TRABAJO ESPECIAL DE GRADO

CAPACIDAD DISIPATIVA DE CONEXIONES ESTRUCTURALES EN GFRP PULTRUSO.

TUTOR ACADÉMICO: Dr. Rosario Ceravolo

Presentado ante la Ilustre
Universidad Central de Venezuela
en el marco del Convenio de doble titulación
con el Politecnico di Torino
Por el Br.:
Azar Mekel, Emilio Elias
Para optar al Título de
Ingeniero Civil

Caracas, 2014

Azar Mekel Emilio Elias

CAPACIDAD DISIPATIVA DE CONEXIONES ESTRUCTURALES EN GFRP PULTRUSO.

Tutor Académico: Dr. Rosario Ceravolo.

Trabajo Especial de Grado. Presentado en el marco del Convenio de doble titulación PDT. Torino, U.C.V. Facultad de Ingeniería.

Escuela de Ingeniería Civil. Año, nº pág. (1).

Palabras Clave: (Disipación de energía, Pultrusion, ANSYS 14, Rotura progresiva)

La tesis descrita a continuación busca poner en evidencia el comportamiento de dos tipos de conexiones, la primera una conexión tipo viga-columna mientras que la segunda una conexión tipo base-columna. Las conexiones están compuestas por perfiles tipo I hechos en GFRP (Glass Fiber Reinforced Polymer), con propiedades geométricas y mecánicas establecidas por el fabricante de dichos perfiles. Los análisis a realizarse son aplicación de esfuerzos axiales a compresión, momento y por ultimo ciclos histéricos mediante la aplicación de desplazamientos.

Todos los elementos vienen modelados con el programa FEM ANSYS14, con el cual fue posible modelar la geometría, propiedades mecánicas y deformativas de cada una de las conexiones, así como también aplicar diferentes steps de carga y poder procesar la progresiva de daño. En cuanto a la disipación de energía se usó el criterio de Jacobsen para medir la energía disipada en cada una de las conexiones

Aplicando las diferentes combinaciones de carga, se demostró que los perfiles desarrollan mayor resistencia a momento a medida que aumenta el esfuerzo de compresión en los mismos, en cuanto a la disipación de energía se constató que es muy pequeña y disminuye aún más a medida que aumenta el esfuerzo a compresión en los perfiles.

POLITECNICO DI TORINO

Corso di Laurea Magistrale in Ingegneria Civile

Final Degree Project

PROGRESSIVE DAMAGE AND DISSIPATION CAPACITY OF GFRP PULTRUDED JOINTS

Advisor: Prof. Rosario Ceravolo

Co Advisor: PhD. Carlo Casalegno

Candidate
Emilio Elias Azar Mekel

Index

1 Introduction

Over the last decade there has been significant growth in the use of fiber- reinforced polymer (FRP) composite materials as construction materials in structural engineering, which for the purposes of this book is defined as the field of engineering that covers the analysis and design of primary, load- bearing structural members and systems in buildings and bridges by civil and structural engineers.

Also known as fiber-reinforced plastics, or advanced composite materials, these materials have proven themselves to be valuable for use in the construction of new buildings and bridges and for the upgrading of existing buildings and bridges. As these materials have transitioned from the research laboratory to implementation in actual structures, so have codes and specifications developed for them for use in civil engineering structural design in the last decade. Now, at the beginning of the twenty-first century, the structural engineering community is about to enter a stage in which structural design with FRP composites is poised to become as routine as structural design with classical structural materials such as masonry, wood, steel, and concrete.

One of the biggest problems of the FRP composites is poor ductility in the material. Ductility in materials allows redistribution of internal forces, increase the security in the structures to seismic hazards or other unexpected situation instead that the composite material has a fragile behavior, and some pseudo-ductility phenomena.

To understand better this phenomenon in this final degree project two different connections are going to be model, in a FEM program (ANSYS). The two connections are made of pultruded GFRP profiles, steel bolts and steel plates. These two connections are going to be subjected to different solicitations, as bending moment, axial compression and hysteretic cycles, all of this to describe failure mechanism, load capacity and energy dissipation of each one. Also results are going to be compare with other previous analyses, to validate results and the FEM model. Once defined these results can be used to calculate different parameters or rules to project structures in pultruded GFRP elements, necessary for improve security under particular conditions as seismic hazard, wind and others.

2 Historical Background

FRP composites have been used on a limited basis in structural engineering for almost 50 years for both new construction and for repair and rehabilitation of existing structures. Structural and civil engineers have been affixing their professional stamps to designs for buildings and bridges for many years, even though these materials have not been recognized by official building codes, and no code-approved design procedures have existed until very recently. These forward-thinking engineers have tended to be people who have specialized expertise in the use of FRP composites in structural engineering or who were in-house structural engineers directly affiliated with a manufacturer of FRP components. In addition to being registered structural engineers involved in engineering practice, many of these engineers have had fundamental knowledge of the materials, manufacturing methods, and fabrication and installation methods for FRP composite in civil engineering structures. Many have worked on teams to develop new FRP components for civil engineering structures (Bank, 1993b). Since the mid-1990s, however, other structural engineers and architects have begun to design with FRP composites on a fairly routine basis. In general, these engineers and architects have not had specialized training or exposure to FRP composites as construction materials. These designs are completed with the aid of published design procedures or by proof testing, and often, with the aid of an in-house engineer from an FRP product manufacturer, who advises on the details of the design and provides sample specifications for the FRP material for the contract documents. Many structural engineers of this type have also affixed their professional seals to these designs over the past decade.

The historical review provides selected examples of where FRP composites have been used in building and bridges in the past half-century. More attention is paid to the applications from the 1990s, which were designed in a routine fashion by structural engineers, as opposed to those from before the 1990s, which were generally designed by engineers with a specialized knowledge of composites. The review describes applications that used FRP components and products available at the time of their manufacture. Many FRP products used in these projects are no longer produced or have been replaced by improved parts and products.

The state of the art of the early work, from 1980 to 1990, in the area of FRP composites for reinforcing and retrofitting of concrete structures in the United States, Japan, Canada, and Europe is detailed in collections of papers and reports edited by Iyer and Sen (1991) and Nanni (1993b). In 1993, a series of biannual international symposia devoted to FRP reinforcement of concrete structures was initiated. At about this time, international research interest in the use of FRP in concrete increased dramatically. Collections of papers on the use of FRP profile sections in structures have been published by the American Society of Civil Engineers (ASCE) since the early 1980s by the now-disbanded Structural Plastics Research Council (SPRC) and in proceedings of the ASCE Materials Congresses. In 1997, the American Society of Civil Engineers (ASCE) founded the *Journal of Composites for Construction*, which today is the main international archive for reporting on research and development in the field of FRP materials for the AEC industry. In 2003, the International Institute for FRP in Construction (IIFC) was established in Hong Kong. To date, thousands of research studies and structural engineering projects using FRP materials have been reported worldwide.

2.1 FRP Reinforcements for new concrete structural members.

FRP reinforcements for new concrete structural members have been of interest to structural engineers since the earliest days of the FRP composites industry. In 1954, in his seminal paper on the development of pultrusion technology, Brandt Goldsworthy speculated that ‘‘the chemical inertness of this material allows its use in concrete reinforcing and all types of

structural members that are subject to corrosive action in chemical plants or other areas here corrosive conditions exist'' (Goldsworthy, 1954).

2.1.1 FRP Bars or Grids for Reinforced Concrete Members

The use of FRP reinforcing bars and grids for concrete is a growing segment of the application of FRP composites in structural engineering for new construction. From 1950s to the 1970s, a small number of feasibility studies were conducted to investigate the use of small-diameter glass FRP rods, with and without surface deformations, to reinforce or prestress concrete structural members. In the early 1980s, glass helical–strand deformed reinforcing bars were produced for structural engineering applications by Vega Technologies, Inc. of Marshall, Arkansas (Pleimann, 1991). These bars were used to build magnetic resonance imaging facilities, due to their electromagnetic transparency. At the time, these FRP bars were cost-competitive with stainless steel bars, which were the only other alternative for this application. Many single-story cast- in-place wall and slab structures, which look identical to conventional rein- forced concrete structures, were built. Designs were performed by registered structural engineers using the working stress design basis, and the buildings were constructed using conventional construction technology.

In the late 1980s, interest in the use of FRP received a boost as attention focused on ways to mitigate corrosion in steel-reinforced concrete structures exposed to the elements, especially highway bridge decks. In the United States, International Grating, Inc. developed a sand-coated glass fiber– reinforced bar that was used experimentally in a number of bridge deck projects. This was followed in the 1990s by the development of deformed FRP bars by Marshall Composites, Inc. A number of companies experimented with FRP bars with helically wound spiral outer surfaces. These included Creative Pultrusions, Glasforms, Vega Technologies, International Grating, Hughes Brothers, and Pultrall. In the late 1990s a number of these producers also experimented with carbon fiber FRP bars with deformed, helically wound, and sand-coated surfaces. Extensive research was conducted in the 1990s on the behavior of concrete beams and slabs reinforced with various types of FRP bars (Daniali, 1990; Faza and GangaRao, 1990, 1993; Nanni, 1993a; Benmokrane et al., 1996a,b; Michaluk et al., 1998). Studies were also con- ducted on the use of glass fiber pultruded FRP gratings in reinforced concrete slabs (Bank and Xi, 1993). ACI published its first design guide, ACI 440.1R- 01, for FRP-reinforced concrete in 2001 (ACI, 2001). The guide was subsequently revised in 2003 (ACI 440.1R-03), and the current version, ACI 440.1R-06, was published in 2006 (ACI, 2006). Figure 1 shows samples of a number of commercially produced glass- and carbon-reinforced FRP bars for concrete reinforcing.

At the same time that glass fiber FRP bars were being developed for reinforcing concrete in corrosive environments in the United States, a parallel effort was under way in Japan. The Japanese effort focused, to a large extent, on carbon fiber reinforcement, due to concern for the degradation of glass fibers in alkaline environments. A two-dimensional grid product called NEF- MAC (new fiber composite material for reinforced concrete) was developed successfully and commercialized by Shimizu Corporation. Grids with carbon fibers, glass fibers, and carbon glass hybrid fibers were produced. The majority of applications of NEFMAC appear to have been in tunnels, where the noncorrosive properties and panel sizes of the grids were very effective when used with shotcreteing methods. Design guides for reinforced concrete design with FRP bars were published in Japan in 1995 and 1997 (BRI, 1995; JSCE, 1997). Efforts were also directed to developing polyvinyl alcohol (PVA) FRP bars, but these were never commercialized. Figure1.2 shows carbon and glass NEFMAC grids developed in Japan in the 1980s.

Today, FRP reinforcing bars for concrete with both glass and carbon fibers are produced by a number of companies in North America, Asia, and Europe. The use of FRP bars has become mainstream and is no longer confined to demonstration projects. However, this is still a niche area in structural engineering; competition among manufacturers is fairly fierce and only the strong.

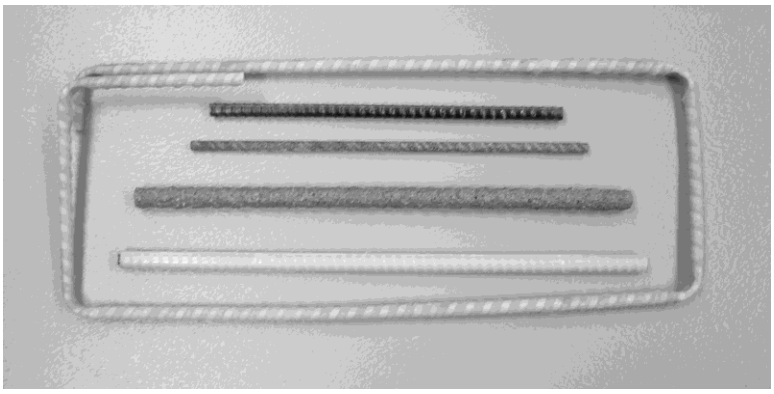

Figure 1.1. Glass- and carbon-reinforced FRP bars.

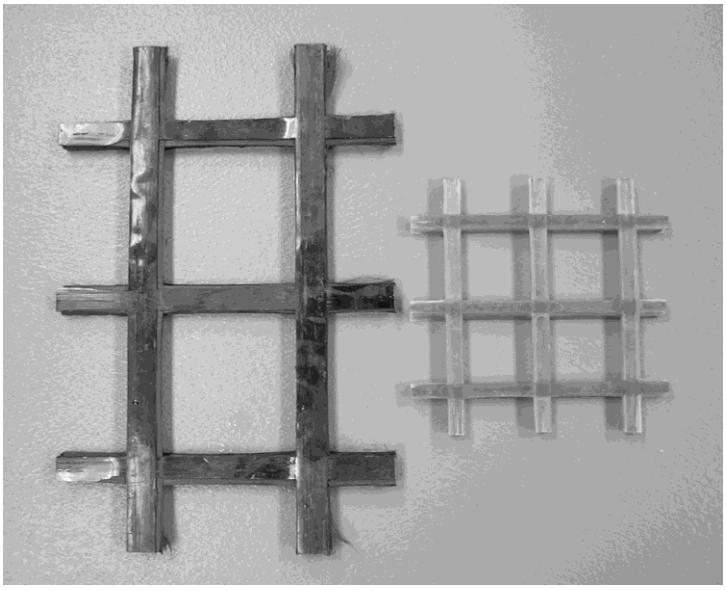

Figure 1.2. NEFMAC FRP grids.

Companies are surviving. Applications have become routine for certain specialized environments. Most current applications appear to be in underground tunnels and in bridge decks. Figure 1.3 shows a large glass fiber FRP rein- forcing cage being readied for placement in forms for a tunneling application. The FRP bars are used to create a ‘‘soft eye’’ for subsequent drilling through a vertical concrete shaft wall. These FRP bars are lap spliced to the steel bars in a conventional fashion. Figure 1.4 shows a bridge deck slab with a glass FRP top mat being poured.

In addition to FRP bars for reinforcing concrete, FRP dowel bars for concrete highway pavements and FRP ground anchors have also been commercialized successfully in recent years. Explicit design procedures according to the ACI are given in this book for the design of concrete structures reinforced with FRP bars.

Figure 1.3. Reinforcing cage being readied for placement in forms for a tunneling application.

Figure 1.4. Bridge deck slab with a glass FRP top mat being poured.

2.1.2 FRP Tendons for Prestressed Concrete MemberS

Development of FRP tendons for prestressing concrete took place in Holland, Germany, and Japan in the early 1980s. This was motivated primarily by the desire to reduce corrosion in prestressed concrete elements. A rectangular aramid FRP strip called Arapree was developed in Holland by the Hollandsche Beton Groep (HBG) and Akzo, and a glass fiber tendon in an external polymer sheath called Polystal was developed by Strabag Bau AG and Bayer AG in Germany. These products were used in a number of bridge demon stration projects in Europe, but their production has been discontinued. Arapree is now produced by Sireg in Italy. In the 1980s in Japan, a national project was undertaken to develop FRP reinforcements for concrete that focused primarily on tendons (Fukuyama, 1999). Many different aramid and carbon fiber products were developed and over 50 demonstration projects were completed. The Advanced Composite Cable Club (ACC Club) was founded to coordinate and commercialize FRP

prestressing products in Japan.
These included twisted-strand carbon tendons called carbon fiber composite cable (CFCC), known as Tokyo Rope, by Tokyo Seiko K.K.; aramid fiber rods and strips, called Arapree (under license from HBG), by Nippon Aramid Co.; aramid fiber rods, called Technora Rods, by Teijin Ltd.; aramid fiber tendons, called FiBRA, by Kobe Steel Cable; and carbon fiber tendons, called Leadline, by Mitsubishi Chemical Corporation. As conventional steel chucks and anchors could not be used, due to the low transverse strength of FRP tendons, all the manufacturers developed specialized prestressing anchors. This has proved to be the Achilles heel of the FRP prestressing industry. Both technical difficulties with the anchors and their high prices made them unattractive to the construction industry. Through the 1990s a number of demonstration projects were conducted in the United States and Canada using Japanese and European FRP prestressing products, but routine use of these FRP tendons has not occurred. These FRP rods have also been used as conventional reinforcing bars in a number of demonstration projects.

2.1.3 Stay-in-Place FRP Formwork for Reinforced Concrete Members

The use of FRP composites as stay-in-place (SIP) formwork has been explored for a number of years. FRP SIP formwork systems that act to reinforce the concrete after it has cured and systems used only as SIP forms have been developed. A stay-in-place bridge deck panel produced by Diversified Composites, Inc. in the United States has been used on two multispan highway bridges in Dayton, Ohio (1999) and Waupun, Wisconsin (2003). The deck form has a corrugated profile and is intended as a no corroding substitute for stay-in-place metal and prestressed concrete deck forms. When used as a stay-in-place deck form, the FRP composite serves as the tensile reinforcement after the concrete has hardened.

FRP tubular stay-in-place forms have also been used to manufacture beam and column members. They are also referred to as concrete-filled FRP tubes. A carbon shell system consisting of concrete-filled carbon FRP tubes has been used to produce girders for the superstructure of a highway bridge in California.

2.2 FRP Strengthening of existing structural members

FRP materials used to strengthen and repair load-bearing structural members are popular applications of FRP composites in structural engineering. Collectively, these applications are known as retrofitting applications, as they are used in existing structures and not in the construction of new structures. Retrofitting applications can be classified broadly into two types. One type is strengthening, where the original structure's strength or ductility (typically, its displacement capacity) is increased from the loads (or displacements) for which it was originally designed. This increase may be necessitated by the desire to make the structure compatible with existing building codes (particularly in the case of seismic retrofitting) or may be desired due to changes in use of the structure. FRP retrofitting to improve the performance (load carrying and ductility) of a structure when subjected to blast and impact loading has become of interest of late. The other type of FRP retrofitting can be classified as repair. In this case, the FRP composite is used to retrofit an existing and deteriorated structure to bring its load-carrying capacity or ductility back to the loads or displacements for which it was designed (and hence is, in fact, a type of strengthening). Repair is necessitated when the original structure has deteriorated due to environmental effects, such as corrosion of steel reinforcing in concrete structures or when the original structure has been damaged in service or was not constructed according to the original design. For example, reinforcing bars may be omitted in a beam at the time of construction due to a design or construction error. Although these two types of applications are similar, there are important differences that are related primarily to evaluation of the existing structural capacity and the nature of the repair to be undertaken before FRP can be used. In many cases, a repair design will include strengthening to add a level of safety to the repaired structure and to account for uncertainty in the retrofit design.

FRP retrofitting has been used successfully on reinforced concrete structures, prestressed concrete structures, timber structures, and masonry and metal structures. At this time, code design guidance is only available for FRP retrofitting of reinforced concrete structures, particularly as applied to strengthening. Consequently, this historical review focuses primarily on the use of FRP retrofitting technologies for reinforced concrete and prestressed concrete structures.

Two primary methods are used to attach FRP composite materials to concrete structures (and to masonry, timber, and even metallic structures) for retrofitting purposes. One method employs pre-manufactured rigid FRP strips that are adhesively bonded to the surface of the structural member. The other method, known as hand layup, consists of in situ forming of the FRP composite on the surface of the structural member using flexible dry fiber fabrics or sheets of width approximately 6 to 60 in. (150 to 1500 mm) and liquid polymers. In recent years a new variant of the premanufactured strip method called near surface mounting (NSM) has been developed. In this method, a thin, narrow FRP or small-diameter round FRP is inserted and then bonded adhesively into a machined groove at the surface of the concrete member.
FRP retrofitting has been used with bridge and building structures to strengthen static loads, and for dynamic loads (such as strengthening for improved seismic or blast response in a bridge or building structure). FRP composites have been used successfully for flexural strengthening of concrete beams and slabs, shear strengthening of concrete beams, and axial strengthening and ductility enhancement of concrete columns.

The use of FRP composites for retrofitting concrete structures appears to have evolved at approximately the same time, in the late 1980s, in Europe (particularly in Switzerland) and in Japan. Both of these initiatives were followed very soon afterward by research and applications in the United States and Canada. Initially, research focused on flexural strengthening of structural members (concrete and timber). This was followed very closely by studies on confinement of concrete columns with FRP composite fabrics and sheets, known as wraps, to address a number of deficiencies in concrete columns, particularly in highway bridges, subjected to lateral loads due to earthquakes. Both of these FRP applications grew out of the experience gained with retrofitting of reinforced concrete using steel plates or steel jackets. The use of steel plates to strengthen reinforced concrete structural members was an accepted technology by the mid-1980s, particularly for bridge retrofitting. The use of steel jackets to retrofit concrete columns developed into a routine practice in the United Sates following the Loma Prieta earthquake in 1989. FRP shear strengthening of concrete beams has been studied since the early 1990s and numerous applications in concrete structures, particularly precast prestressed concrete T-beams, have been undertaken. Strengthening of concrete slabs for punching shear has been studied in recent years but is not yet an accepted technology.

Adhesively bonded precured carbon fiber-reinforced epoxy FRP strengthening strips for flexural strengthening of concrete beams was first studied and used in Switzerland in the late. An FRP strengthening strip known as Carbodur was developed at EMPA and commercialized by Sika.

The fire safety and fatigue life of the system have been studied at EMPA. These strips have been used in hundreds of building, bridge, and chimney retrofit projects in Europe (Taerwe and Matthys, 1999). An L-shaped precured strip has recently been developed by EMPA for shear strengthening of beams. Today, precured strips are produced by a number of manufacturers, including S&P Clever Reinforcement Company in Austria; Hughes Brothers, Strongwell, and FyfeCo in the United States; and Sika in Switzerland. Since the mid-1990s, following commercialization of the precured FRP strip, hundreds of research projects and thousands of FRP retrofits for static or nonseismic dynamic loads (e.g., vehicular loads, wind loads) have been carried out throughout the world.

Manufacturers of FRP products themselves have traditionally provided de- sign guidance for the use of precured FRP strengthening strips. The first English-language edition of the Sika Carbodur design guide appeared. Current editions have replaced earlier editions as more information has become

available and new FRP strengthening products have been introduced. A design guide is published by the S&P Reinforcement Company that covers their products (S&P, 1998). More recently, professional organizations have developed general-purpose design guides for use of precured (and bonded) FRP strengthening products for concrete structures, which in time will probably replace manufacturers' guides (TR 55, 2004; FIB, 2001; ACI, 2002; CSA, 2002). Code guidance for NSM systems is currently being

Early work in the United States on FRP strengthening of concrete structures was undertaken for the purpose of seismic retrofitting of reinforced concrete columns. The Fyfe Company developed a glass fabric and epoxy hand-layup system for column retrofitting in the early 1990s that was tested at the University of California San Diego (UCSD) (Priestley et al., 1992). This work was followed by further development and testing of FRP column wrapping systems, with research being conducted primarily at UCSD (Priest- ley and Seible, 1995). Based on much of this earlier work, Acceptance Criteria 125 was published by the International Conference of Building Officials (ICBO) to provide guidance to contractors and designers who wished to use the method in the United States (AC 125, 1997).

Simultaneously, a number of researchers in the United States studied flexural strengthening of beams using hand-layup fiber sheets and fabrics of glass or carbon fibers (Saadamanesh, 1994). The Forca tow sheet carbon sheet strengthening system, called the MBrace System (MBrace, 1998), was commercialized in the United States by Master Builders, Inc. of Ohio together with Structural Preservation Systems of Maryland. The Fyfe Company developed and commercialized the Tyfo System (Tyfo, 1998). Installation of a fabric sheet is shown in Figure 1.10. Hexcel supplies fabric strengthening systems for Sika known as SikaHex. Nowadays numerous companies market a variety of fabric and sheet strengthening materials in the United States, including VSL, Edge Structural Composites, and Quakewrap. Figure 1.5 shows installation of an FRP wrap on a rectangular column.

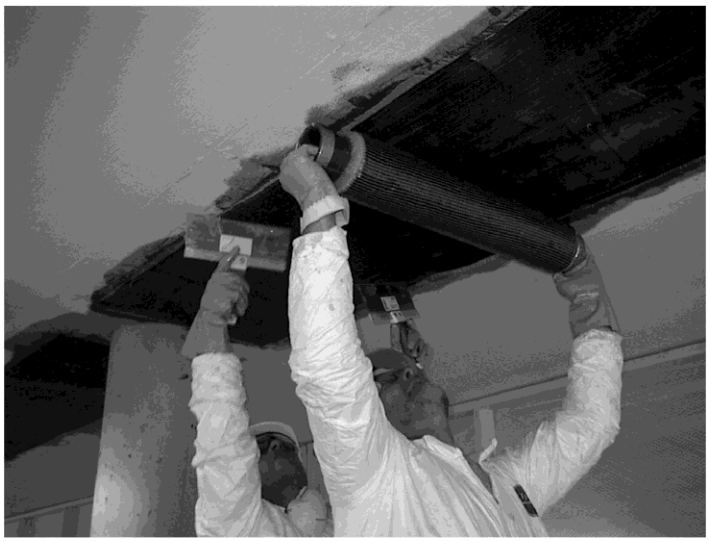

Figure 1.5 Installation of a carbon fiber fabric sheet.

2.3 FRP Profiles for new structures

A cost-effective method of producing high-quality constant-cross-section FRP profile shapes, called pultrusion, was developed in the 1950s in the United States. Initially, small profiles were produced primarily for industrial applications, but the method was always envisioned as being used for developing FRP substitutes for conventional beams and columns in buildings and bridges. To quote Brandt Goldsworthy again: ''The chemical inertness of this material allows its use in . . . all types of structural members that are subject to corrosive action in chemical plants or other areas where corrosive conditions exist'' (Goldsworthy, 1954). By the late 1960s and early 1970s a number of

pultrusion companies were producing ‘‘standard’’ I-shaped and tubular pro- files. The Structural Plastics Research Council (SPRC) was established in 1971 by the American Society of Civil Engineers (ASCE), and a manual was developed for the design of structural plastics (McCormick, 1988). Called the Structural Plastics Design Manual (SPDM), it was originally published in 1979 as an FHWA report and subsequently by the ASCE in 1984 (ASCE, 1984). This guide was not restricted to pultruded profiles. In 1996, a European design guide for polymer composite structures was published (Eurocomp, 1996), and in 2002 the European Union published the first standard specification for pultruded profiles (CEN, 2002a).

The first large structures constructed from FRP profiles were single-story gable frames that were used in the emerging computer and electronics industry for Electromagnetic Interference (EMI) test laboratories. The electromagnetic transparency of the FRP profiles was a key benefit in these buildings which required no magnetic material above the foundation level. Custom pultruded profiles and building systems were developed and commercialized by Composites Technology, Inc. (CTI), founded by Andrew Green in Texas in the 1960s (Smallowitz, 1985). In 1985, CTI designed and constructed an innovative EMI building for Apple Computer. Similar structures were also constructed from FRP pultruded profiles produced by Morrison Molded Fiberglass Company (MMFG, now Strongwell) in Virginia for IBM and othersin the 1980s. Figure 6 shows a FRP gable frame building during the installation of the FRP cladding. For much of this time, designing was done by an MMFG subsidiary called Glass-Steel. A design manual for the MMFG profile shape Extren was published in 1973. Creative Pultrusions began producing standard shapes in the late 1970s, called Pultex, and developed a design manual. Current editions of these manuals are published regularly and are available from these two companies.

The next major development in building systems for FRP profiles, which continues to be the largest market segment for large pultruded building com- ponents, was in the cooling tower industry. An FRP building system was developed in the 1980s by Composite Technology, Inc. for Ceramic Cooling Tower (CCT) and commercialized as the Unilite system (Green et al., 1994). The Unilite system consisted of a number of unique beam, column, and panel FRP pultruded components.

In addition to custom cooling tower structures, FRP profiles have been used in ‘‘stick-built’’ cooling towers since the late 1980s. These systems are typically constructed using tubular FRP sections 2x2 in. (50x50 mm) and 3x3 in. (75x 75 mm) covered with an FRP or no reinforced polymer cladding system. Designers typically use standard off-the-shelf pultruded pro- files in these structures and design them according to applicable building codes.
To date, standard FRP profile shapes have not seen much use in multistory frame building structures for commercial or residential construction. One of the major difficulties with multistory frame structures using FRP profiles is the development of economical and effective means of connecting the individual members. Research has been conducted on the subject of FRP connections since the early 1990s, but no simple and effective connection system has yet been developed or commercialized for FRP pultruded profiles. Most current designs use steel-like connection details that are not optimized for FRP profiles. A prototype multistory framed building called the Eyecatcher, constructed by Fiberline Composites in Basel, Switzerland in 1999, is shown in Fig. 1.7. The building was constructed for the Swissbau Fair as a dem- onstration of the potential for FRP profile shapes (Keller, 1999).

In the field of bridge engineering, FRP profile shapes have seen increased application since the mid-1970s. Both the light weight of the FRP components and their noncorrosive properties serve to make them attractive as bridge decking panels and as superstructure members. Hundreds of 30 to 90 ft (9 to 27 m)-long short span pedestrian footbridges of the truss variety have been designed and constructed worldwide using small FRP profiles. In 1992, a 131-m-long cable-stayed pedestrian bridge was constructed in Aberfeldy, Scotland, using the Advanced Composite Construction System (ACCS), a FRP plank system designed by Maunsell Structural Plastics (Bur- goyne and Head, 1993; Cadei and Stratford, 2002). A fiber rope called Parafil was used for the cable stays. In 1997, a 40.3-m cable-stayed

pedestrian bridge was constructed over a railway line using FRP profiles in Kolding, Denmark (Braestrup, 1999). Both of these structures are worth noting, due to their extensive use of FRP pultruded profiles that facilitated rapid and economical construction.

Figure 1.6 FRP frame structure under construction.

Figure 1.7 Eyecatcher building.

Figure 1.8 Light-truss pedestrian bridge pultruded structure.

In the 1990s, a significant effort was undertaken by a number of FRP manufacturers to develop an FRP bridge deck system that could be used on conventional steel or concrete girders. Besides the potential for long-term durability of an FRP bridge deck, an added benefit exists when FRP decks are used to replace deteriorated reinforced concrete decks. Due to the significant decrease in dead weight of the structure, the live-load capacity for the re-decked structure can be increased, which

may be beneficial, especially on bridges with load postings. FRP deck systems have been developed and commercialized by Creative Pultrusions, Martin Marietta Composites, Atlantic Research Corp., Hardcore Composites, and others (Bakis et al., 2002). As with FRP frame systems, the connections between the prefabricated FRP deck panels and those between the FRP deck and the superstructure have been sources of the greatest difficulty in realizing this technology. The high cost of glass FRP decks compared with conventional concrete decks does not appear to be able to offset savings in weight and construction productivity. Developing an approved bridge guardrail for FRP deck systems has also proved to be a challenge that has not been resolved satisfactorily at this time. In 2001, a glass–carbon FRP pultruded profile 36 in. high by 18 in. wide known as the *double-web beam* (DWB) was developed by Strongwell for use as a bridge girder. Figure 1.20 shows FRP girders on the Dickey Creek Bridge in Virginia in 2001. FRP rods have also been developed for use as guy wires for towers and for suspension cables for bridges. Pultruded glass FRP rods have been used since the mid-1970s in numerous applications in the United States as guy wires or bracing cables in antenna towers. The use of carbon FRP cables for bridges was first suggested in the early 1980s by Urs Meier of the Swiss Federal Laboratories for Materials Testing and Research (EMPA) in Dubendorf, Switzerland, as an alternative to steel cables for very long span suspension bridges, where the weight of the cable itself can be a limiting factor (Meier, 1986). Since then, EMPA and BBR Ltd. in Zurich, Ciba AG in Basle, and Stesalit AG in Zullwil, Switzerland, have worked together on developing carbon FRP cables for bridges. In 1997, two carbon FRP cables consisting of 241 5-mm (0.2-in.)-diameter carbon–epoxy FRP rods were used in the Storchen cable-stayed bridge in Winterthur, Switzerland. Figure 1.21 is a close-up of the multistrand carbon FRP cable used. FRP profiles have also been used as stays in the Kolding FRP pedestrian bridge constructed in Den- mark in 1997, and carbon fiber cables were used in the Laroin footbridge constructed in France in 2002.

Figure 1.9 FRP DWB girders on Dickey Creek bridge.

3 Materials and Manufacturing

To produce an FRP composite material, two primary raw material constituents are required, reinforcing fibers and a polymer resin matrix. In this section we review key properties and characteristics of the raw materials used to produce FRP products for structural engineering. We do not provide information on how the raw materials are produced; the reader is referred to the composite materials literature for coverage of this subject (e.g., Schwartz, 1997a,b). However, it is worth noting that all the raw materials are produced at high temperatures in industrialized processes that require highly specialized equipment and control. Analogous to the state of affairs that exists today, where a structural engineer does not typically have extensive knowledge of how port- land cement is produced from limestone, a structural engineer is not expected to have extensive knowledge of how polymer resin is produced from crude oil or how glass fiber is produced from silica sand.

Except in very rare circumstances, the raw fiber and polymer constituents cannot be used in their as-produced forms to manufacture an FRP composite material. After the fiber filaments are produced, they are post processed in a number of secondary operations to produce fiber products such as strands, sheets, fabrics, and mats that can be used in a manufacturing process. Similarly, the raw polymer, which is generally referred to as the base polymer or neat resin, is often blended with other resins and mixed with a variety of additives and process aids to produce a resin system (or resin mix) for manufacturing. The fiber and resin systems are discussed later in the manufacturing sections of this chapter, as they are manufacturing method–dependent. Numerous companies manufacture and distribute both raw and post processed raw materials for use in production of FRP composites. The annual Source- book (Sourcebook, 2006) provides an extensive list of U.S.-based manufacturers and suppliers.

3.1 Reinforcing Fibers

The fiber phase of an FRP composite material consists of thousands of individual micrometer-diameter individual filaments. In the large majority of fiber forms used in FRP products for structural engineering, these fibers are indefinitely long and are called continuous. This is to differentiate them from short fibers of length 10 to 50 mm that are used in the spray-up process for boat building and consumer products or in reinforced cementitious materials [known as glass-reinforced cements (GRCs) or fiber- reinforced cementitous (FRC) composites]. Continuous fibers are used at a relatively high volume percentage (from 20 to 60%) to reinforce the polymer resin: thus the term fiber-reinforced polymer (FRP). The mechanical properties of the fibers are typically orders of magnitude greater than those of the polymer resins that they reinforce; however, due to their filamentary nature they cannot be used as stand-alone construction materials and must be used in a synergistic fashion with polymer resins to realize their superior mechanical properties.

Glass Fibers Glass fibers are used in a multitude of FRP products for structural engineering, from FRP reinforcing bars for concrete, to FRP strengthening fabrics, to FRP structural profile shapes. Glass is an amorphous inorganic compound of primarily metallic oxides that is produced in fibrous form in a number of standard formulations or types. Silica dioxideis the largest single compound in all glass formulations, constituting from 50 to 70% by weight of the glass. Different grades of glass fiber are identified by letter nomenclature. A borosilicate glass known as E-glass (electrical glass) because of its high electrical resistivity is used to produce the vast majority of glass fiber used in FRP products for structural engineering. A-glass and C-glass are used to produce specialized products for use in structural engineering. S-glass (structural or high-strength glass) is used to produce the high-performance fibers used primarily in the aerospace industry. The diameter of an individual glass fiber or filament ranges from approximately 3 to 24 1-m. The 17-1-m Diameter fiber is most commonly used for FRP products for structural engineering. A glass fiber has a distinctive bright white color to the naked eye. Glass is usually considered to be an isotropic material. Approximate properties of

commonly used grades of glass fibers are given in Table 2.1. Values presented in Table 3.1 are intended as a guide and should not be used in design calculations. Glass fibers are produced at melt temperatures of about 1400°C. Individual filaments are produced with a surface coating called a sizing that serves to protect the filaments when they are formed into a bundle or a strand.

TABLE 3.1 Approximate Properties of Common Grades of Glass Fibers

Grade of Glass Fiber	Density [g/cm^3]	Tensile Modulus [GPa]	Tensile Strength [MPa]	Max. Elongation (%)
E	2.57 (0.093)	72.5 (10.5)	3400 (493)	2.5
A	2.46 (0.089)	73 (10.6)	2760 (400)	2.5
C	2.46 (0.089)	74 (10.7)	2350 (340)	2.5
S	2.47 (0.089)	88 (12.8)	4600 (667)	3.0

The sizing also contains coupling agents, usually silanes, that are specially formulated to enhance bonding between the glass fiber and the particular polymer resin being used when making a glass-reinforced FRP composite material. Today, most commercially available glass fibers can be obtained with sizings that are compatible with the three major thermosetting resin systems used in structural engineering: epoxy, polyester, and vinyl ester. The commonly used term fiberglass is generally used to refer to the glass fiber- reinforced polymer composite material itself and not solely to the glass fiber constituent material. When referring to the fibrous reinforcement alone, the term glass fiber is preferred. Glass fibers are particularly sensitive to moisture, especially in the presence of salts and elevated alkalinity, and need to be well protected by the resin system used in the FRP part. Glass fibers are also susceptible to creep rupture and lose strength under sustained stresses (Bank et al., 1995b). The endurance limit of glass fibers is generally lower than 60% of the ultimate strength. Glass fibers are excellent thermal and electrical insulators (hence, their extensive use in buildings and the electric power industry as insulation materials) and are the most inexpensive of the high-performance fibers.

Carbon Fibers Carbon fibers are used in structural engineering applications today in FRP strengthening sheets and fabrics, in FRP strengthening strips, and in FRP prestressing tendons. Carbon fiber is a solid semi crystalline organic material consisting on the atomic level of planar two-dimensional arrays of carbon atoms. The two-dimensional sheet like array is usually known as the *graphitic form;* hence, the fibers are also known as graphite fibers (the three-dimensional array is well known as the *diamond form*).

Carbon fibers have diameters from about 5 to 10 1-m. Carbon fiber has a characteristic charcoal-black color. Due to their two- dimensional atomic structure, carbon fibers are considered to be transversely isotropic, having different properties in the longitudinal direction of the atomic array than in the transverse direction. The longitudinal axis of the fiber is parallel to the graphitic planes and gives the fiber its high longitudinal modulus and strength. Approximate properties of common grades of carbon fibers are given in Table 3.2.

Carbon fiber is produced at high temperatures [1200 to 2400°C] from three possible precursor materials: a natural cellulosic rayon textile fiber, a synthetic polyacrilonitrile (PAN) textile fiber, or pitch (coal tar). Pitch-based fibers, produced as a by-product of petroleum processing, are generally lower cost than PAN- and rayon-based fibers. As the temperature of the heat treatment increases during production of the carbon fiber, the atomic structure develops more of the sheet like planar graphitic array, giving the fiber higher and higher longitudinal modulus. For this reason, early carbon fibers were also known as *graphite fibers.* The term *carbon fiber* is used to describe all carbon fibers used in structural engineering applications. The term *graphite fiber* is still used in the aerospace industry; however, this term is slowly dying out. Similar to glass fibers, carbon fibers need to be sized to be compatible with a resin system. Historically, carbon fibers have been used primarily with epoxy resins, and suitable sizing for epoxy resin systems are readily available.

Nowadays, carbon fibers are being used with vinylester and blended vinylester–polyester resins for FRP profiles and FRP strengthening strips. Sizing for carbon fibers for polyester and vinylester resins are not as common. Care must be taken when specifying a carbon fiber for use with a nonepoxy resin system to ensure that the fiber is properly sized for the resin system used.

TABLE 3.2 Approximate Properties of Common Grades of Carbon Fibers

Grade of Carbon Fiber	Density [g/cm^3]	Tensile Modulus [GPa]	Tensile Strength [MPa]	Max. Elongation (%)
Standard	1.7 (0.061)	250 (36.3)	3700 (537)	1.2
High strength	1.8 (0.065)	250 (36.3)	4800 (696)	1.4
High modulus	1.9 (0.068)	500 (72.5)	3000 (435)	0.5
Ultrahigh modulus	2.1 (0.076)	800 (116.0)	2400 (348)	0.2

Carbon fibers are very durable and perform very well in hot and moist environments and when subjected to fatigue loads. They do not absorb moisture. They have a negative or very low coefficient of thermal expansion in their longitudinal direction, giving them excellent dimensional stability. They are, however, thermally and electrically conductive. Care must be taken when they are used in contact with metallic materials, as a galvanic cell can develop due to the electro potential mismatch between the carbon fiber and most metallic materials. Some research has suggested that this can lead to degradation of the polymer resin in the FRP composite, especially in the presence of chlorides and to corrosion of the metallic material (Alias and Brown, 1992; Torres-Acosta, 2002).

Aramid Fibers Aramid fibers were used to produce first-generation FRP prestressing tendons in the 1980s in Europe and Japan; however, few manufacturers still produce aramid fiber FRP reinforcing bars or tendons. Aramid fabrics are occasionally used in FRP strengthening applications to wrap columns and as sparse-volume weft (fill) fibers in unidirectional glass or carbon fabrics for FRP strengthening. Aramid fibers consist of aromatic polyamide molecular chains. They were first developed, and patented, by DuPont in 1965 under the trade name Kevlar.
A combination of their relatively high price, difficulty in processing, high moisture absorption (up to 6% by weight), low melting temperatures, and relatively poor compressive properties have made them less attractive for FRP parts for structural engineering applications. Their advantages include extremely high tenacity and toughness, and consequently, they are used in many industrial products, either in bare fabric form or as reinforcements for FRP composites where energy absorption is required, such as in bulletproof vests (body armor), helmets, and automotive crash attenuators. They have a distinctive yellow color and are similar in cost to carbon fibers. Like carbon fibers, they have a negative coefficient of thermal expansion in the fiber longitudinal direction. They are the lightest of the high- performance fibers, having a density of around 1.4 g / cm3 (0.051 lb / in3). Depending on the type of aramid fiber, the fiber longitudinal tensile strength ranges from 3400 to 4100 MPa, and its longitudinal tensile modulus ranges from 70 to 125 GPa.

Other Fibers Other fibers that are now in the development phase for use in FRP products for structural engineering include thermoplastic ultrahigh- molecular-weight (UHMW) polyethylene fibers and polyvinyl alcohol (PVA) fibers. PVA fibers have been used in FRP bars and FRP strengthening sheets in Japan. UHMW short fibers are being used in the development of ductile fiber-reinforced cements (FRCs) but have not yet been used in FRP products for structural engineering. Inorganic basalt fibers, produced in Russia and the Ukraine, may see future applications in FRP products in structural engineering, due to their superior corrosion resistance and similar mechanical properties to glass fibers. Thin steel wires have been developed for use in FRP strengthening fabrics with either polymer or cementitious binders. Natural fibers such as hemp, sisal, and flax, as well as bamboo fibers, have been used in experimental applications to produce FRP composites, but no commercial FRP products are available that contain these fibers at this time. It is anticipated that FRP products in structural engineering that will be developed in the first half of the twenty-first century will probably use more of

these natural fibers as sustainability and recyclability become more important drivers in the construction industry.

3.2 Polymer Resins

The term polymer is used to describe an array of extremely large molecules, called macromolecules that consist of repeating units or chains, in which the atoms are held together by covalent bonds. The term polymer is generally used to describe an organic material of this type; however, it can also be used to describe an inorganic material. The term polymer resin, or simply resin, is used in the composites industry to refer to the primary polymer ingredient in the non fibrous part of the FRP material that binds the fibers together. This non fibrous part is also known as the matrix or binder. When used in commercial and industrial products a polymer-based material is often known as a plastic and the acronym FRP is also often used to denote a fiber-reinforced plastic. The acronym RP is often used to connote a reinforced plastic, al- though this is mostly used to describe short-fiber-reinforced plastic products of lower strength and stiffness.

The differences between organic polymers depend on the functional groups present in the polymer chains and the extent of the interaction between these chains. Chains, which have a molecular backbone, may be linear or branched. (Seymour, 1987). Two primary groups of polymers exist today, thermosetting polymers and thermoplastic polymers. They are distinguished from one an- other by how the polymer chains are connected when the polymer is in its solid form. Thermosetting polymers are cross-linked, which means that their molecular chains are joined to form a continuous three-dimensional network by strong covalently bonded atoms. Thermoplastic polymers are not cross-linked, and their molecular chains are held together by weak van der Waals forces or by hydrogen bonds (Schwartz, 1997b). This affects their mechanical and physical properties. Due to cross-linking, a thermosetting polymer's structure is set when it solidifies or cures during the polymerization process, and it cannot be heated and softened and then re-formed into a different shape. On the other hand, a thermoplastic polymer does not set but remains plastic, and the molecular chains can ''flow'' when the solid polymer is heated such that it softens and can be reset into a different shape upon cooling.

Synthetic organic polymers are produced by polymerization techniques, either chain (or additional) polymerization or step (or condensation) polymerization. Most high-performance polymers are produced by condensation of dysfunctional reactants. The best known chain polymerization reaction is free- radical polymerization, in which an electron-deficient molecule (or free radical) is initially added to a monomer, forming a new, larger free radical. The chain reaction continues until the reactive constituents are expended.

The thermal response of polymers plays a large role in their processing, properties, and behavior. Pure crystalline solids such as metals undergo a phase change from solid to liquid at a transition temperature, called the melting point, Tm. This is the only thermal transition possible in a pure crystalline solid. Since polymers are semi crystalline solids that contain non crystalline amorphous regions, other thermal transitions occur at lower temperatures than Tm. A thermal transition of particular interest to structural engineering, known as the glass transition temperature, Tg, occurs in the amorphous region of the polymer at a temperature below the melting temperature. The physical (density, heat capacity) and mechanical (stiffness, damping) properties of the polymer undergo a change. When the temperature approaches Tg from below, the polymer changes from a rigid (known as glassy) to a viscous (known as rubbery) state. The glass transition temperature may be referred to as the heat distortion temperature or heat deflection temperature in polymer manufacturer's literature. Although not precisely the same property, these three transition temperatures are usually close in value (within 10°C) and are used interchangeably in the industry to describe roughly the same physical phenomenon. Both thermosetting and thermoplastic polymers have glass transition temperatures. A thermoplastic polymer liquefies at its melting temperature, whereas a thermosetting polymer begins to decompose at its melting temperature. Above the melting temperature a thermoplastic or thermosetting polymer will pyrolysis in an oxygen-rich atmosphere.

In structural engineering, FRP composites must be used in their rigid states at operating temperatures below their glass transition temperatures. At temperatures higher than the glass transition temperature, the modulus of the resin, and hence the FRP composite, decreases. Since deflection criteria are used routinely in structural engineering design, an FRP part can become un- serviceable at temperatures close to its glass transition temperature. In addition, the FRP part will be less durable and will have lower strength at temperatures above its glass transition temperature. On the other hand, elastomeric polymers like those used in asphalt binders are used above their glass transition temperatures in their viscous state. When these polymers are used below their glass transition temperatures, they become brittle and crack.

Polymer resins are good insulators and do not conduct heat or electricity provided that they have low void ratios. Water in the voids of a polymer composite can allow the composite to conduct electricity. For glass-reinforced polymer electric power parts, stringent limits are placed on the void ratio (usually less than 1%). Polymer resins are usually considered to be isotropic viscoelastic materials. They creep under sustained stresses or loads and relax under constant strains or displacements. Most polymer resins are susceptible to degradation in ultraviolet light (White and Turnbull, 1994). Thermosetting polymer resins are generally not suitable for use at temperatures greater than 180°C and in fires if not protected in a fashion similar to steel structural members. Polymer materials have been shown to have acceptable fire ratings when used in appropriately designed protection systems and fire- retarding additives. Thermoplastic polymers have been developed for high temperatures up to 450°C. Most liquid polymer resins have a shelf life between 6 and 12 months and should be stored at cool temperatures between 10 and 15°C (50 to 60°F).

Unsaturated Polyester Resin Polyester resin is widely used to make pultruded FRP profiles for use in structural engineering and is also used to make some FRP rebars. When greater corrosion resistance is desired in FRP parts, higher-priced vinyl ester resins are generally recommended, although the corrosion resistance of some polyester resins may be as good as that of vinyl ester resins. Polyester resins can also be used for FRP strengthening for structures. However, epoxy resins are preferred at this time for FRP strengthening applications because of their adhesive properties, low shrinkage, and environ- mental durability.

Unsaturated polyester resin is the most widely used resin system for producing industrial and commercial FRP composite material parts. It is referred to as an unsaturated polymer because the double-covalent bonds in its polymer chains are not saturated with hydrogen atoms. By dissolving the polymer in a reactive diluent, typically a styrene monomer, an exothermic free-radical polymerization chain reaction takes place. This polymerization reaction occurs only in the presence of a catalyst, usually peroxide. The reactive styrene is added at concentrations of 20 to 60 parts per hundred of the total resin mix by weight. Based on the type of acid monomer used in the production of the resin, three types of polyester resin, having increasingly better physical and mechanical properties, are produced: orthophthalic, isophthalic, and teraphthalic polyesters. The first unsaturated polyester resin was produced by Ellis and Rust in 1940 (Seymour, 1987).

Epoxy Resins Epoxy resins are used in many FRP products for structural engineering applications. Most carbon fiber–reinforced precured FRP strips for structural strengthening are made with epoxy resins. In addition, epoxy resin adhesives are used to bond precured FRP strips to concrete (and other materials) in the FRP strengthening process. Epoxy resins are also used extensively in FRP strengthening applications, where the epoxy resin is applied to the dry fiber sheet or fabric in the field and then cured in situ, acting as both the matrix for the FRP composite and as the adhesive to attach the FRP composite to the substrate. When applied to dry fiber sheets or fabrics, the epoxy resins are often referred to saturants. Epoxy resins have also been used to manufacture FRP tendons for prestressing concrete and FRP stay cables for bridges. They are not used extensively to produce larger FRP profiles, due to their higher costs and the difficulty entailed in processing large pultruded FRP parts.

An epoxy resin contains one or more epoxide (or oxirane) groups that react with hydroxyl groups. Most common are the reaction products of bisphenol A and epichlorohydrin, called bis A epoxies, or those made from phenol or alkylated phenol and formaldehyde and called novolacs. The resins are cured (or hardened) with amines, acid anhydrides, (Lewis acids) by condensation polymerization and not, like polyesters, by free-radical chain polymerization. The epoxy resin and the curing agent (or hardener) are supplied in two parts and are mixed in specific proportions (usually about 2 to 3 parts to 1 part by weight) just prior to use to cause the curing reaction. The first epoxy resin was produced by Schlack in 1939 (Seymour, 1987).

Epoxy resins are particularly versatile and can be formulated in a range of properties to serve as matrix materials for FRP composites or to serve as adhesives. The epoxies used as the resins in FRP parts for structural engineering belong to the same family as the more familiar epoxies currently used in a variety of structural engineering applications, such as for concrete crack injection, as anchors for concrete, and for bonding precast concrete elements. Epoxy resins are known to have excellent corrosion resistance and to undergo significantly less shrinkage than polyester or vinyl ester resins when cured. Consequently, they are less prone to cracking under thermal loads. Epoxy resins have been developed for high-temperature applications of 180°C (350°F) and higher and have been the thermosetting resins of choice in the aerospace industry for the last 50 years. Epoxies based on bisphenol

Vinylester Resins Developed in the last 20 years, vinyl ester resins have become attractive polymer resins for FRP products for structural engineering due to their good properties, especially their corrosion resistance and their ease of processing (Blankenship et al. 1989). Today, vinyl ester resins are used to make the majority of FRP rebars sold in the world and are also used widely in FRP pultruded profiles. Most manufacturers of pultruded profiles make profiles of identical shapes in both a polyester and a vinyl ester resin series. Vinyl ester resins have also been used to make FRP strengthening strips and FRP rods for near-surface-mounting applications. They are generally replacing polyester resins in FRP products in structural engineering, due to their superior environmental durability in alkaline environments.

A vinyl ester resin is a hybrid of an epoxy and an unsaturated polyester resin and is sometimes referred to as an epoxy vinyl ester resin or a modified epoxy resin. It is an unsaturated polymer that is produced from an epoxy and an acrylic ester monomer. When it is dissolved in styrene, it reacts with the styrene monomer in the same way as an unsaturated polyester does and cures by free-radical chain polymerization with a peroxide catalyst. Consequently, it tends to have many of the desirable physical properties of an epoxy resin and many of the desirable processing properties of a polyester resin. The two major groups of epoxies used to produce vinyl ester resins are bisphenol A and novolac epoxies (Starr, 2000).Vinylester resins can be filled and pigmented. They have densities from 1.05 to 1.10 g / cm3 (0.038 to 0.042 lb / in3) and glass transition temperatures from 40 to 120°C. They can be cured at room temperatures or at elevated temperatures.

Phenolic Resins Phenolic resins are the oldest and most widely used thermosetting resins; however, they have only recently been used for FRP products for structural engineering, due to the difficulty of reinforcing them and curing them by condensation polymerization. They were first developed by Leo Baekeland in the early 1900s and called Bakelite when filled with wood flour (Seymour, 1987). Until the 1980s they had to be cured at high temperatures from 150 to 300°C. They are used extensively in the production of plywood and other engineered wood products. They are being introduced into FRP products for structural engineering because they have superior fire resistance, and they char and release water when burned. They can be filled and reinforced; however, they are difficult to pigment and have a characteristic brownish color.

Polyurethane Resins Thermosetting polyurethane resins have recently been introduced into the

market as structural resins. They were first produced in the 1930s by Otto Bayer and consist of long-chain urethane molecules of isocyanate and hydroxyl-containing molecules. They have been used extensively in their thermoplastic formulation to produce insulation and structural polymer foam materials for decades. Only recently have they been produced in high-density forms that can be used in resin molding and pultrusion operations (Connolly et al., 2005). Polyurethane resins have high toughness and when used with glass fibers produce composites with high transverse tensile and impact strengths. Their cost is approximately the same as that of high-performance vinyl ester resins. Polyurethane resins do not require styrene to polymerize as do unsaturated polyester and vinyl ester resins.

Other Polymer Resins Thermoplastic resin systems such as polyethylene teraphthalate (PET, a saturated polyester), polypropylene, and nylon have been used in a very limited fashion to produce FRP parts for structural engineering. Thermoplastic composites based on polyether ether ketone (PEEK), polyphenylene sulfide (PPS), and polyimide (PI) thermoplastic resins, as well as many others, are being used extensively in the high-temperature aerospace composites market. The attractiveness of using thermoplastic resin systems in structural engineering is due to their ability to be heated, softened, and re- formed, which may give the parts the potential to be joined by a local heating processes, akin to welding of metals. In addition, they are generally less expensive than thermosetting resins and are recyclable. However, they are difficult to process and generally have lower strength and stiffness than thermosets. They do, however, have higher elongations than thermosets (up to 20%), making them tougher and more ductile. A comparison of the properties of thermosetting resins for FRP products for structural engineering is given in Table 2.3. FRP products produced for use in structural engineering can include significantly more ingredients than just the primary constituents: fibers and polymer resins. Fibers are produced with surface coatings called sizing's and are supplied in many different strand and broad good forms. Resins can contain fillers, catalysts, accelerators, hardeners, curing agents, pigments, ultraviolet stabilizers, fire retardants, mold release agents, and other additives. These have different functions, from causing the resin to polymerize to helping the processing to modifying the final properties of the FRP part. These many different supplementary constituents are manufacturing method–dependent and are discussed below.

2.3 Manufacturing Methods

Two main manufacturing methods are used to produce FRP composite material products for use in structural engineering. The one method is an auto- mated industrialized process, developed in the early 1950s, called pultrusion, in which the FRP products are produced in a factory and shipped to the construction site for fabrication and installation or erection. The other method is a manual method, known as hand layup or wet layup, in which the FRP product is manufactured in situ at the construction site at the time it is installed. It is the original method used to produce fiber-reinforced polymer composites and dates back to the development of FRP materials in the 1940s. However, as described below, the hand-layup method as it is used in structural engineering is significantly different from that used in the rest of the com- posites industry.

The pultrusion process is used to manufacturer FRP reinforcing bars, FRP strengthening strips, and FRP profiles and is the most cost-competitive method for producing high-quality FRP parts for use in structural engineering. The hand-layup method is used to manufacture and install dry fiber strengthening sheets and fabrics and is also very cost-competitive, as it is particularly easy to use in the field. Other methods that have been used to produce specialized FRP products for use in structural engineering, such as filament winding and resin transfer molding, are discussed very briefly since code-based design guides for use of these products in structural engineering are either not avail- able or are insufficiently developed at this time.

TABLE 2.3 Approximate Properties of Thermosetting Polymer Resins

	Density [g/cm^3 (lb/in^3)]	Tensile Modulus [GPa (Msi)]	Tensile Strength [MPa (ksi)]	Max. Elongation (%)
Polyester	1.2 (0.043)	4.0 (0.58)	65 (9.4)	2.5
Epoxy	1.2 (0.043)	3.0 (0.44)	90 (13.1)	8.0
Vinylester	1.12 (0.041)	3.5 (0.51)	82 (11.9)	6.0
Phenolic	1.24 (0.045)	2.5 (0.36)	40 (5.8)	1.8
Polyurethane	varies	2.9 (0.42)	71 (10.3)	5.9

2.3.1 Pultrusion

Pultrusion is an automated and continuous process used to produce FRP parts from raw materials. Figure 2.1 shows a photograph of typical FRP pultruded parts used in structural engineering. A pultruded part can have an open cross section, such as a plate or a wide-flange profile; a single closed cross section, such as a hollow tube; or a multicellular cross section, such as panel with internal webs. The cross section does not have to have a constant thickness throughout. Although there is great flexibility in the shape, thickness variation, and size of the part cross section, the cross section must remain constant along its length. In addition, the part must be straight and cannot be cured into a curved shape. A pultruded part can be produced to any desired length, and if it is flexible enough, it can be coiled onto a spool for shipping (such as a thin FRP strip for strengthening or a small-diameter FRP rebar). Modifications to the pultrusion process have been developed for non-constant cross sections or for producing curved parts; however, these are no routine variants of the pultrusion process. In other variants, a core material is used in a cellular part to fill the cavity in the part.

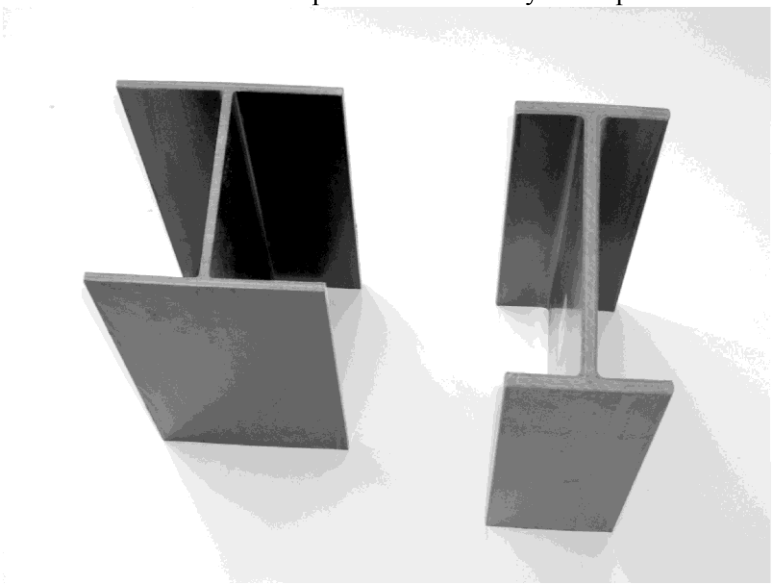

Figure 2.1 Pultruded I-shaped beams.

A pultrusion line or a pultrusion machine is used to produce the pultruded part. The first pultrusion machine, called the Glastruder, was developed by Brandt Goldsworthy in the early 1950s (Goldsworthy, 1954). In 1959, a U.S. patent for a pultrusion machine and the method for producing pultruded parts was awarded to Goldsworthy and Landgraf (1959). Pultrusion machines can now be purchased from a number of companies or can be built from scratch from available off-the-shelf materials and parts. Experienced pultrusion companies tend to develop and build their own pultrusion machines in-house. A schematic of a typical pultrusion line or machine is shown in Fig. 2.2.

To produce FRP parts for structural engineering, dry fibers impregnated with a low-viscosity4 liquid thermosetting polymer resin are guided into a heated chrome-plated steel die, where they are cured to

form the desired FRP part. The FRP is cured as the material is pulled through the die by a pulling apparatus: hence, the name pultrusion. A number of variations of this basic process exist and are described by Meyer (1970). After exiting the die and extending past the pullers, the part is cut to length by a diamond blade cutoff saw. The rate of production of a pultruded part depends on the size of the part. Small round pultruded rods can be produced at rate of up to 60 in. / min, although larger complex multicellular parts can be produced at a rate of only a few inches per minute. As the surface area of the cross section increases, a greater amount of force is needed to overcome the frictional forces to pull the part through the die. Typical pultrusion machines have pulling capacities of 10,000, 20,000, and 40,000 lb (approximately 50, 100, and 200 kN).

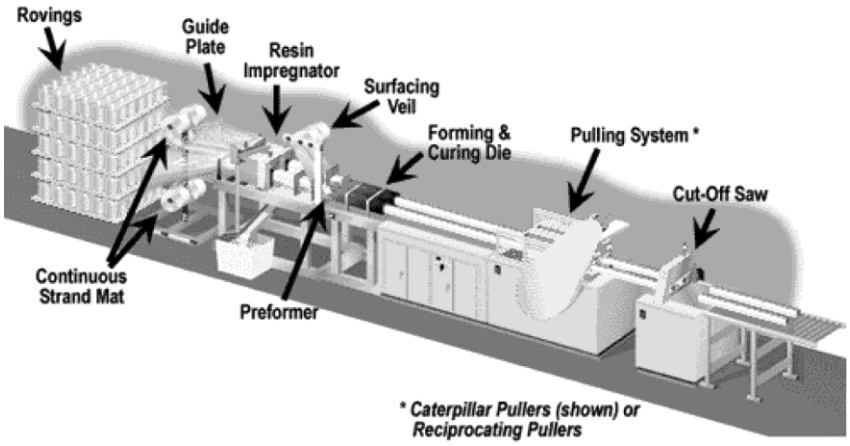

Figure 2.2 Pultrusion line.

The length of the heated steel die used to produce an FRP part is typically from 20 to 40 in. (500 to 1000 mm). The die, which is heated by electric resistance heaters or oil heat, is often heated in two or three separate regions along its length to different temperatures from 200 to 400°F in order to develop the best curing conditions for the type of resin system used in the part. The entrance to the die is typically cooled to prevent pre- mature curing of the resin system. When parts are not required to have a smooth exterior surface, such as a deformed FRP reinforcing bar, a long die is not used. Rather, the impregnated fiber is pulled though a forming ring and is then cured by radiant heat in 6- to 8-ft long cylindrical ovens. The pulling apparatus and the cutoff saw are located downstream of the ovens. When thick parts are pultruded, radio-frequency (RF) heating is frequently used to preheat the resin before the part enters the heated die to assist the curing process.

The dry fiber is supplied in various forms on spools or rolls and is spliced ‘‘on-the-fly’’ to create a never-ending source of fiber. The dry fiber is usually impregnated or wet-out in a resin bath, which is continuously refilled and is usually open to the environment, which is ventilated. Most pultrusion manufacturers run their machines on a 24-hour continuous cycle and do not stop the process until the required lot of the FRP part is produced. Typically, only one operator is needed to oversee the line when it is running smoothly. Setup time for a pultrusion line can take from a few hours to a few days, depending on the complexity of the part, and typically involves two to three operators. Cleanup time for the line usually takes a few hours. Acetone is typically used to clean the parts of the pultrusion line that have been exposed to the polymer resin.

The raw materials that are used in the pultrusion process can be broadly viewed as breaking down into two main systems: the fiber system and the resin system. The fiber system contains all the dry reinforcements that are pulled into the resin system for wetting-out prior to entering the die. The resin system refers to the mix of ingredients that is used to saturate the fibers. The resin system is typically premixed in large batches in a mixing room in a pultrusion plant before it is brought to the pultrusion line and pumped or poured into the resin bath.

Fiber System for Pultrusion The fiber system used in an FRP pultruded part can consist of different types and architectures of fiber materials. The raw fiber is processed and supplied either in strand form on a spool and known as roving or tow, or in broad goods form on a roll and known as mat, fabric, veil, or tissue. The dry fiber is fed into the pultrusion die in a specific arrangement so as to locate the various different fibers and fiber forms in specific parts of the part cross section. High-density polyethylene (HDPE) or Teflon-coated plates with holes and slits or vinyl tubes, through which the individual fiber types pass guide the fibers through the resin bath and into the die. The guides also help to remove excess resin from the resin-saturated fibers before the fibers enter the die mouth. In FRP profiles, individual strands and mats or fabrics are usually laid out in symmetric and balanced alternating layers, giving the pultruded material a laminated or layered internal architecture. Glass and carbon fiber are currently used to reinforce most FRP pultruded parts for structural engineering applications. A very small amount of aramid fiber is used in pultrusion. Glass fiber is used in pultruded profiles due to its low cost. Carbon fiber is used in FRP strengthening strips due to its high modulus. A small number of profiles and strips have been produced with a mixture of glass and carbon fibers to optimize the mechanical properties and costs of the part. These FRP pultruded parts are called hybrids. In addition to the reinforcing fibers, which give the FRP composite its strength and stiff- ness, no reinforcing polyester and glass surfacing mats or veils are used at the surface of the part to aid in processing and to create a smooth surface finish.

Glass Fiber Rovings Individual continuous glass filaments are bundled, generally without a twist, into multifilament strands known as rovings that are used in the pultrusion process either as is or in fabrics produced from roving's. In the United States, roving quantity is traditionally measured in units of yield Roving is produced in yields of 56, 62, 113, 225, 250, 450, 495, 650, and 675. Not all producers manufacture all yields. The number of filaments in an individual roving with a specific yield depends on the fiber diameter of the filament. The most common roving used in pultruded parts is a 113 yield roving, which has approximately 4000 filaments, usually having a diameter of 24 1-m each. Figure 2.3 shows a spool of 113 yield glass fiber roving. In the metric system, roving quantity is measured in units of TEX (g / km). A 113 yield roving is equal to a 4390 TEX roving. Its cross- sectional fiber area is 0.00268 in2 (1.729 mm2).

Rovings are supplied on spools weighing approximately 50 lb (22 kg) each. Typically, tens to hundreds of separate rovings are pulled into a pultruded FRP part. Many large industrial companies manufacture glass fiber roving throughout the world. In 2004, the price of glass fiber roving was about $0.70 per pound ($1.5 per kilogram). In the pultrusion process, the rovings are aligned along the direction of the pultruded part, which is known as the machine direction or lengthwise (LW) direction. In composite mechanics, this direction is known as the longitudinal or zero-degree (0°) direction of the composite material. In structural design, this direction typically coincides with the longitudinal axis of the FRP bar, FRP strip, FRP beam, or FRP column.

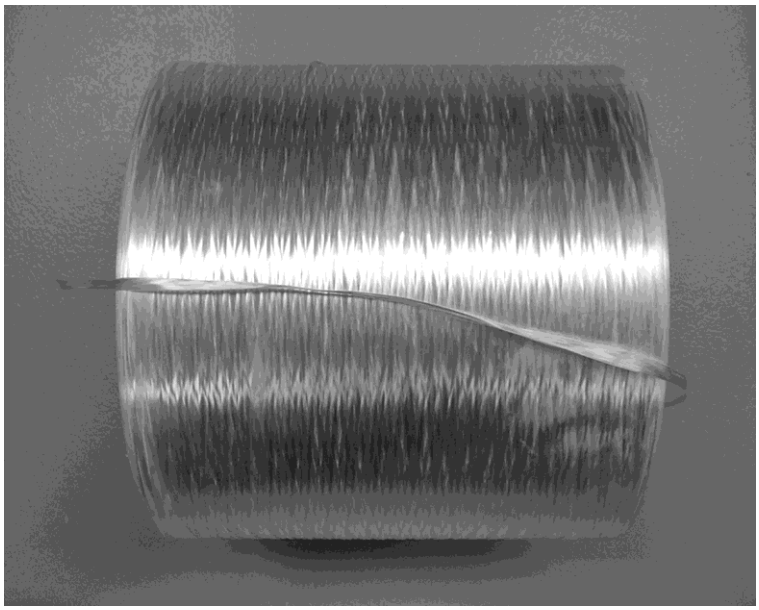

Figure 2.3 113 yield glass roving on a spool.

Consequently, the rovings provide the pultruded part with the majority of its axial and flexural strength and stiffness. For parts requiring only high longitudinal strength and stiffness, such as FRP reinforcing bars or thin FRP strengthening strips, high percentages of rovings on the order of 50 to 60% of the total volume of the FRP composite are used. However, such parts have low crosswise (CW) or transverse strength and stiffness. To develop transverse strength and stiffness in a pultruded part, fiber mats and fabrics are used in addition to the rovings. The polymer resin is typically relied on to provide the out-of-plane and transverse shear properties of the pultruded material. When producing tubular parts, glass fiber roving can also be wound in the circumferential direction around the tube to provide an outer layer of hoop reinforcement. Three-dimensional fiber reinforcement preforms for pultrusion that can give out-of-plane, or through-the-thickness, strength and stiffness are not used in regular parts, and a typical pultruded part has a plate like layered structure with alternating layers of roving and mats or fabrics through the plate thickness.

In the pultrusion operation, the roving spools are stacked on metal racks called creels. Creel racks should be metal and grounded to prevent electro- static charge buildup during production. The roving is pulled off the individual spools and guided into the resin bath, where it is saturated with liquid resin (also known as wet-out). The roving is usually the first fiber reinforcement material to be wet-out. It is important to ensure that the roving bundles do not bunch together in the resin bath, as this can lead to rovings not being fully wet-out, which will lead to dry-fiber areas in the finished product, which is highly undesirable.

Glass Fiber Mats Continuous filament mat (CFM), also referred to in the United States as continuous strand mat, is the second most widely employed glass fiber product used in the pultrusion industry. CFM is used to provide crosswise (CW) or transverse strength and stiffness in plate like parts or portions of parts (e.g., the flange of a wide-flange profile). CFMs consist of random, swirled, indefinitely long continuous glass fiber filaments held together by a resin-soluble polymeric binder. They are different from copped strand mats (CSMs), which consist of short [1 to 2 in. (25 to 50 mm)] fibers held together in mat form by a resin-soluble binder 6 which are used mainly in sheet molding compounds. Because of the pulling forces exerted on the mats in the pultrusion processes, chopped stand mats are generally not suit- able for pultrusion except when used together with a preformed combination fabric system (these fabrics are discussed below). Continuous filament mats also help to keep the individual rovings in position as they move through the die. Due to the random orientation of the fibers in the plane of the continuous mat, the mat, and hence the layer of the cured pultruded material that contains the mat, can be assumed to have equal properties in all directions in its plane.

In the pultrusion operation, the CFM is typically wet-out after the rovings. A hose, funnel, or chute may be used to pour the liquid resin directly onto the mat surface as it is fed through guides. When the mat is light, it is often simply wet-out by the excess resin that is carried by the rovings into the forming guides. When the saturated mat and rovings enter the die, they are squeezed into the die opening. This squeezing produces an internal die pressure of around 80 psi. The pressure tends to compress the mat layers. Figure 2.5 shows an E-glass CFM.

Glass Fiber Fabrics Since unidirectional rovings give the pultruded com- posite reinforcement in its longitudinal direction, and the continuous stand mats give reinforcement in all in-plane directions equally (i.e., isotropically), the range of mechanical properties of the pultruded composite consisting of only rovings and mats is limited. To obtain a greater range of properties and to ‘‘tailor’’ the layup (or the fiber architecture) of the pultruded composite to yield specific structural properties, fabric reinforcements can be used in which fibers are oriented in specific directions and at specific volume percentages to the pultrusion axis.

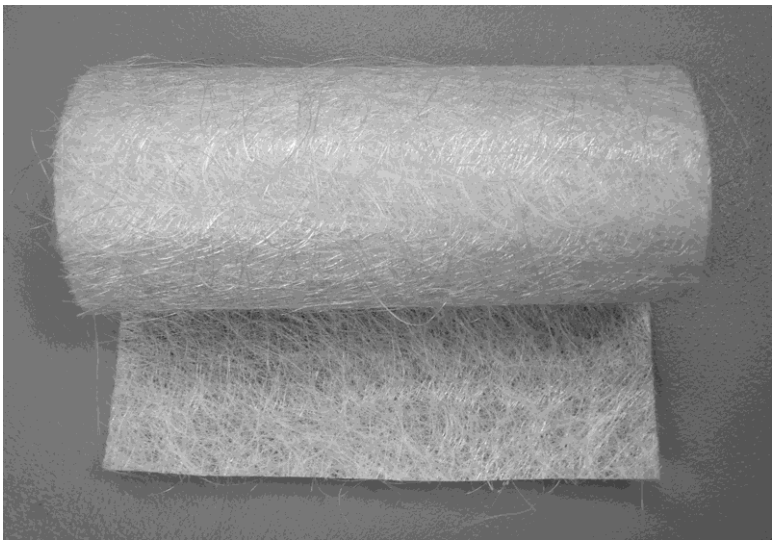

Figure 2.4 1.5-oz/ft^2 E-glass continuous filament mat.

This design approach, in which multiaxial plies (or layers) are used, is routine in the hand-layup technique; however, it is only in recent years that multiaxial fabrics have been used successfully in the pultrusion process. This is because pulling an off-axis ply (say, one with a 45° orientation to the pultrusion direction) is a nontrivial matter and special preformed fabrics are needed that can be pulled without causing distortion of the fiber orientations. Although now available, multiaxial fabrics are still used only in very special pultruded parts, as their costs can be considerably more than that of mats. They are not as easy to wet-out and pull as rovings and CFMs. It is, however, generally recognized in the composites industry that to optimize the mechanical properties of pultruded profiles for structural engineering, the next generation of profiles will need to use more multiaxial fabrics, possibly with hybrid fiber types, and have more sophisticated cross- sectional shapes. The recent double-web beam produced by Strongwell, shown in Fig. 2.5, is an example of such a engineered hybrid profile developed for bridge girders.

Glass fiber fabric materials for pultrusion are generally of two types. One type is a woven roving fabric; the other type is a stitched roving fabric. Woven roving is used routinely in hand-layup applications such as boat building and is supplied in weights between 200 to 1600 g/m^2 and has fiber orientations of 0° and 90°. The percentage of 0° and 90° fibers [known as the *warp* and the *weft* directions in the textile industry] depends on the weave pattern. Most woven fabrics made for use in pultrusion are of the plain or square pattern, with almost equal percentages of fibers in the two directions.

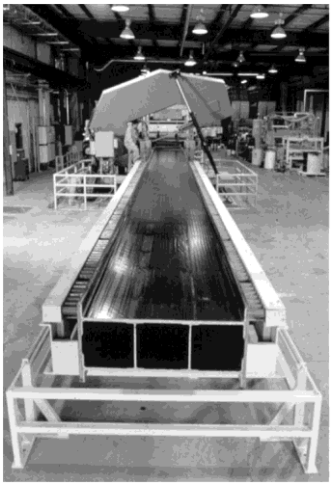

Figure 2.5 Double-web hybrid fiber pultruded beams.

To use a woven roving in a pultrusion process, it needs to be attached to a glass mat (usually, a chopped strand mat) to prevent it from distorting when pulled. Powder bonding, stitching with a polyester or glass yarn, or needling are used to attach the woven fabric to the mat, which is then known as a combination fabric. Many different combinations of woven roving weights and mat weights are available. Commonly used types are 18- oz/ yd2 woven roving with a 1-oz / ft2 mat.

The other type of fabric type that is used in pultrusion is a stitched fabric where the unidirectional layers of rovings in different directions are stitched together with or without a chopped mat. Popular types of stitched fabrics are biaxial (having equal percentages of 0° and 90° or +45° and -45° fiber orientations) and triaxial (having fibers in the 0°, +45°, and -45° fiber orientations). +45° and -45° fiber orientations are used to give a pultruded part high in-plane shear strength and stiffness properties. Unidirectional stitched fabrics in which the fibers in one direction are stitched to a mat can also be obtained. These are particularly useful when 90° fiber orientation is needed in a pultruded part to give it high transverse strength and stiffness. For unique applications, unbalanced stitched fabrics can be obtained. As noted previously, it is important to ensure that the resulting layup is both symmetric and balanced when using stitched and combination-stitched fabrics.

Resin System for Pultrusion The three main thermosetting resins used in the pultrusion process are unsaturated polyesters, unsaturated vinyl esters, and epoxies. To each of these base resins supplementary constituents are added to cause the polymerization reaction to occur, to modify the processing variables, and to tailor the properties of the final FRP pultruded part. The additional constituents that are added can be broadly grouped into three main categories: polymerization agents, fillers, and additives. Polymerization agents are known as either catalysts or curing agents (or even hardeners), depending on the resin type being used. Fillers are sometimes called extenders. Additives are also known as modifiers or process aids. Examples of some sample pultrusion resin systems, with trade names and precise quantities of the various constituents used, can be found in Meyer (1985) and Starr (2000). Most pultruders regard their mixes as proprietary and therefore usually do not openly publicize the exact details of their resin systems. Resin systems are typically developed by a pultrusion company in collaboration with a resin manufacturer.

Polymerization Agents Unsaturated polyester and vinyl ester resins that react with a styrene monomer are catalyzed with organic peroxides. The peroxide is used to ‘‘kick-off’’ or initiate the curing reaction and is heat-activated by the die so that the resin does not begin to gel and cure in the resin bath.10 Different catalysts are chosen to cause the polymerization processes to occur at a controlled time and

lengthwise position in the pultrusion die. They are referred to as kicker peroxides, medium-reactivity peroxides, and finishing peroxides (Starr, 2000). Peroxides are added in quantities of between 0.25 and 1.5% by weight of the resin and are given as parts per hundred (pph) by weight. It is also not uncommon for additional styrene monomer to be added to the base resin (also known as the neat resin) during the resin mixing operation. Ten to 15% by weight can be added to aid in processing (it decreases the resin viscosity) and to decrease costs. However, the quantity of styrene in the resin mix must be carefully controlled, as unreacted styrene in the cured part can lead to a part with poor environmental durability. Blended polyester and vinyl ester resins are also used in pultrusion to exploit beneficial processing and property characteristics of each resin type.

Epoxy resins used in pultrusion are polymerized by the addition of curing agents, typically of the amine type. The curing agent or hardener is usually referred to as part B, and the epoxy resin is referred to as part A. Curing agents are generally added at ratios of 25 to 50% by weight of the epoxy resin. Curing agent accelerators may also be used in small percentages (less than 1% by weight). Epoxy resins are significantly more difficult to pultruded than polyester or vinyl ester resins because of their lower shrinkage, higher viscosity, and longer gel times (Starr, 2000). Because of this, the pultrusion line is usually slower and requires more pulling force when an epoxy resin is used. Specially formulated epoxies that cure only at high temperatures are also required. Limited epoxy formulations are used in pultrusion. Epoxies are used where significant mechanical or physical property advantages can be obtained. At this time, no routinely produced standard FRP profile shapes are made with epoxy resin systems; however, most pultruded FRP strengthening strips are produced with epoxy resins.

Fillers Inorganic particulate fillers are used to fill or ‘‘extend’’ the base polymer resin used for pultrusion for three primary reasons: to improve processing dynamics, to reduce cost, and to alter cured part properties (Lackey and Vaughan, 2002). Inorganic fillers have particle sizes between 0.5 and 8 1-m and can have spherical or plate like geometries. The three primary types of inorganic fillers used in pultrusion are kaolin clay (aluminum silicate), calcium carbonate, and alumina trihydrate (ATH). Typical polyester and vinylester pultruded FRP profiles shapes and FRP rebars have between 10 and 30% by weight of filler in the resin mix. Small pultruded parts having primarily unidirectional roving reinforcement usually have low filler percentages, from no filler to 5% by weight. Epoxy resin pultrusions can also be filled. Small parts such as FRP strengthening strips are generally not filled. The density of the inorganic fillers is between 2.4 and 2.6 g / cm3 (0.0865 to 0.0937 lb / in3), making it approximately equal to glass fiber and about twice the density of the resin. Fillers are substantially less costly than either resins or fibers. In addition to serving as a filler, alumina trihydrate serves a dual role as a fire-retardant additive. Fillers usually decrease the key longitudinal mechanical properties and the corrosion resistance of an FRP pultruded part (Lackey et al., 1999). However, fillers can be used to improve properties, especially in the transverse direction and to modify the physical properties (Meyer, 1985) of an FRP pultruded part. Recently, pultruders have begun to experiment with nanosized particle fillers, and results show FRP parts with greater corrosion resistance.

Additives the third groups of constituents that are added to the resin mix are those used to assist in the processing or to modify the properties of the cured FRP part (Lackey and Vaughan, 2002). Chemical release agents, typically metallic stearates, fatty acids, or waxes, are used to prevent the FRP part from sticking to the die interior. A foaming agent is often used to remove entrained air from the resin mix. Pigments, or colorants, are mixed in the resin to give the finished part different colors. Ultraviolet stabilizers are added to protect the resin in the cured part from the effects of sunlight. Additives that retard flame spread in the cured FRP part, such as antimony trioxide, may be added to FRP profiles to meet code-stipulated fire and flammability ratings.[12] In addition, thickening agents, toughening agents, and viscosity control agents may be used to modify the characteristics of the resin mix. These additives are generally added in quantities less than 1% by weight of the resin. The one additive that is often added in a significantly higher percentage is a low- profile or shrink additive. Low-profile additives are usually thermoplastic polymer materials and are added to the mix to prevent shrinkage cracking in the interior of thick parts and at the surface

of thin parts. Silane coupling agents may be added to the resin mix to improve the bond between the fibers and the resin; however, these coupling agents are usually in the sizing on the fiber itself. It is important to note that all of these additives can influence both the physical and mechanical properties of the FRP part since they all affect the resin chemistry (Lackey and Vaughan, 2002). Even a seemingly innocuous additive such as a pigment can have a significant effect on properties, and changing the color of a FRP pultruded part is not necessarily a trivial matter.

4 Progressive failure analysis

4.1 Bolted Pultruded Connections

The vast majority of light-truss and heavy-frame pultruded connections in load-bearing pultruded structures that are made with mechanical fasteners use bolted connections with either steel (typically, galvanized or stainless) or FRP fastener hardware. As noted previously, adhesive bonding may be used in addition to the bolting but is very rarely used as the sole means of making a pultruded truss or frame connection. There are many reasons for using bolted connections in pultruded structures:

1. The fabrication of the individual connection parts and the profiles to be connected is relatively easy and is generally familiar to construction workers skilled in steel and wood frame construction.
2. The connection is easy to assemble in the field or in the shop, and no surface preparation of the base materials is required (as in the case of adhesive bonding).
3. The connections are easy to inspect after assembly.
4. The connection can be assembled quickly and achieve its full strength and stiffness immediately (as opposed to an adhesively bonded connection).
5. If no adhesive is used in addition to the bolting, the connection can be disassembled easily if necessary.
6. Bolted connections can be economical when the cost of both shop and field labor work is taken into account. In the United States, fabrication of drilled holes in pultruded materials can be quite costly and is generally in the order of $1 per hole.
7. Specified manufacturing tolerances (out-of-straightness and twist) in pultruded profiles can be accommodated since the connection parts can usually be worked into place, due to their low stiffness.
8. Minor misfits due to bolt hole sizes or locations can usually be fixed in the field using simple hand tools.

However, there are also a number of issues to consider when using bolted connections in pultruded structures:

1. The bolt holes cause stress concentrations and reduce the net section in the pultruded material and thereby reduce the efficiency of the connection. In addition, the load on fastener groups does not typically dis- tribute evenly to multiple rows of bolts as in steel-bolted connections.
2. The pultruded parts used in the connection are made of orthotropic materials, and therefore the orientation of the individual parts in the connection is critical, unlike in steel-bolted connections, where the base material is isotropic and not orientation dependent. This is particularly relevant for the pultruded angles used in beam-to-column connections, where the major fiber orientation is often placed perpendicular to the primary load direction
3. Conventional glass pultruded materials have low through-the-thickness stiffness and strength properties and can therefore be crushed if high bolt torques are used. Since the base material can creep, the bolt tension can decrease over time, due to strain relaxation. If FRP bolts are used, the bolts themselves will lose tension due to strain relaxation. In addition, if small nuts (without washers) are used, the entire fastener can punch through or crush the base pultruded material when the connection is loaded. For this reason, only bearing connections are used in pultruded bolted connections, and slip-critical or friction connections are not possible in pultruded connections.
4. There is limited availability of FRP nuts and bolts or threaded rods sizes, and no FRP

parts are available that have unthreaded shanks such that material will bear on the threaded portion of the fastener, which is undesirable. Since the threads are machined into FRP bolts and threaded rods, they have a tendency to strip-off under bolt shear loads, and thus the tensile capacity of the FRP bolt is quite limited.

5. There is limited availability of pultruded angle thicknessesand sizes (2 to 6 in leg equal angles) used in typical beam-to-column.
6. The properties of pultruded plate material used for connection gusset plates and miscellaneous filler parts are typically less than the properties of the pultruded profiles in the connection.
7. Holes drilled in the pultruded material for a bolted connection provide a pathway for ingress of moisture and other chemical agents that can degrade the pultruded material. Therefore, all drilled holes in pultruded materials must be sealed with a thin epoxy resin coating. This is typi- cally done in the shop after the parts are drilled.
8. Holes in pultruded material must be drilled, preferably using special diamond-tipped bits. Holes cannot be punched like steel parts, due to the properties of the pultruded materials.

Bolted pultruded connections can fail in significantly different ways from steel connections even though the connection geometries may look similar. Pultruded connections can fail due to failure in the pultruded material of the members being connected, in the pultruded material of the pultruded connection parts (angles and gussets), or in the mechanical fasteners themselves (the bolts, nuts, rods, and washers). FRP bolts or threaded rods can fail in transverse shear, in longitudinal shear due to thread stripping, and in longitudinal tension or compression. FRP nuts can fail due to longitudinal thread shear. The pultruded material in the connected members or in the parts can fail due to in-plane or out-of- plane loads or a combination of the two, depending on the type of pultruded connection. Bolted connections are used for both light-truss and heavy-frame pultruded connections, as noted previously; however, different considerations apply in their design, which are due primarily to the types of forces and eccentricities of the fasteners relative to the centerline of the members being connected.

4.2 Lap Joint Connections

In the studies referred to above, the researchers have investigated the influences of pultruded material orientation, fastener size, bolt torque, pultruded plate thickness, bolt spacing, washer presence and size, and single- and multibolt configurations on connection failure modes and capacities. Most of these data, together with more recent test results, has been assembled by Mottram and Turvey (2003) in a comprehensive review to that date. Recommendations for lap joint connection geometries and equations for checking different elementary failure modes, based on the research cited above, are presented in what follows. The failure modes of single-bolt lap joints are usually identified as net- tension failure, shear-out failure, splitting (also called *cleavage*) failure, cleavage (also called *block shear*) failure, and bearing failure. These are shown graphically in Fig. 4.1 . It is important to recognize that these failure modes are expected to occur in FRP plates with unidirectional, bidirectional, or quasi-isotropic layups and are not necessarily applicable to conventional pultruded materials unless they are loaded at either 0° or 90° (i.e., parallel to transverse to the pultrusion direction).

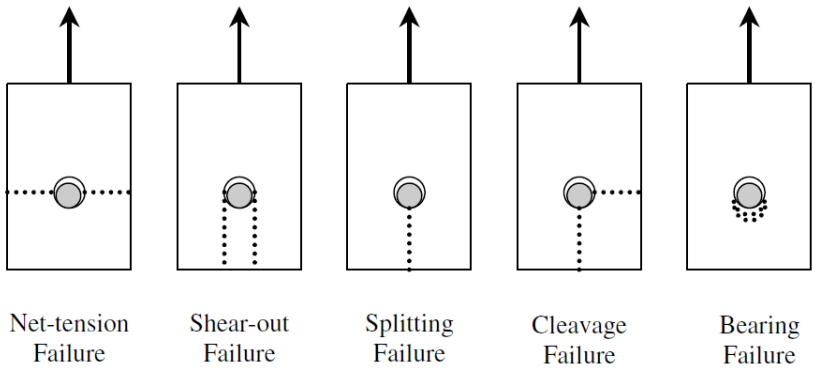

Figure 4.1 Failure modes of single-bolt lap joint in plane connections

If a pultruded material is loaded in an off-axis orientation (such as the chord of the truss shown in Fig. 3.2) the failure will typically occur in combined net tension and shear along a plane that is parallel to the roving orientation.

In this case, detailing recommendations based on assuming the failure modes shown above may not be appropriate. Therefore, a designer should attempt to place the longitudinal direction of the pultruded part used in the connection either parallel (preferably) or perpendicular to the load, or conduct tests of the pul- truded material (or profile) loaded in the direction of interest.

A review of the extensive research data obtained for pultruded plate materials has led to recommendations, shown in Table 3.1, for spacing and edge distances for lap joints in pultruded connections made of conventional glass FRP pultruded plate loaded by in-plane loads in tension. These recommendations apply to structures in operating environments of normal room temperature and humidity.

TABLE 3.1 Recommended Geometric Parameters for Lap Joint Connections

	Research Data		Manufacturer[a]	
	Recommended	Minimum	Recommended	Minimum
End[b] distance to bolt diameter, e/d_b	≥ 3	2	≥ 3	2
Plate width to bolt diameter, w/d_b	≥ 5	3	≥ 4	3
Side distance to bolt diameter, s/d_b	≥ 2	1.5	≥ 2	1.5
Longitudinal spacing (pitch) to bolt diameter, p/d_b	≥ 4	3	≥ 5	4
Transverse spacing (gage) to bolt diameter, g/d_b	≥ 4	3	≥ 5	4
Bolt diameter to plate thickness, d_b/t_{pl}	≥ 1	0.5	2	1
Washer diameter to bolt diameter, d_w/d_b	≥ 2	2	NR	NR
Hole size clearance, $d_h - d_b$	tight fit ($0.05d_b$)	$\frac{1}{16}$ in.[c]	$\frac{1}{16}$ in.	NA

It is important to note that these recommendations were obtained from testing pultruded plate (flat sheet), which has properties that differ from those of the pultruded material in conventional profiles

It is important to note that the geometric design recommendations pre- sented above are for lap joints loaded in tension. The geometric recommen- dations are intended to cause bearing failure in

the pultruded base material at the locations of the fasteners when the material is loaded in the longitudinal direction, and to avoid net-tension or cleavage failure modes, which are brittle failures modes. However, this is generally true only for single-bolt joints. Bearing failure is regarded as a ductile failure mode and consists of local crushing and delamination of the pultruded material in direct contact with the bolt. As the lap joint continues to be displaced longitudinally, the bearing failure can become a shear-out failure. Shear-out failure can occur either be- tween the bolt and the part end, or between fasteners in a column of bolts parallel to the load direction. If the end distance (or the longitudinal spacing) is sufficiently long (e.g., $e/d_b > 5$), this failure can also be a progressive pseudoductile failure mode in pultruded materials.

4.3 Heavy Frame pultruded connections

In heavy-frame connections, the connection parts used to connect the mem- bers, which are usually at right angles, are eccentrically located with respect to the centroid of the members being connected. As a result, the connection parts are subjected to loads that are offset from, or eccentric to, the line of the fasteners. This causes a localized bending moment to develop in the plane of the web, in addition to the in-plane loads that occur in lap joint connections seen in light trusses. For the in-plane component of the forces, the same discussion and the guidance cited previously for lap joints is applicable to the parts of the heavy pultruded connection that carry in-plane loads

The moment causes out-of-plane forces to develop at the face of the connected members which generate prying forces at the top and compressive forces at the bottom of the connection. For example, a web clip subjected to a bending moment causes the top of the clip to pull away, or pry away, from the column flange, and the bottom part of the clip angle to be compressed into the flange of the column This eventually leads to the failure of the clip angle, due to delamination due to tensile and flexural stresses at the top of the angle.

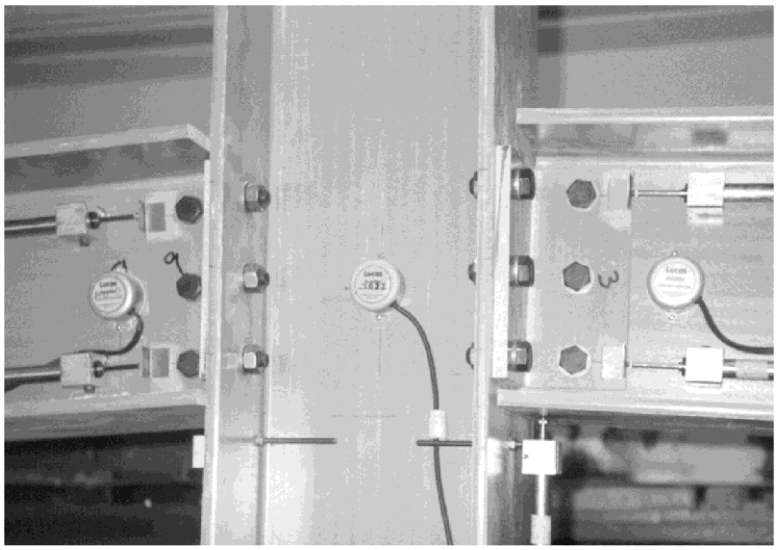

Figure 4.2 Out-of-plane forces in clip angle simple shear beam-to-column connections.

4.4 Progressive damage analysis

This analysis in usually used to measure the nonlinear behavior of the composite materials due to threw evolution of the damage. A simple scheme to illustrate the steps of the analysis could be:

1 Build the FEM model
2 Increase the loading
3 Solution

4 Control of the damage, based in the failure criterion
   4.1) If isn't damage follow step 2
   4.2) If is damage follow step 5
5 Application of a damage law of the elastic properties of the material
5 Follow step 3

4.5 Laminate Strength Analyses

The failure criteria previously described deal with lamina failure. In order to predict laminate strength, the progressive accumulation of damage leading to final failure needs to be taken into account. Clearly, this is a difficult task, since failure mechanisms in laminates are a great deal more complicated than those in a unidirectional composite under in-plane loading. New damage mechanisms, such as delamination, and complex interactions between intralaminar and interlaminar damage mechanisms may occur in a laminate. The effects of delamination are usually treated separately from intralaminar damage mechanisms, although recent work has taken into consideration all the damage mechanisms in the failure analysis of a skin-stiffener composite structure. Experimental evidence has shown that the failure in a laminated composite is very often progressive in nature, occurring by a process of damage accumulation. Therefore, the progressive loss of lamina stiffness must be taken into account as a function of the type of damage predicted. The typical procedure to predict the strength of a laminate when intralaminar damage mechanisms are dominant is:

1. Lamina strain and stress analyses.
2. Lamina failure criteria.
3. Stiffness degradation models (as a function of type of failure predicted at lamina level).
4. Laminate failure criterion.

The stiffness degradation (point 3) is usually performed using a reduction of ply elastic properties, typically reducing E1 for fiber failures and both E2 and G12 for matrix transverse of shear cracking [25]-[26]. This reduction may be sudden [25] or progressive [26]. For transverse matrix cracking, the progressive degradation of elastic properties has a good physical basis, since it represents the progressive accumulation of transverse cracks until the crack density saturation (CDS) is achieved. The reduction of the transverse elastic properties can also be a function of the stress state [25]. This consideration is also reasonable, since a matrix crack under compressive stresses can still carry some load. A number of procedures have been proposed to determine ultimate laminate failure (point 4). A common procedure is to assume ultimate laminate failure when fiber fracture occurs in any lamina. This procedure is inadequate when stress concentrations are present, like in access holes and bolted joints, since localized fiber fracture, actually relieving stress concentrations, occur without laminate failure [27]. Furthermore, in matrix dominated laminates, such as $(\pm 45^{o})s$ laminates, failure may occur without fiber fracture. It is then clear that the guidelines for implementation of lamina failure criteria should be based on a study taking into account no only lamina failure criteria, but also stiffness degradation models and laminate failure criterion.

4.6 Delamination

Delamination is one of the predominant forms of failure in laminated composites due to the lack of reinforcement in the thickness direction. Delamination as a result of impact or a manufacturing defect can cause significant reductions in the compressive load-carrying capacity and bending stiffness of a structure. The stress gradients that occur near geometric discontinuities such as ply drop-offs, stiffener terminations and flanges, bonded and bolted joints, and access holes promote delamination initiation, trigger intralaminar damage mechanisms, and may cause a significant loss of structural integrity. Without including the delamination failure mode, the predictive capabilities of progressive failure analyses will remain limited The analysis of delamination is commonly divided into the study of the initiation and the analysis of the propagation of an already initiated area. Delamination initiation analysis is usually based on stresses and use of criteria such as the quadratic interaction of the interlaminar stresses in conjunction with a characteristic distance [30]. This distance is a function of

specimen geometry and material properties, and its determination always requires extensive testing. Delamination propagation, on the other hand, is usually predicted using Fracture Mechanics. The Fracture Mechanics approach avoids the difficulties associated with the stress singularity at a crack front. Two main approaches have been proposed:

The virtual crack closure technique (VCCT), based on the assumption that when a crack extends by a small amount, the energy absorbed in the process is equal to the work required to close the crack to its original length. The use of decohesion finite elements placed between the composite material layers. Decohesion elements combine a stress based formulation with a Fracture Mechanics based formulation and are used to define the non-linear constitutive law of the material at the interface between laminar. This approach has been used to simulate delamination onset and growth in laminated composites.

4.7 Maximum Stress Failure Criterion

Perhaps the most widely used failure criterion for unidirectional composites is the maximum stress failure criterion (Tsai, 1987; Nahas, 1986), which predicts that a material will fail when the magnitude of the stress in any direction exceeds its corresponding allowable level in that direction. This criterion is valid for both isotropic and anisotropic materials. However, it does not consider interactions between the various stress components and, therefore, has the potential to be inaccurate for multi-axial stress states. The most significant advantage of this failure criterion is that it identifies the specific mode of failure within a ply. Failure in any principal direction of the material is predicted when any of the following conditions exist:

if $\sigma1>0$ and if $\sigma1>$XlT, then the failure mode is fiber tension.
if $\sigma1<0$ and if $|\sigma1|>$XlC, then the failure mode is fiber compression.
if $\sigma2>0$ and if $\sigma2>$X2T, then the failure mode is matrix tension.
if $\sigma2<0$ and if $|\sigma2|>$X2C, then the failure mode is matrix compression.
if $\sigma3>0$ and if $\sigma3>$X3T, then the failure mode is matrix tension.
if $\sigma3<0$ and if $|\sigma3|>$X3C, then the failure mode is matrix compression.
if $|\sigma4| >$ X23, then the failure mode is interlaminar shear.
if $|\sigma5| >$ X13, then the failure mode is interlaminar shear.
if $|\sigma6| >$ X12, then the failure mode is in-plane shear.

In Equations, $\sigma1$ through $\sigma6$, are the six principal ply stresses, XlT is the tensile strength in the 1-direction (longitudinal), XlC is the compressive strength in the l-direction, X2T is the tensile strength in the 2-direction (transverse), X2C is the compressive strength in the 2-direction, X3T is the tensile strength in the 3-direction, X3C is the compressive strength in the 3-direction, X23 is the shear strength in the 23-plane, Xl3 is the shear strength in the 13-plane, and Xl2 is the shear strength in the 12-plane

4.7 Puck failure Theory

The Puck criterion identifies fiber failure and inter-fiber failure in a unidirectional composite.The Puck criterion also separates fiber failure into two different physical modes. To use the Puck failure criterion, you must specify two pieces of information.

-Composite Material Type: Either a carbon fiber reinforced polymer (CFRP) or a glass fiber reinforced polymer (GFRP) must be specified.

-Selected Fiber Properties: Longitudinal modulus, Longitudinal Poisson ratio.

4.8.1Fiber Failure

The Puck criterion recognizes two different modes of fiber failure, the first being a tensile failure, and the second being a compressive "fiber kinking" failure. The tensile fiber failure criterion is

$$\frac{1}{\epsilon_{1T}}\left(\epsilon_1 + \frac{\nu_{f12}}{E_{f1}} m_{\sigma f} \sigma_2\right) = 1 \quad ,$$

and the compressive "fiber kinking" failure is

$$\frac{1}{\epsilon_{1C}}\left|\left(\epsilon_1 + \frac{\nu_{f12}}{E_{f1}} m_{\sigma f} \sigma_2\right)\right| = 1 - (10\gamma_{21})^2 \quad .$$

In the above fiber failure criteria:

$$\epsilon_{1T}\, \epsilon_{1C}$$

Composite strains corresponding to composite longitudinal tensile and compressive failure, respectively.

$$\epsilon_1$$

Uniaxial strain in the composite.

$$\nu_{f12}$$

Longitudinal Poisson ratio of the fiber.

$$E_{f1}$$

Longitudinal tensile modulus of the fiber.

$$\sigma_2$$

Transverse stress of the composite.

$$\gamma_{21}$$

Longitudinal shear strain in the composite.

$$m_{\sigma f}$$

4.8.2 Inter-Fiber Failure (Matrix Cracking)

In the Puck criterion, inter-fiber failure encompasses any matrix cracking or fiber/matrix debonding. The Puck criterion recognizes three different inter-fiber failure modes, referred to as modes A, B, and C. These inter-fiber failure modes are distinguished by the orientation of the fracture planes relative to the reinforcing fibers.

4.8.3 Inter-Fiber Failure Mode A:

Mode A corresponds to a fracture angle of 0°. The criterion is invoked if the transverse stress in the composite is greater than 0 (thus indicating a transverse crack perpendicular to the transverse loading).

$$\sqrt{\left(\frac{\tau_{21}}{S_{21}}\right)^2 + \left(1 - p_{\perp\parallel}^{(+)} \frac{Y_T}{S_{21}}\right)^2 \left(\frac{\sigma_2}{Y_T}\right)^2} + p_{\perp\parallel}^{(+)} \frac{\sigma_2}{S_{21}} = 1 - \left|\frac{\sigma_1}{\sigma_{1D}}\right| \quad .$$

4.8.4 Inter-Fiber Failure Mode B:

Mode B corresponds to a transverse compressive stress (inhibiting crack formation) with a longitudinal shear stress which is below a fracture resistance (coupled with empirical constants).

$$\frac{1}{S_{21}}\left(\sqrt{{\tau_{21}}^2 + \left(p_{\perp\parallel}^{(-)} \sigma_2\right)^2} + p_{\perp\parallel}^{(-)} \frac{\sigma_2}{S_{21}}\right) = 1 - \left|\frac{\sigma_1}{\sigma_{1D}}\right| \quad .$$

The above criterion is evaluated if

$$\sigma_2 < 0 \;\; and \;\; 0 \leq \left|\frac{\sigma_2}{\tau_{21}}\right| \leq \frac{R_{\perp\perp}^A}{|\tau_{21C}|} \quad .$$

4.8.5 Inter-Fiber Failure Mode C:

Mode C corresponds to a transverse compressive stress (inhibiting crack formation) with a longitudinal shear stress which is significantly large enough to cause fracture on an inclined plane to fiber axis. The failure criterion for Mode C is

$$\frac{1}{\left(2\left(1+p_{\perp\perp}^{(-)}\right)\right)}\left(\left(\frac{\tau_{21}}{S_{21}}\right)^2+\left(\frac{\sigma_2}{R_{\perp\perp}^A}\right)^2\right)\frac{R_{\perp\perp}^A}{(-\sigma_2)} = 1 - \left|\frac{\sigma_1}{\sigma_{1D}}\right| \quad .$$

The above criterion is evaluated if

$$\sigma_2 < 0 \;\; and \;\; 0 \leq \left|\frac{\tau_{21}}{\sigma_2}\right| \leq \frac{|\tau_{21C}|}{R_{\perp\perp}^A} \quad .$$

4.8.6 Description of Coefficients and Terms Used in the Inter-Fiber Failure Criteria

In the discussion that follows:

Y_T

Composite transverse tensile strength.

Y_C

Transverse compressive strength.

$p_{\perp\parallel}^{(-)} \;\; p_{\perp\parallel}^{(+)}$

Slopes of the (σ_2, τ_{21}) fracture envelope.

To establish a connection between $p_{\perp\perp}^{(-)}$ and $p_{\perp\parallel}^{(-)}$, it is assumed the following relationship holds

$$\frac{p_{\perp\perp}^{(-)}}{R_{\perp\perp}^A} = \frac{p_{\perp\parallel}^{(+)}}{R_{\perp\parallel}^A} = \left(\frac{p}{R}\right) = const \quad .$$

Therefore, $p_{\perp\perp}^{(-)}$ is given by

$$p_{\perp\perp}^{(-)} = R_{\perp\perp}^A \frac{p_{\perp\parallel}^{(+)}}{R_{\perp\parallel}^A} \quad .$$

where $R_{\perp\parallel}^A$ is assumed to be the same as S_{21}, which allows $R_{\perp\perp}^A$ to be expressed as

$$R_{\perp\perp}^A = \frac{S_{21}}{2p_{\perp\parallel}^{(-)}}\left(\sqrt{1+2p_{\perp\parallel}^{(-)}\frac{Y_C}{S_{21}}}-1\right) \quad .$$

$$\tau_{21c} = S_{21}\sqrt{1+2p_{\perp\parallel}^{(-)}} \quad .$$

Finally, we must define σ_{1D}. This is a "degraded" stress in the composite allowing for pre-fiber failure breakage of individual fibers, which causes localized damage in these areas in the form of microcracking and debonding. To account for this weakening effect, Puck degrades the fracture resistances (R) by a weakening factor f_w. Puck defines two equations for this. The first is for the generalized weakening factor.

$$f_w = 1 - \left(\frac{\sigma_1}{\sigma_{1d}}\right)^n \quad .$$

The second is to give another expression of the weakening factor to keep the fracture conditions homogeneous and of first degree with respect to the stresses.

$$f_w = 1 - \frac{\sigma_1}{\sigma_{1D}} \quad .$$

The Simulation Composite Analysis implementation of the Puck criterion utilizes only the in-plane stress components of the 3-D stress state. In this case, the two equations above should be equivalent expressions since there are no iterative calculations on fracture planes being performed. Therefore, we can write

$$\sigma_{1D} = \frac{\sigma_1}{\left(\frac{\sigma_1}{\sigma_{1d}}\right)^n} \quad .$$

Based on the recommendations of Puck, Simulation Composite Analysis uses n=6 for the exponent and empirically computes σ_{1d} as 1.1XT or -1.1XC depending on the sign of σ_1.
It should be emphasized that the Simulation Composite Analysis implementation of the Puck criterion only uses the in-plane components of the 3-D stress and strain state, i.e., σ13, σ23, σ33, are not used to evaluate material failure.

4.9 Hashin Failure Criterion

The Hashin criterion identifies four different modes of failure for the composite material.
The four modes are: tensile fiber failure, compressive fiber failure, tensile matrix failure, compressive matrix failure.

S_{11}^+ = Value of σ_{11} at longitudinal tensile failure

S_{11}^- = Value of σ_{11} at longitudinal compressive failure

S_{22}^+ = Value of σ_{22} at transverse tensile failure

S_{22}^- = Value of σ_{22} at transverse compressive failure

S_{12} = Absolute value of σ_{12} at longitudinal shear failure

S_{23} = Absolute value of σ_{23} at transverse shear failure

If $\sigma_{11} \geq 0$, the Tensile **Fiber** Failure Criterion is:

$$F_f^+ \equiv \left(\frac{\sigma_{11}}{S_{11}^+}\right)^2 + \alpha\left(\frac{\sigma_{12}}{S_{12}}\right)^2 \geq 1.0$$

If $\sigma_{11} < 0$, the Compressive **Fiber** Failure Criterion is:

$$F_f^- \equiv \left(\frac{\sigma_{11}}{S_{11}^-}\right)^2 \geq 1.0$$

If $\sigma_{22} \geq 0$, the Tensile **Matrix** Failure Criterion is:

$$F_m^+ \equiv \left(\frac{\sigma_{22}}{S_{22}^+}\right)^2 + \left(\frac{\sigma_{12}}{S_{12}}\right)^2 \geq 1.0$$

If $\sigma_{22} < 0$, the Compressive **Matrix** Failure Criterion is:

$$F_m^- \equiv \left(\frac{\sigma_{22}}{2S_{23}}\right)^2 + \left[\left(\frac{S_{22}^-}{2S_{23}}\right)^2 - 1\right]\frac{\sigma_{22}}{S_{22}^-} + \left(\frac{\sigma_{12}}{S_{12}}\right)^2 \geq 1.0$$

5 Connection Analysis

In this final project degree was decided to model two pultruded GFRP connection, specifically column attached to a steel end plate, with a particular geometry, stiffness and material properties and the second one a beam-column connection . As first schemes of the connections, Figure 1 and 2 represents an isometric view of the models.

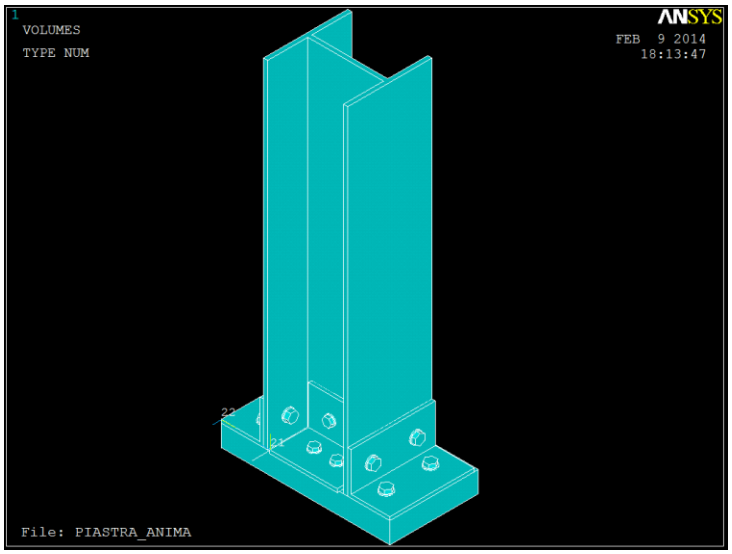

Figure 5.1. Geometry of the Connection 1

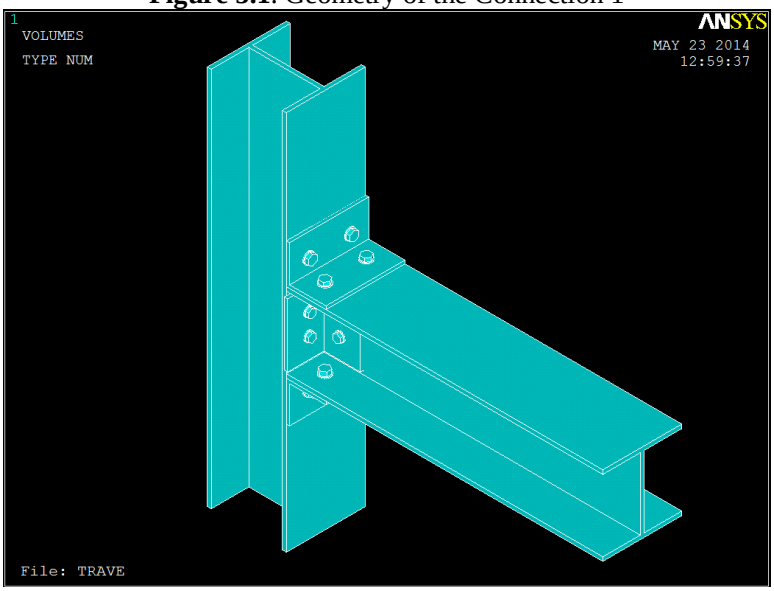

Figure 5.2. Geometry of the Connection2

The connection 1 is composed by one column (200x200x10mm), 4 cleats (100x100x8 mm) between the web and the flange of the column and 14 steel bolts, which 8 are attached to an end plate made by same material properties. In the other hand connection 2 is composed by one column (200x200x10mm), one beam (200x200x10mm), and also 14 steel bolts and 4 cleats that make the union between them. The column, the beam and the cleats are made of pultruded GFRP.

The material has an orthotropic behavior. The fiber of the pultruded elements are arranged according to the longitudinal section. The elastic characteristics of the pultruded material are defined in the table 1, axis Z is considerate as longitudinal axis, also is attributed and friction coefficient between elements equal to 0.2, namely friction between bolts, packing ring, end plate, cleats and column.

EX (MPa)	EY (MPa)	EZ (MPa)	PRXY	PRYZ	PRXZ	GXY (MPa)	GYZ (MPa)	GXZ (MPa)
8000	8000	23000	0.11	0.23	0.23	3500	3000	3000

Table 5.1

Resistance values of the pultruded elements are listed in table 2.

	X	Y	Z
Tensile Stress (MPa)	50	50	400
Compression Stress (MPa)	-80	-80	220
	XY	YZ	XZ
Shear Stress (MPa)	35	30	30

Table 5.2

Values listed in table 1 and 2 were obtained in the catalogue of TOP GLASS s.p.a. (www.topglass.it) and Creative Pultrusion (www.creativepultrusion.com). Pultruded elements have in case of failure mechanical properties reduce 1/10000 from initial value.
Different analyses are going to be executed, changing steps of loading in each analysis. In all cases the first step of loading is the same, pretension of the bolts equivalent to 3600N.
For each analysis is used 3 different failure criteria, they are:

-Maximum stress
-Puck
-Hashin

Each criterion has its own theories of computation, explained in previous chapters. Puck and Hashin criteria are partially iterative, namely, allowing the difference between fiber and matrix of the pultruded elements. Next are presented images that show where failure begins and how it spreads in the connection until total failure.

5.1 Connection 1

5.1.1 Behavior under compression force

Compression force is applied in the end of the column equivalent to 100N/mm2, next are presented the result for the 3 failure criteria.

Maximum Stress

Failure arrive when compression reach 74.375 N/mm2 (431.375 KN). Figure 5.1.1.1 present the last step of loading, equivalent to failure, in general the column presents damage, however the failure is stronger in the bottom face of the column, the other elements, as plates and bolts, do not present a significant damage or failure.

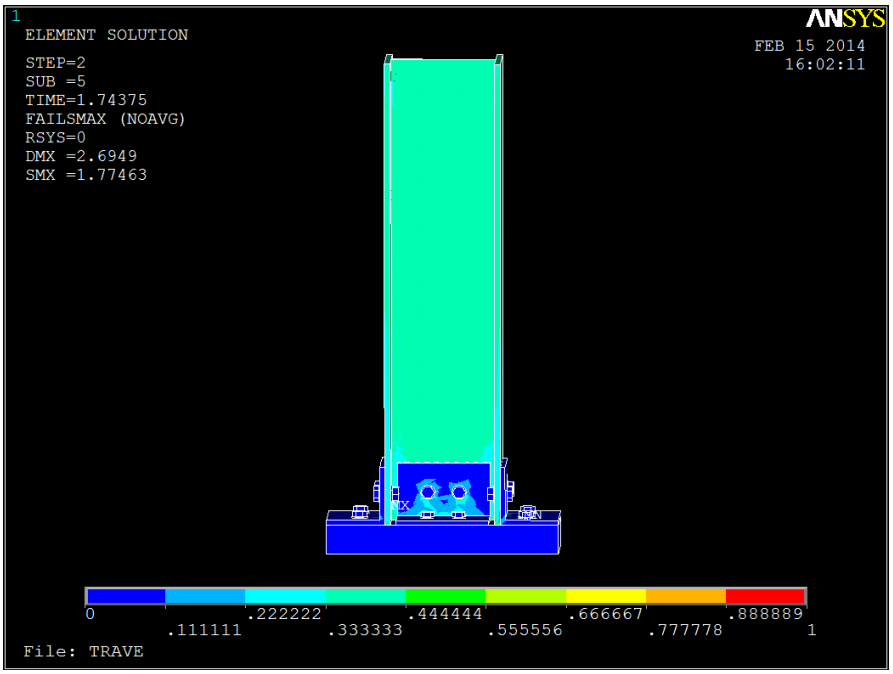

Figure 5.1.1.1 Compression Force 74.375 N/mm2

Hashin

Failure arrives around 45N/mm2, figure 5.1.1.2 and 3 represents the failure of the connection in terms of the matrix and the fiber. Grey zones means failure.

-Matrix

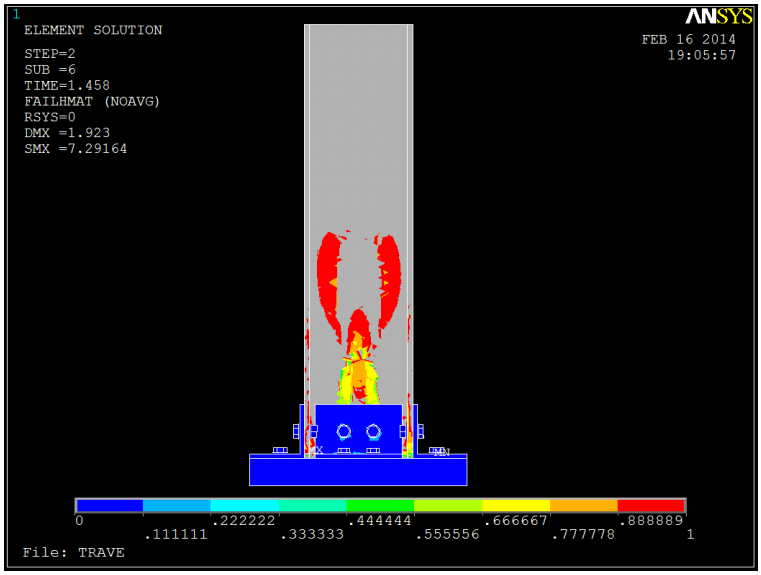

Figure 5.1.1.2. Compression Force 45.8N/mm2

Almost the entire matrix fails under compression load, the other elements barely presents damage.

-Fiber:

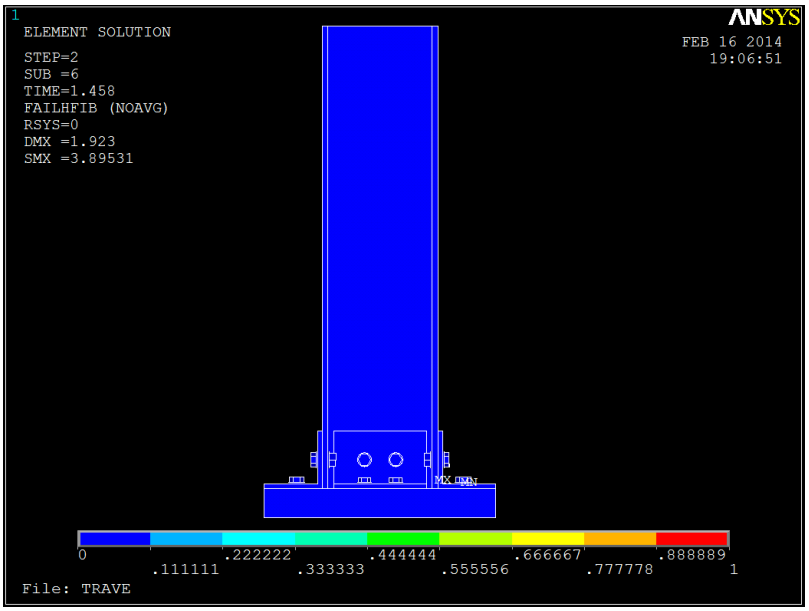

Figure 5.1.1.3. Compression Force 45.8N/mm2

Damage in the fiber is not visible.

Puck

Analogue to Hashin failure arrive reaching 48.78 N/mm2, as before Fiber doesn't arrive to failure instead that matrix fails. Figure 4 and 5 describe the damage for the matrix and the fiber.

-Matrix

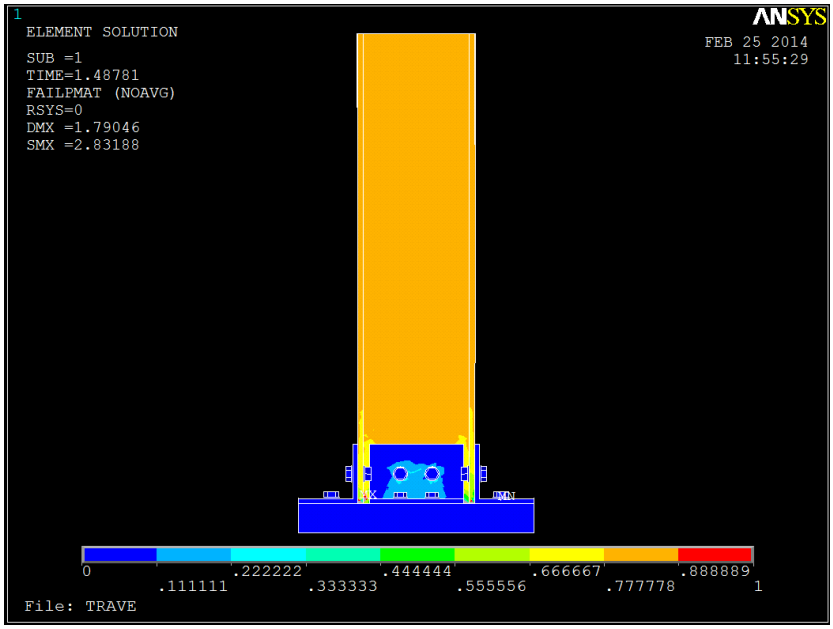

Figure 5.1.1.4. Compression Force 48.78N/mm2

-Fiber

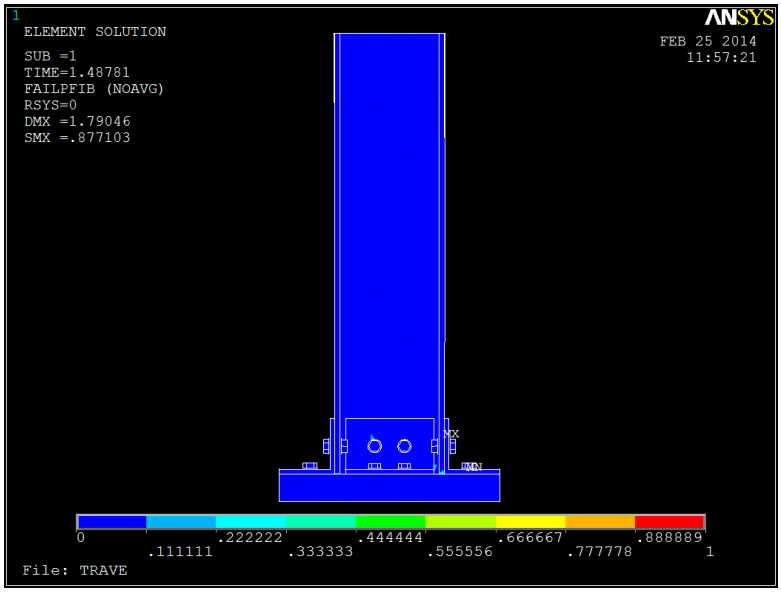

Figure 5.1.15 . Compression Force 48.78N/mm2

5.1.2 Behavior under bending moment

Bending moment is applied in the end of the column equivalent to 8200Nm, next are presented the result for the 3 failure criteria.

Maximum Stress:

The maximum value of resistance is 5868.95 Nm. Figure 1 shows that failure begins at the right cleat of the beam flange, right in the corner then spreads until total failure of the connection, as is possible to see in figures 2, 3 and 4. Web plates are next who are affected; the corner of the plates begins the rupture increasing until failure. Maximum relative displacement of the column is 26.05 mm.

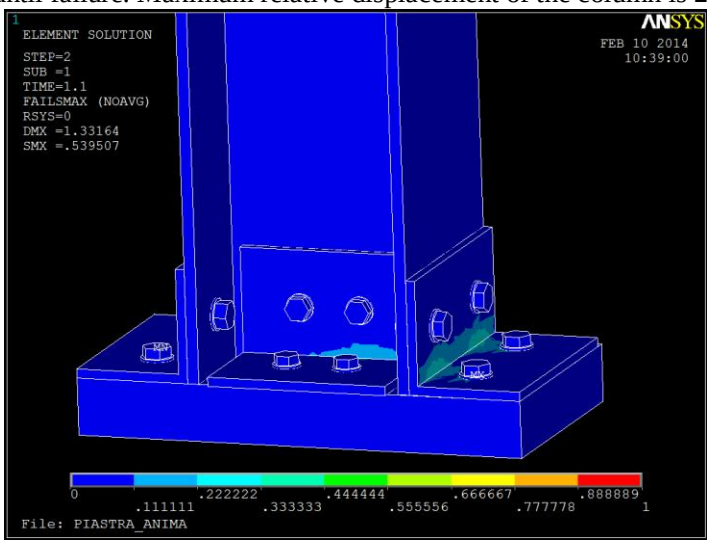

Figure 5.1.2.1. Bending Moment 615 Nm.

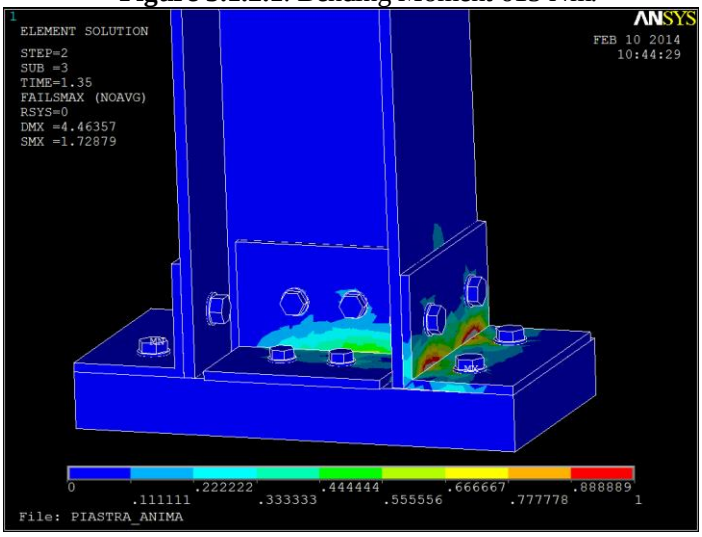

Figure 5.1.2.2. Bending Moment 2152,5 Nm.

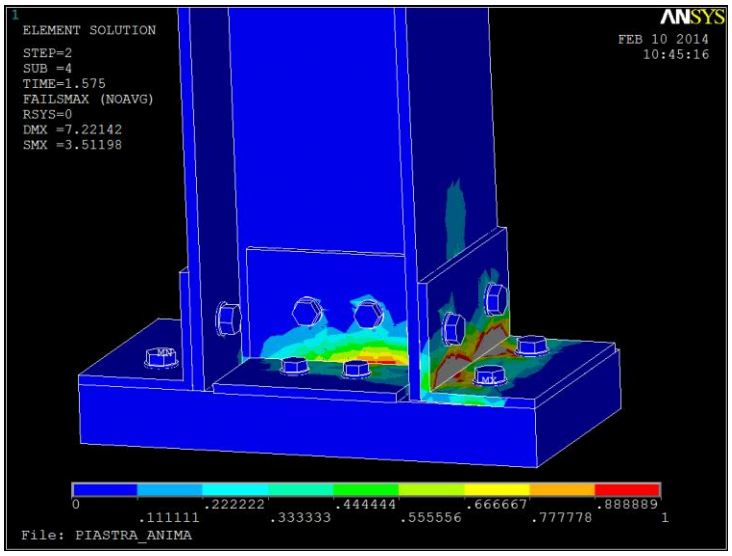

Figure 5.1.2.3 Bending Moment 3536,5 Nm.

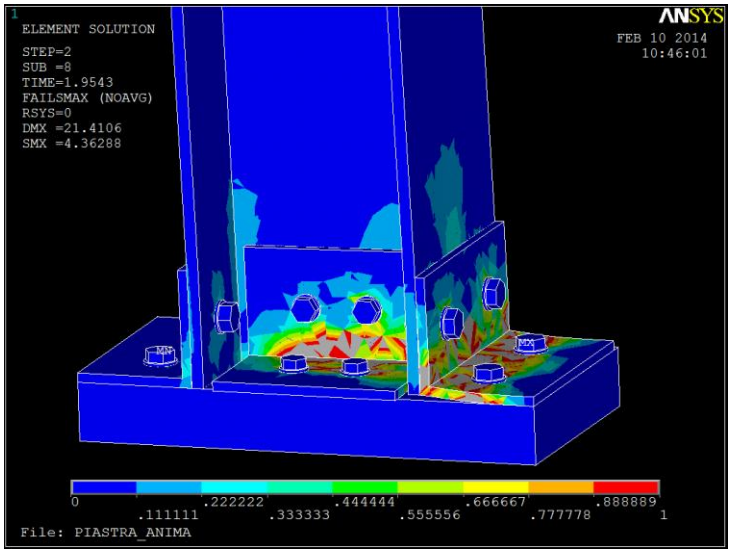

Figure 5.1.2.4. Bending Moment 5868,5 Nm.

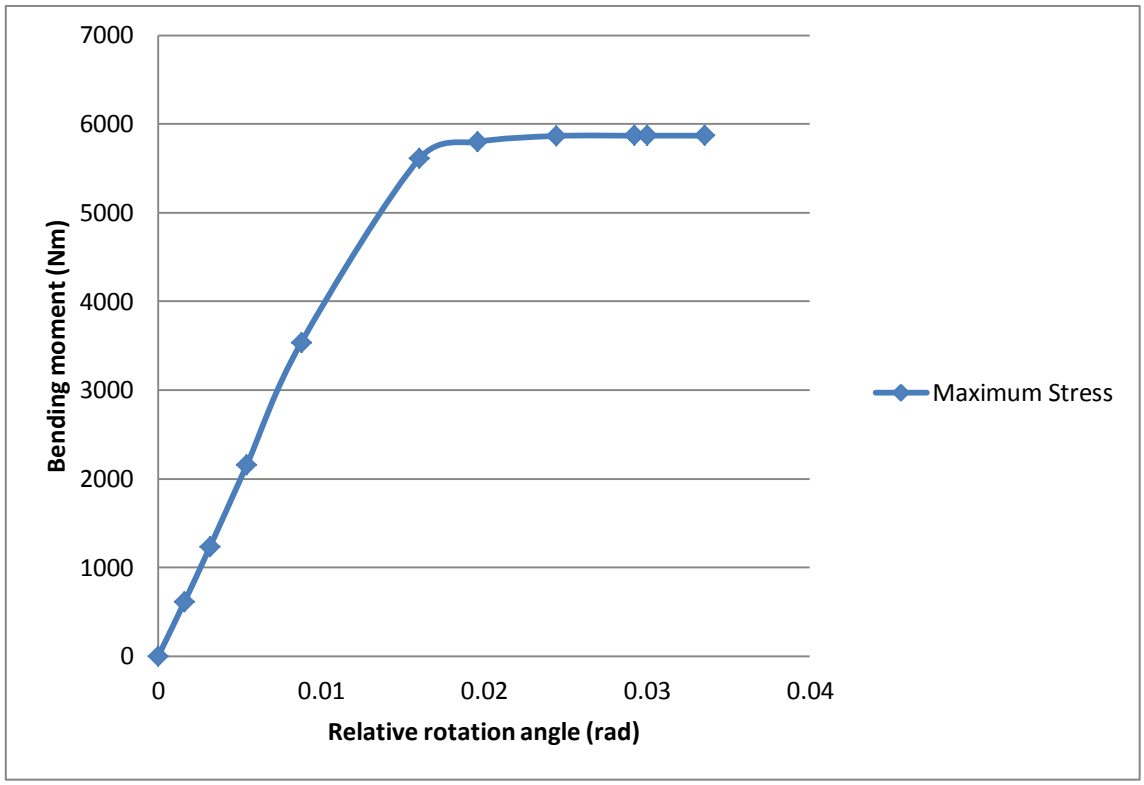

Graph 5.1.2.1. Relative rotation angle (rad)-Bending moment (Nm)

Graph5.1.2.1 shows the relation between the relative rotations angle of the column due to bending moment, thanks to this table is possible to calculate the development of the relative displacement of the column as the analysis progresses.

Hashin

Images show the spread of the failure in the connection. Failure begins around 2835Nm, it will continue until reach 5295.5Nm, as before failure begins at the right cleat of the beam flange, right in the corner then spreads until total failure of the connection. The maximum displacement of the end of the column is 22mm. Matrix presents more damage than the fiber, next figures shows the development of the damage.

Matrix:

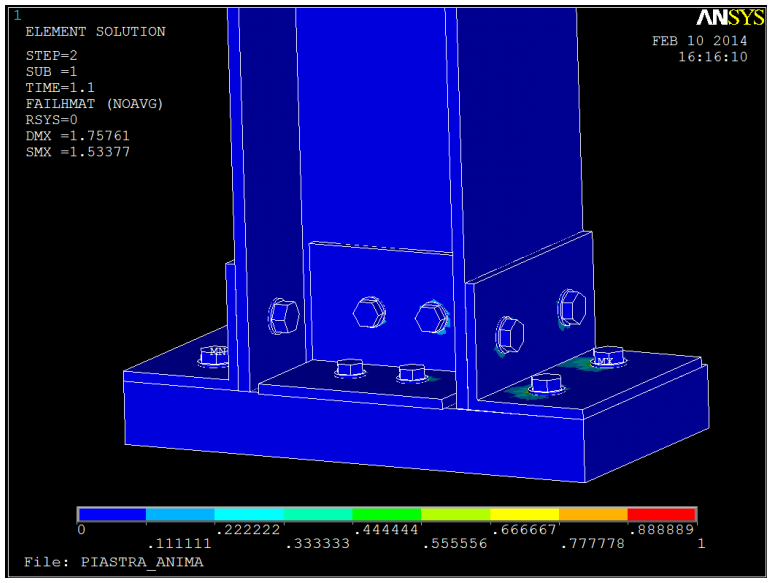

Figure 5.1.2.5. Bending Moment 810 Nm.

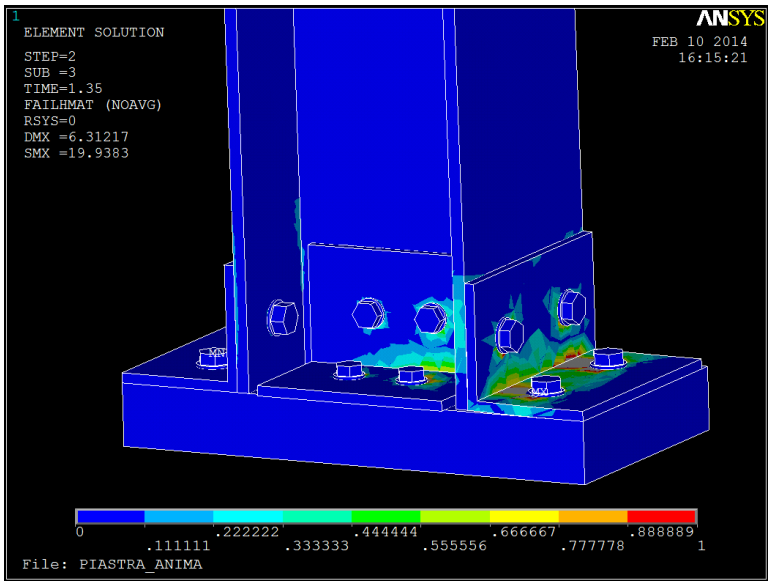

Figure 5.1.2.6. Bending Moment 2835 Nm.

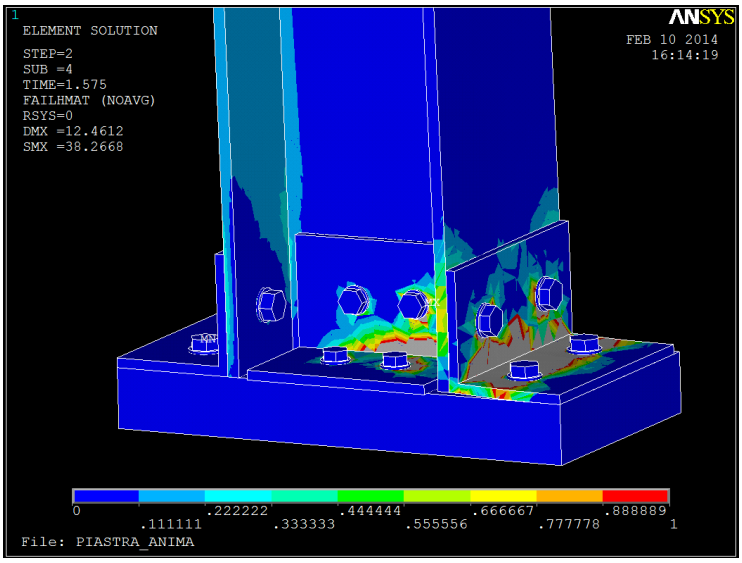

Figure 5.1.2.7 Bending Moment 4657,5 Nm

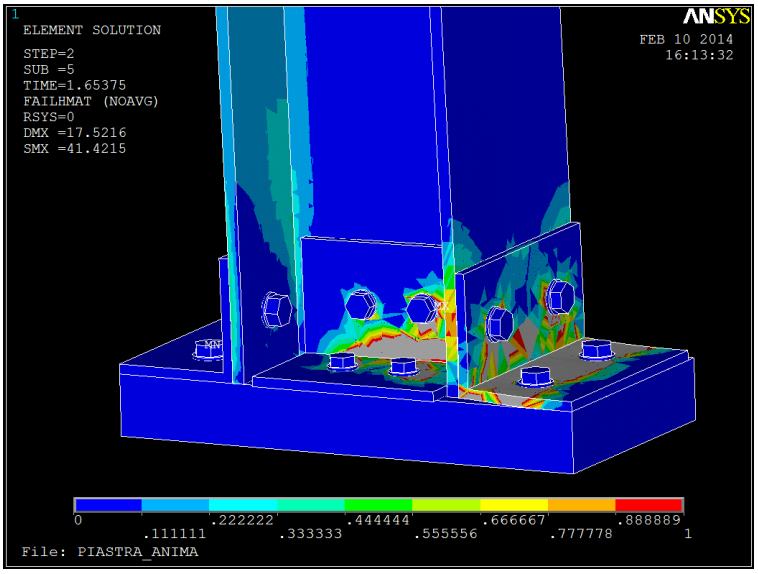

Figure 5.1.2.8. Bending Moment 5295.5 Nm.

Fiber:

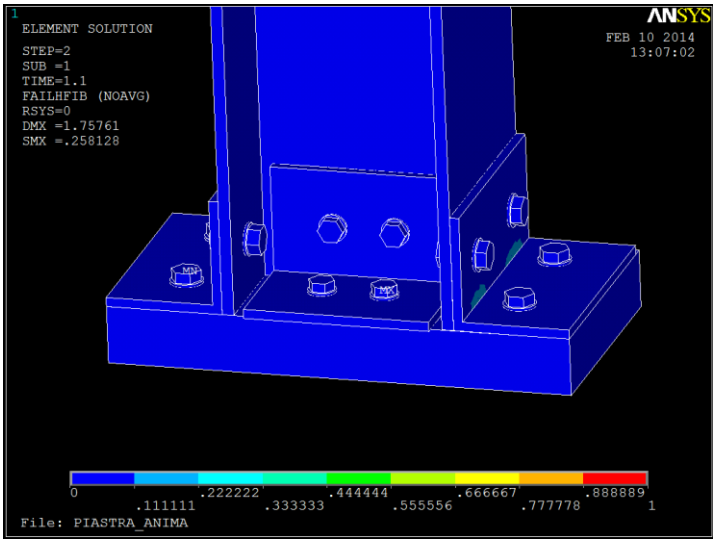

Figure 5.1.2.9. Bending Moment 810 Nm.

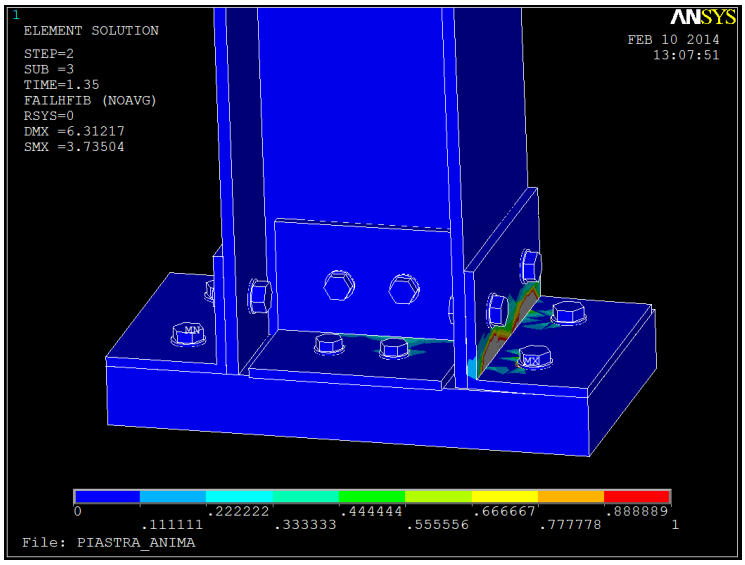

Figure 5.1.2.10. Bending Moment 2835 Nm.

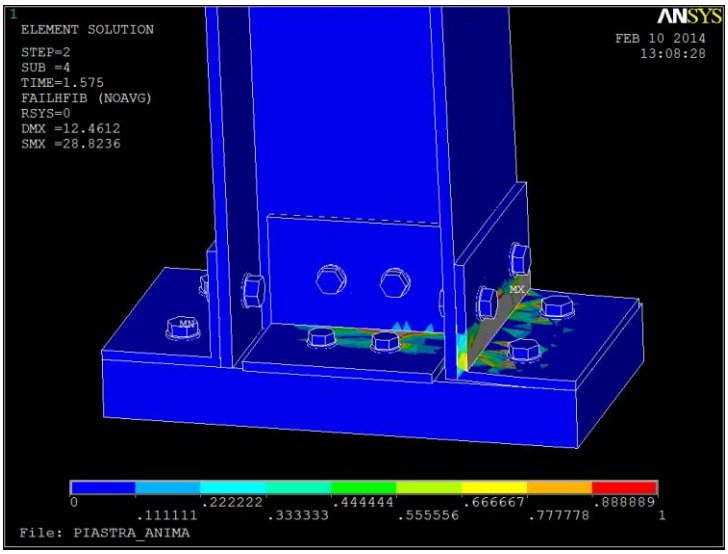

Figure 5.1.2.11. Bending Moment 4657,5 Nm.

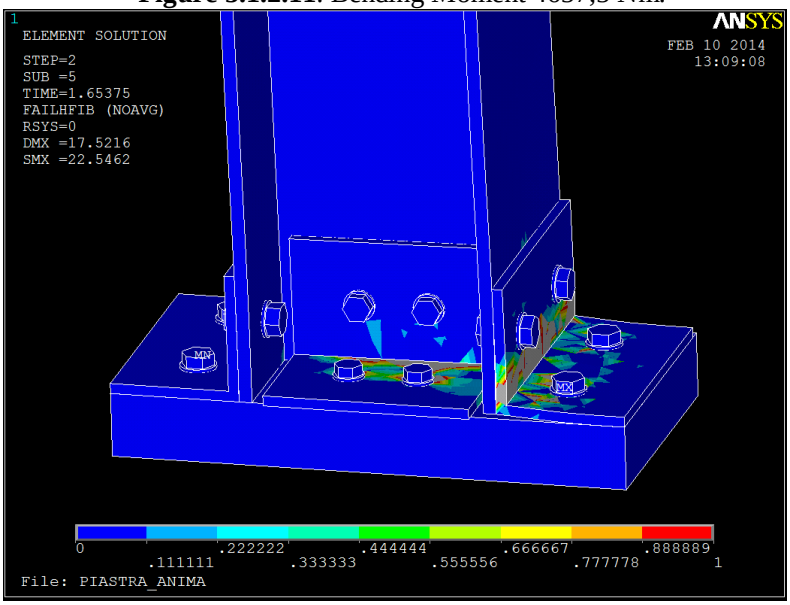

Figure 5.1.2.12. Bending Moment 5295,5 Nm.

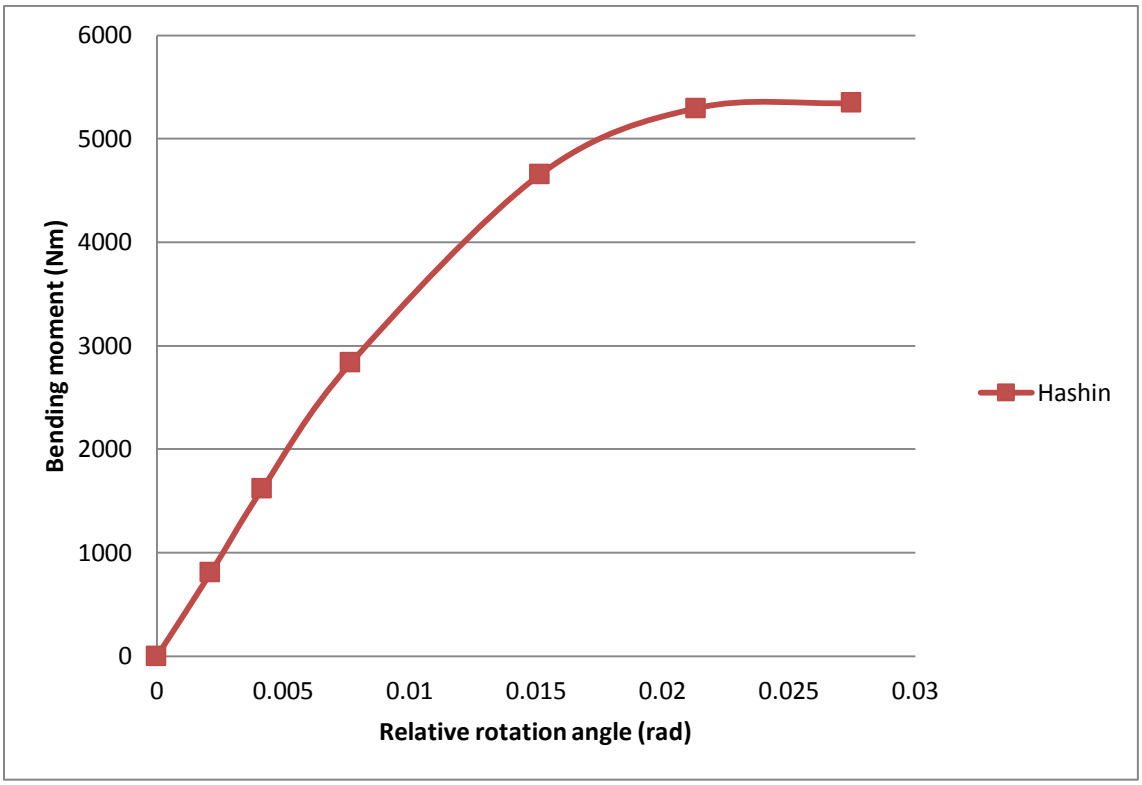

Graph 5.1.2.2. Relative rotation angle (rad)-Bending moment (Nm)

Graph 5.1.2.2 shows the relation between the relative rotation angle of the column due to bending moment, for bending moment under 3000Nm we can see a linear behavior, until this point failure is small predominantly in the right plate of the flange, after this point is appreciated a nonlinear behavior characterized by the loss of mechanical properties until reach total failure of the connection.

Puck

Analogue to Hashin, failure begins around 2835Nm, it will continue until reach 5596.7Nm the maximum displacement of the end of the column is 28.85mm. Matrix presents more damage than the fiber, next figures shows the development of the damage.

Matrix:

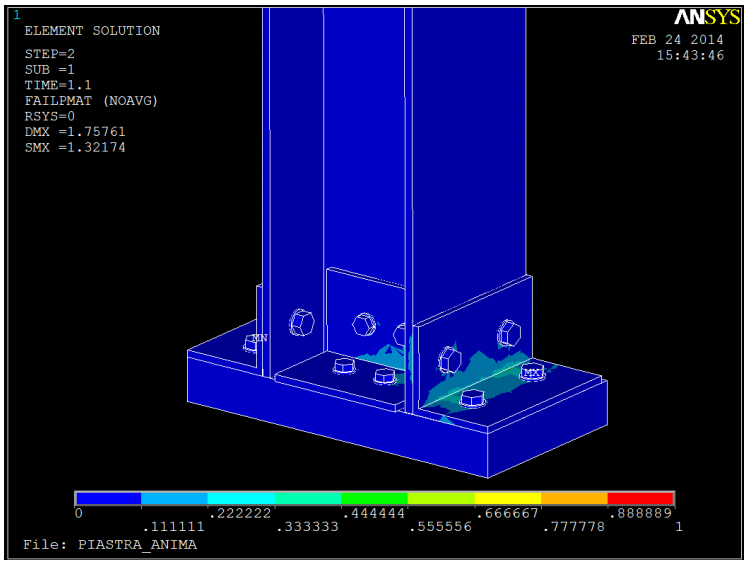

Figure 5.1.2.13. Bending Moment 810 Nm.

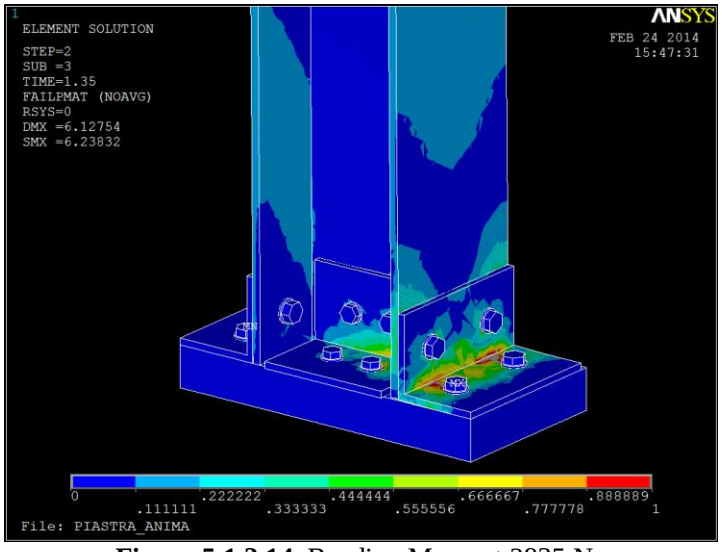

Figure 5.1.2.14. Bending Moment 2835 Nm.

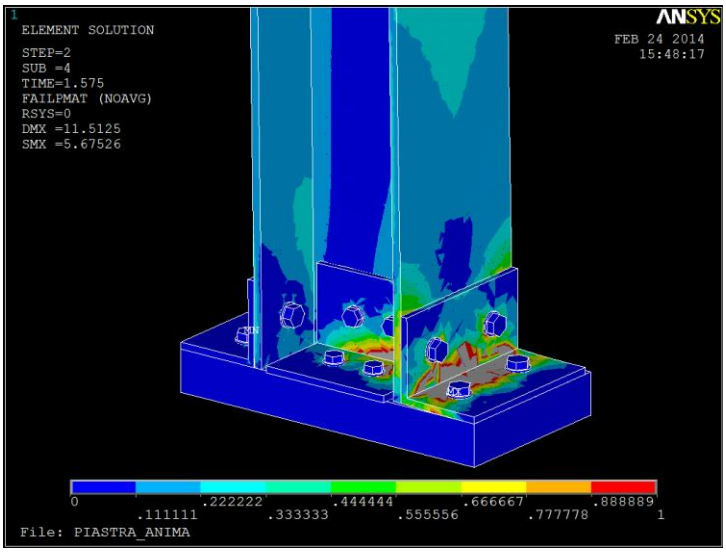

Figure 5.1.2.15. Bending Moment 4657,5 Nm

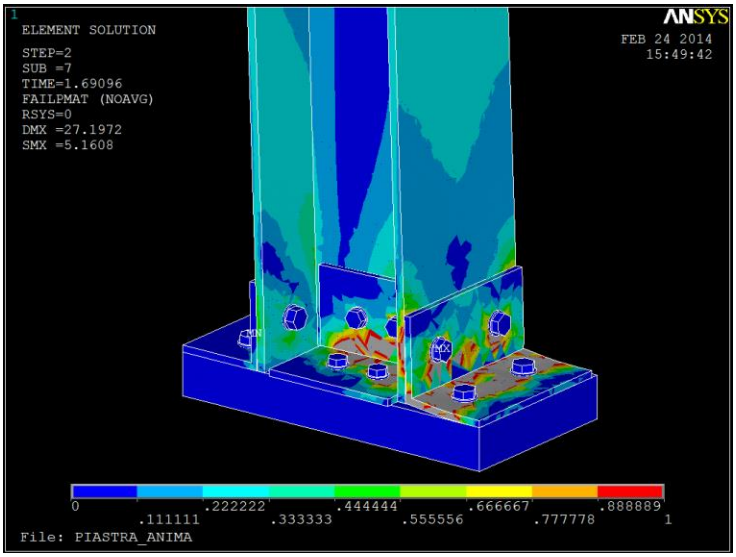

Figure 5.1.2.16. Bending Moment 5596,7 Nm.

Fiber:

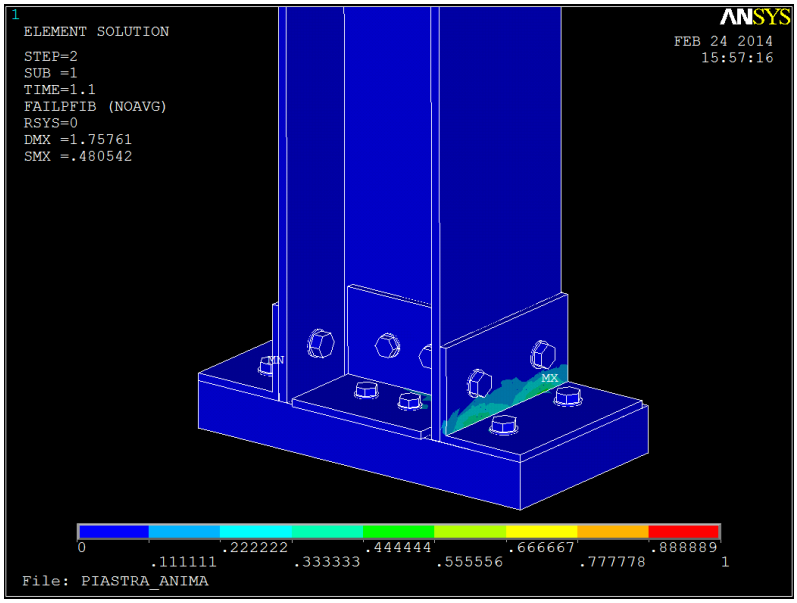

Figure 5.1.2.17. Bending Moment 810 Nm.

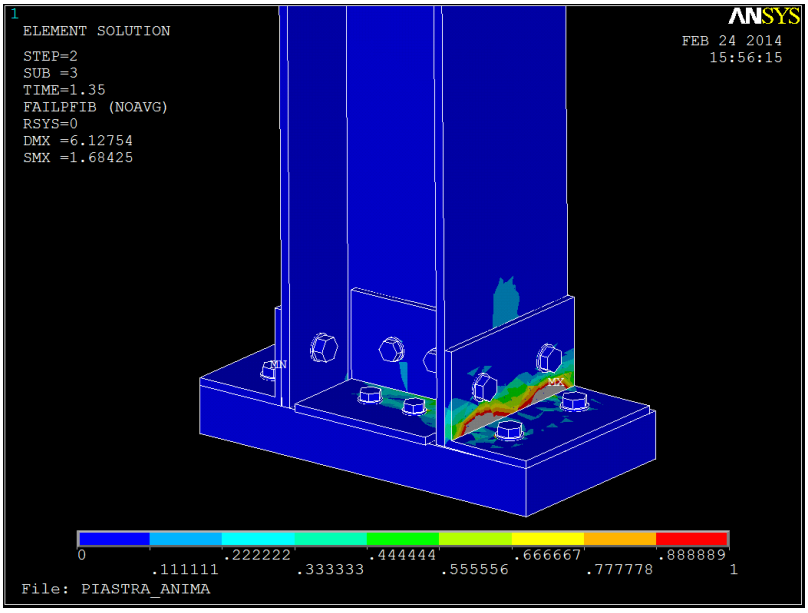

Figure 5.1.2.18 Bending Moment 2835 Nm.

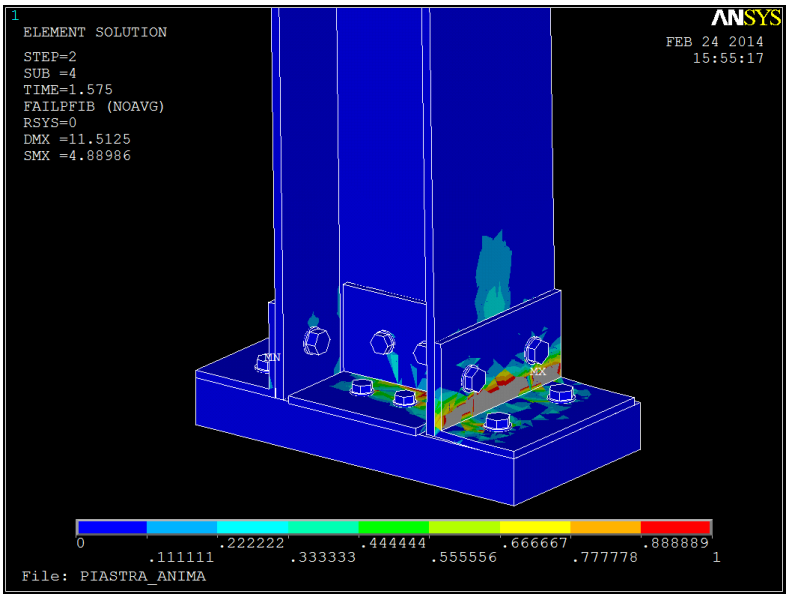

Figure 5.1.2.19. Bending Moment 4657,5 Nm

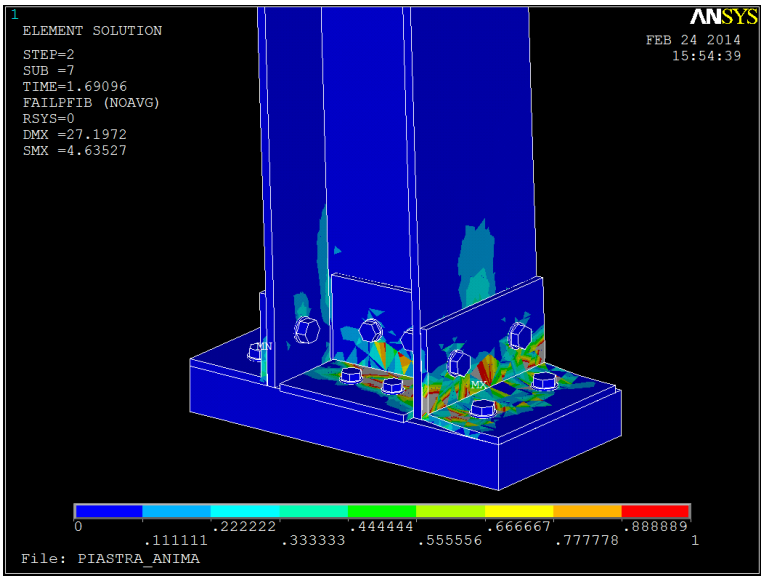

Figure 5.1.2.20. Bending Moment 5596,7 Nm.

Result for the 3 criteria were similar in terms of bending moment, failure of elements and the displacement, next is the Graph 3 that shows a brief resume of the result for each criteria in terms of bending moment and displacement.

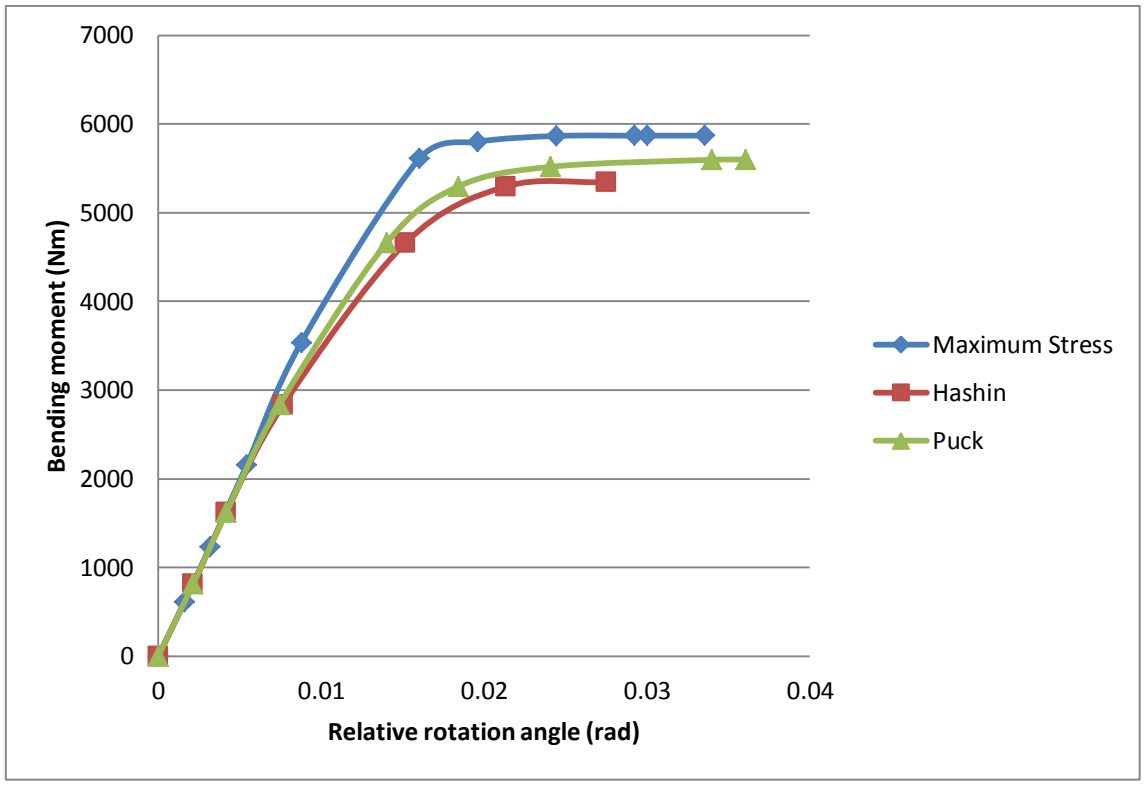

Graph 5.1.2.3. Relative rotation angle (rad)-Bending moment (Nm)

For bending moment under 3000Nm we can see a linear behavior, in fact the 3 curves are practically the same until this point, failure is small predominantly in the right cleat of the flange, after this point is appreciated a nonlinear behavior characterized by the loss of mechanical properties until reach total failure of the connection.

5.1.3 Behavior under compression and bending moment

In this case, it's a combination of the previous analyses, first step to follow is the pretension of the bolts, then subject the column under compression force and finally apply an increasing bending moment in the end of the column until total failure. The analyses can be divided in in 3 different blocks.

- Quarter of failure compression load plus bending moment.
- Half of failure compression load plus bending moment.
- Three quarters of failure compression load plus bending moment.

Each block is evaluated with 3 failure criteria, results are show next:

5.1.3.1 Quarter of failure compression load

Maximum Stress

A quarter of the failure compression load 18.75 N/mm2, then is applied a bending moment equivalent to 12300Nm in the end of the column. The maximum value of resistance in this case is 11015.25 Nm substantially more than the previous analysis. The maximum relative displacement of the column is 45.7 mm. Damage evolution is illustrated in failures 1, 2, 3 and 4, as before partial failure begins on the right cleat of the flange and then spreads to other elements, column and web cleats.

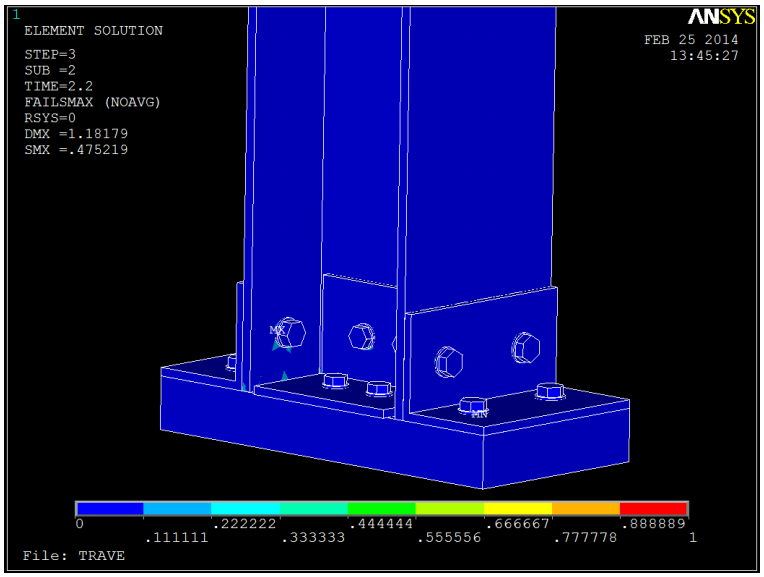

Figure 5.1.3.1. Bending Moment 2460Nm.

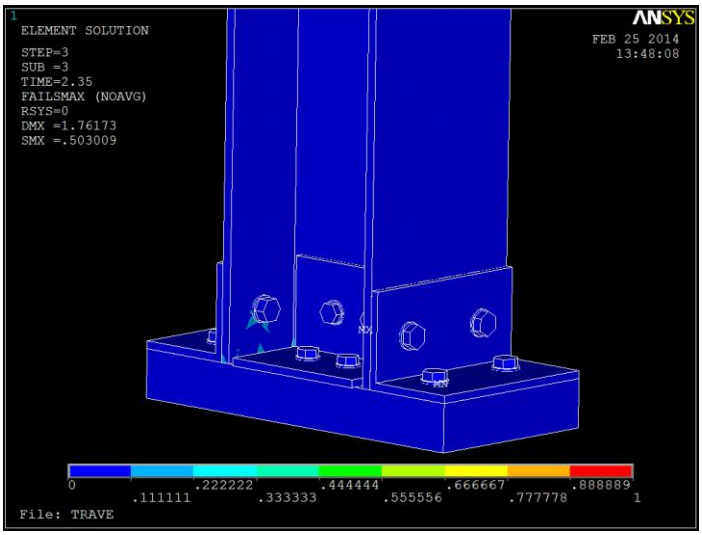

Figure 5.1.3.2 Bending Moment 4305Nm

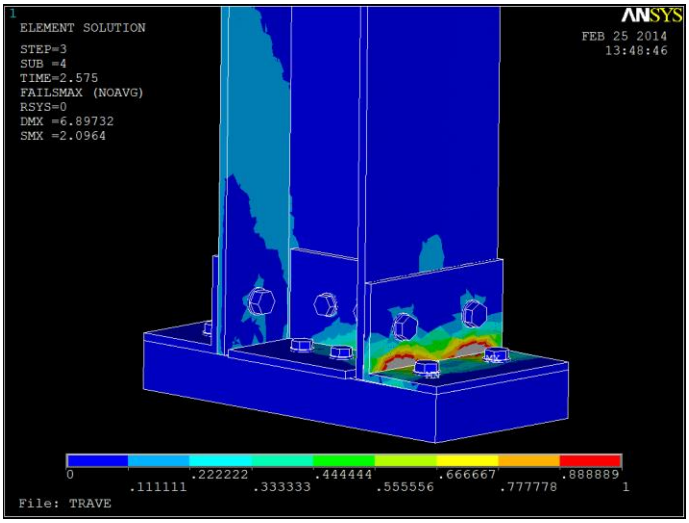

Figure 5.1.3.3. Bending Moment 7072.5Nm

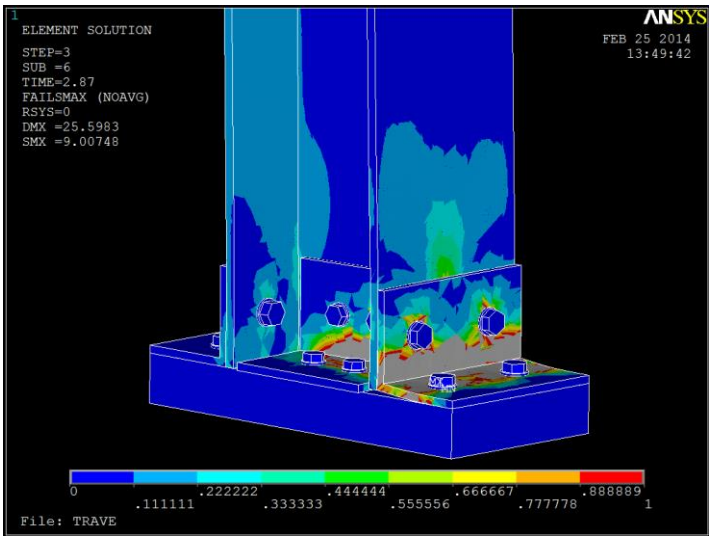

Figure 5.1.3.4 Bending Moment 10209Nm

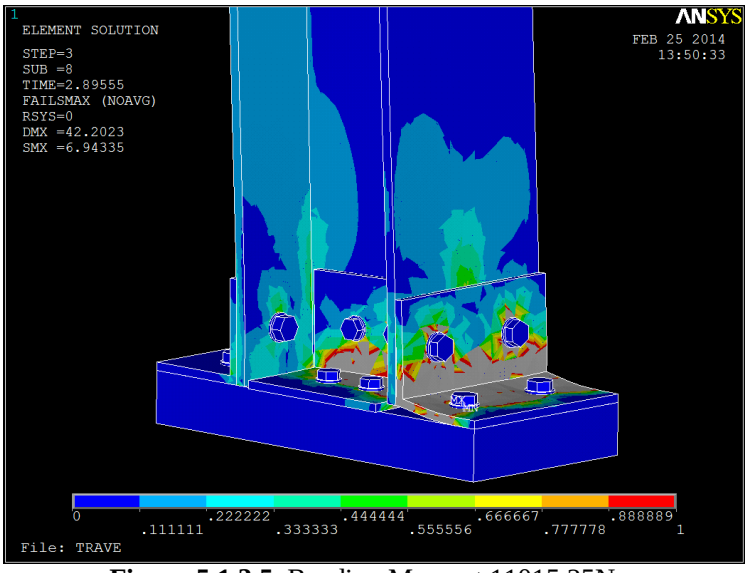

Figure 5.1.3.5. Bending Moment 11015.25Nm

Graph 5.1.3.1 shows the relation between the relative rotation angle of the column due to bending moment, thanks to this table is possible to calculate the development of the relative displacement of the column as the analysis progresses.

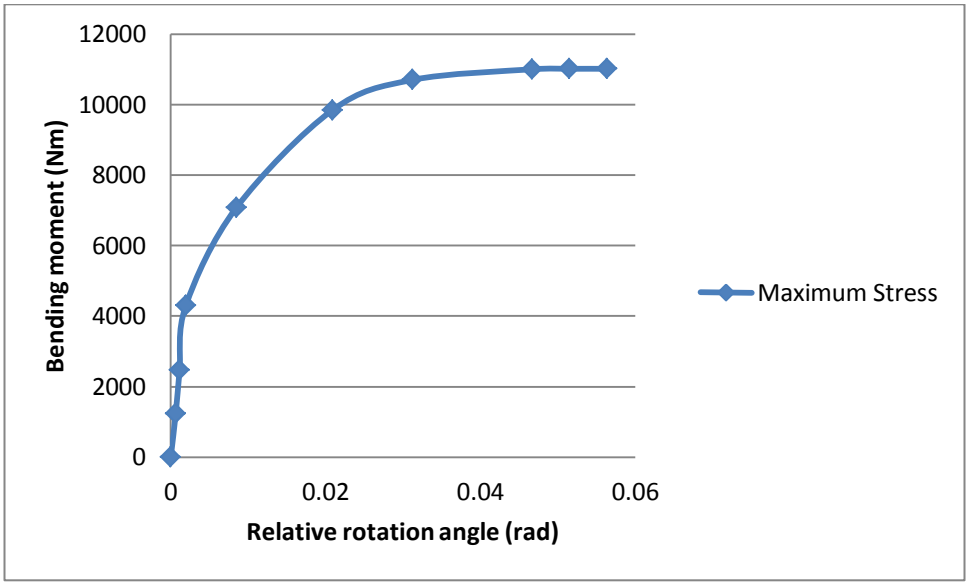

Graph 5.1.3.1. Relative rotation angle (rad)-Bending moment (Nm)

Hashin

Images show the spread of the failure in the connection. Analogue to previous analyses failure begins at the right cleat of the flange. The maximum displacement of the end of the column is 52.65mm and the bending moment 8895.13 Nm. Matrix presents more damage than the fiber, next figures shows the development of the damage.

Matrix

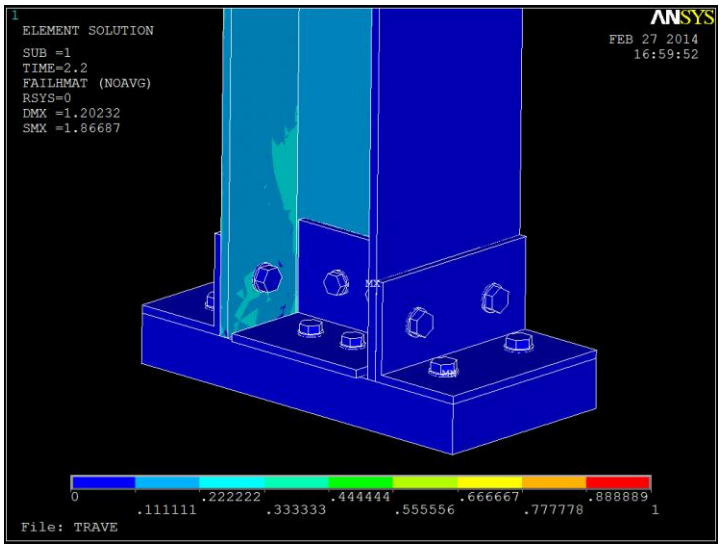

Figure 5.1.3.6. Bending Moment 2870Nm

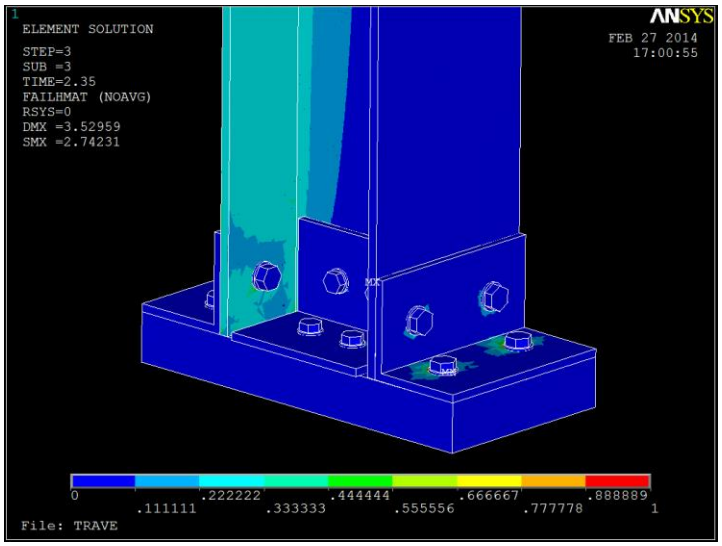

Figure 5.1.3.7 Bending Moment 5022.5Nm

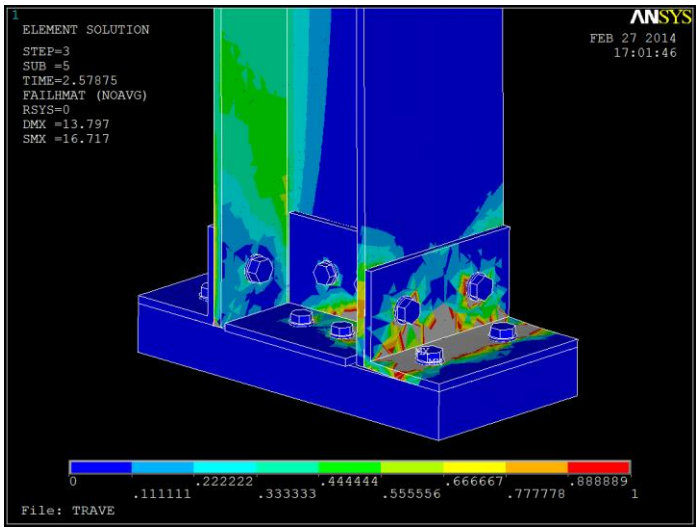

Figure 5.1.3.8. Bending Moment 8305Nm

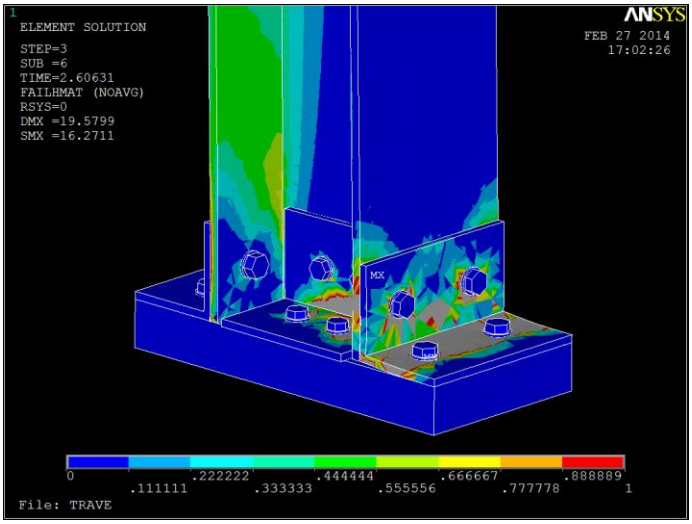

Figure 5.1.3.9. Bending Moment 8700.5Nm

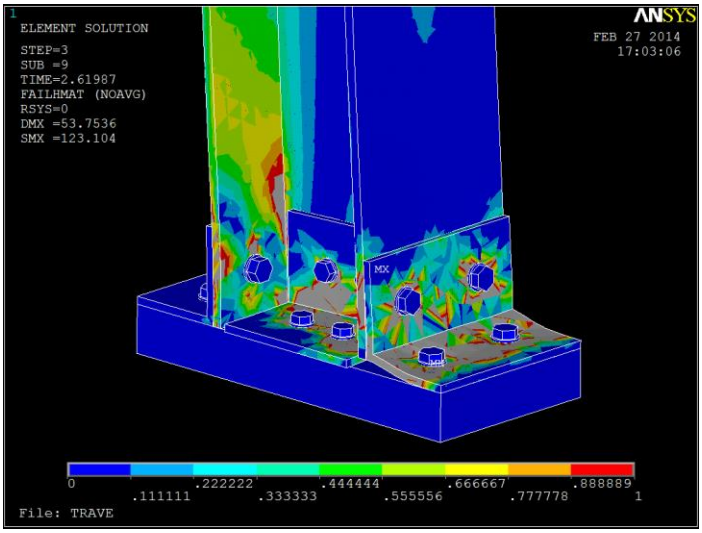

Figure 5.1.3.10. Bending Moment 8895.13Nm

Fiber

Similar to previous analysis fiber has less damage than matrix, however fails in the lasts steps. Next images follow the damage of the connection:

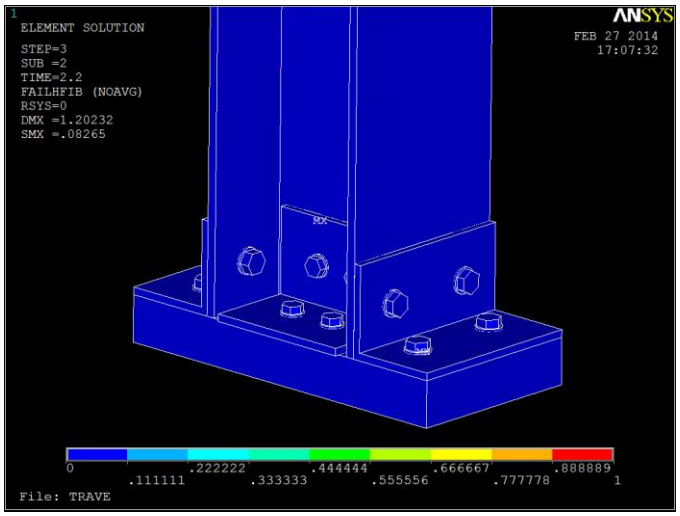

Figure 5.1.3.11. Bending Moment 2870Nm

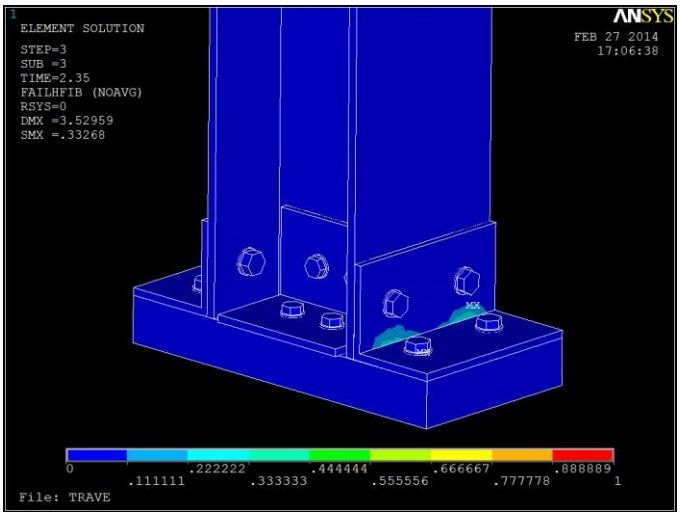

Figure 5.1.3.12. Bending Moment 5022.5Nm

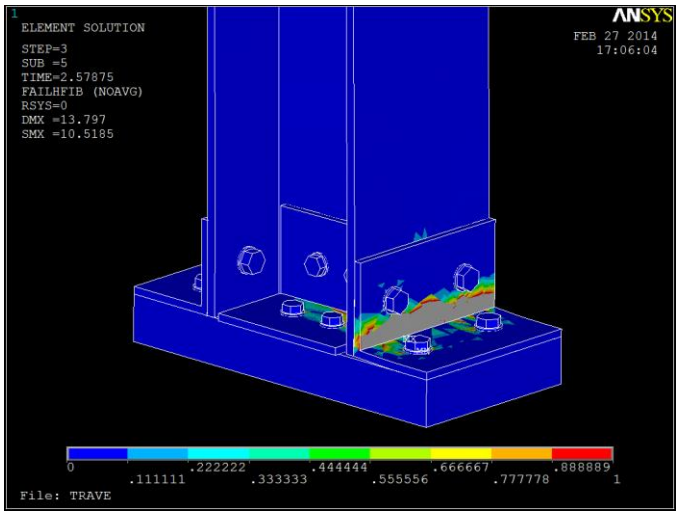

igure 5.1.3.13. Bending Moment 8305Nm

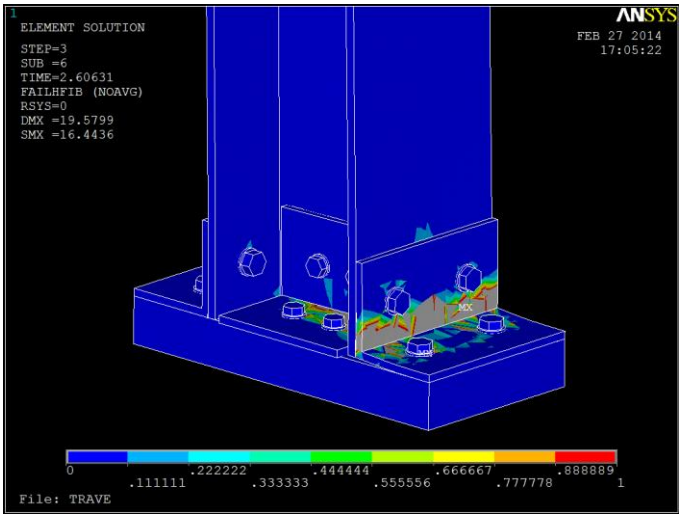

Figure 5.1.3.14 Bending Moment 8700.5Nm

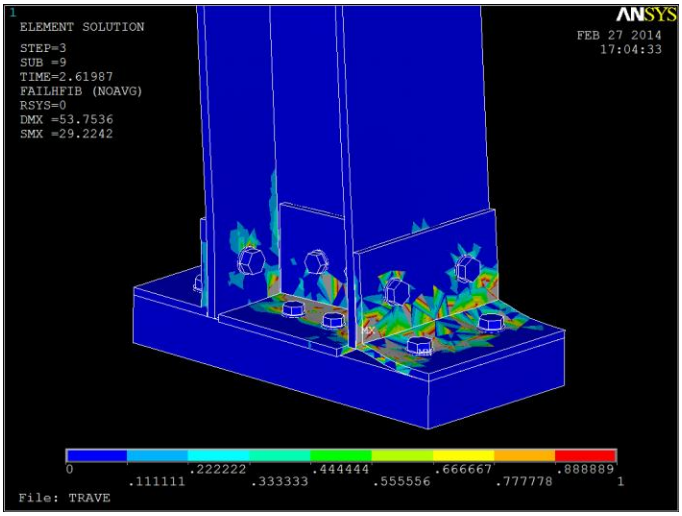

Figure 5.1.3.15. Bending Moment 8895.13Nm

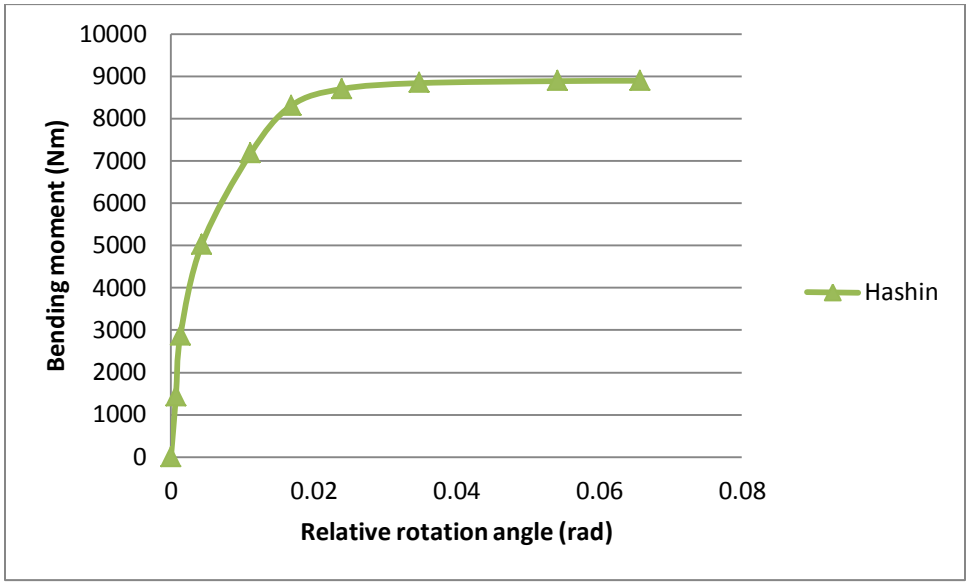

Graph 5.1.3.2. Relative rotation angle (rad)-Bending moment (Nm)

Graph 5.1.3.2 shows the relation between the relative rotation angle of the column due to bending moment, for bending moment under 3000Nm we can see a linear behavior, until this point failure is small predominantly in the right cleat of the flange, after this point is appreciated a nonlinear behavior characterized by the loss of mechanical properties until reach total failure of the connection.

Puck

Analogue to Hashin, total failure is evident at 8906.61Nm. The maximum displacement of the end of the column is 61.18mm. Matrix presents more damage than the fiber, next figures shows the development of the damage.

-Matrix

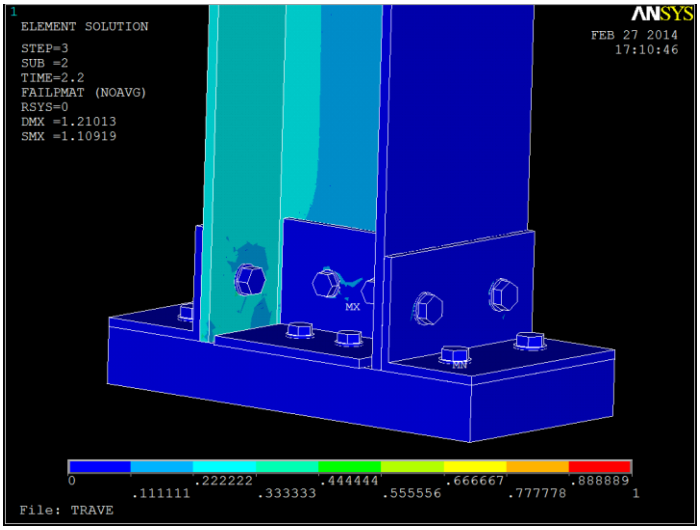

Figure 5.1.3.16. Bending Moment 2870Nm

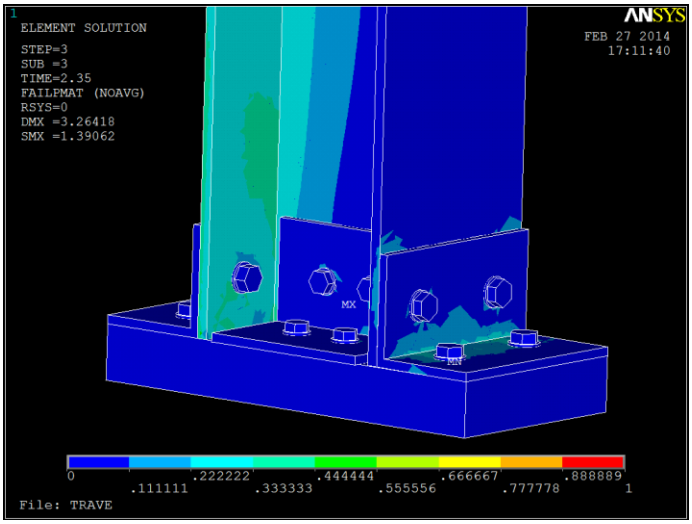

Figure 5.1.3.17. Bending Moment 5022.5Nm

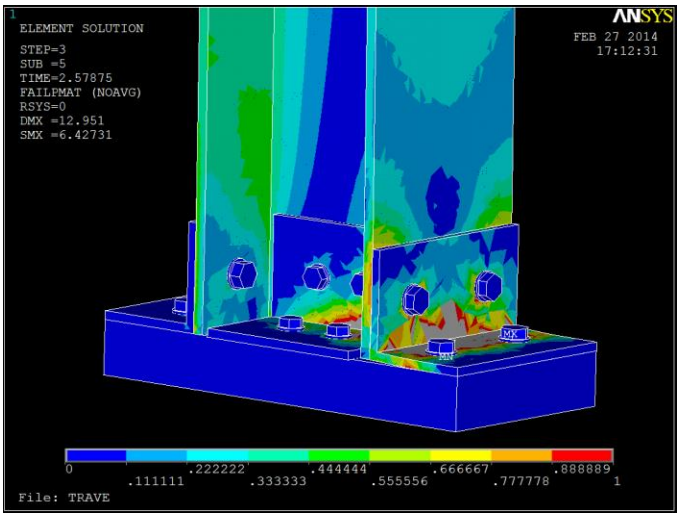

Figure 5.1.3.18. Bending Moment 8305Nm

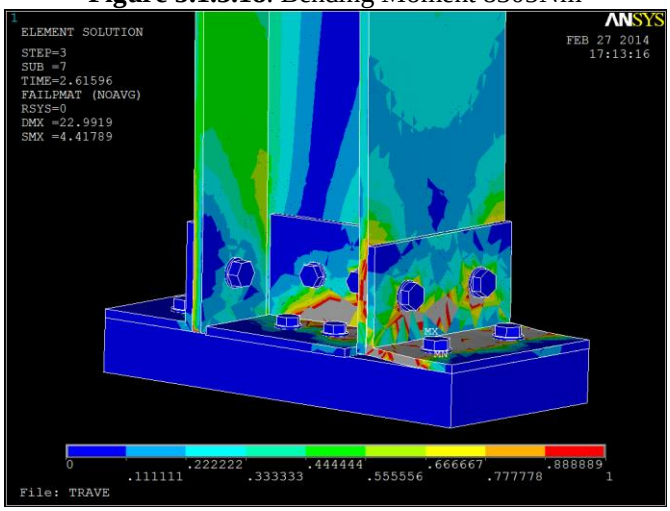

Figure 5.1.3.19. Bending Moment 8839Nm

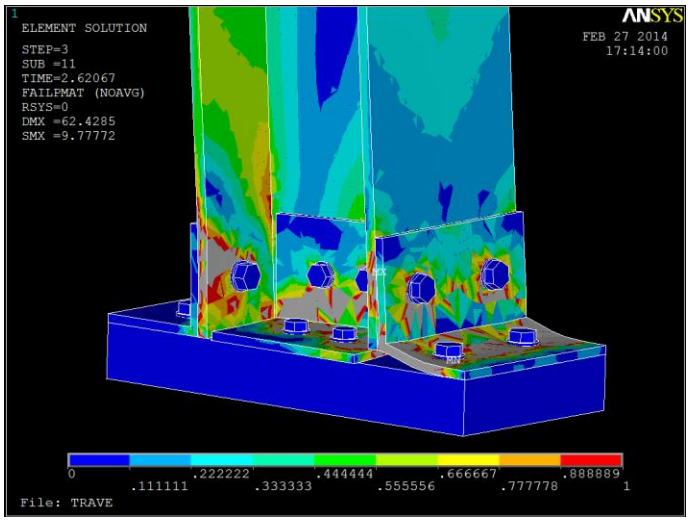

Figure 5.1.3.20. Bending Moment 8906,61Nm

-Fiber

Similar to previous analysis fiber has less damage than matrix, however fails in the lasts steps. Next images follow the damage of the connection:

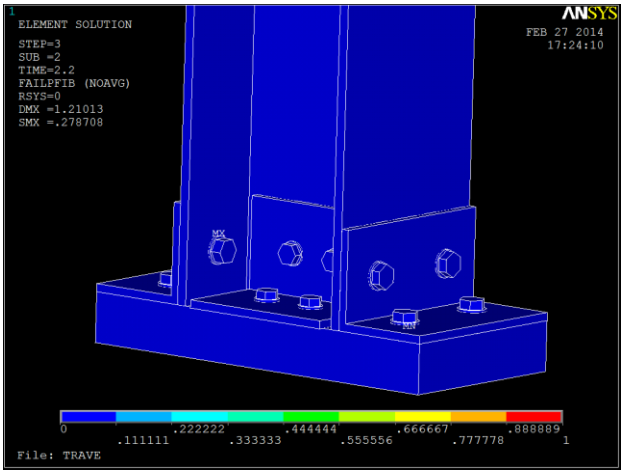

igure 5.1.3.21 Bending Moment 2870Nm

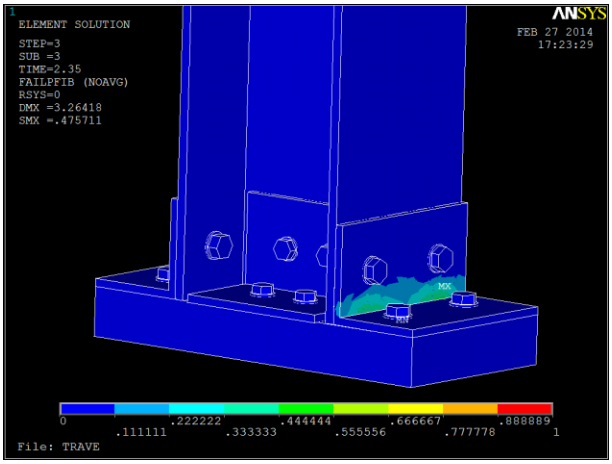

Figure 5.1.3.22. Bending Moment 5022.5Nm

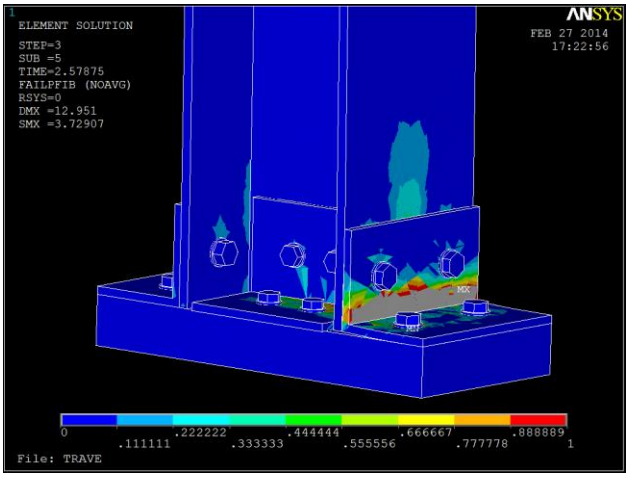

Figure 5.1.3.23. Bending Moment 8305Nm

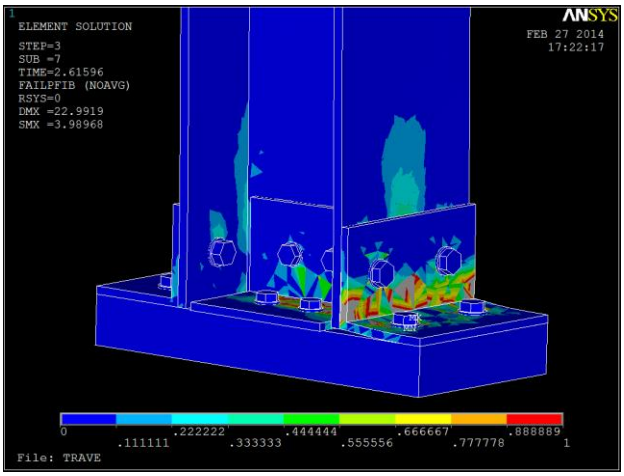

Figure 5.1.3.24. Bending Moment 8839Nm

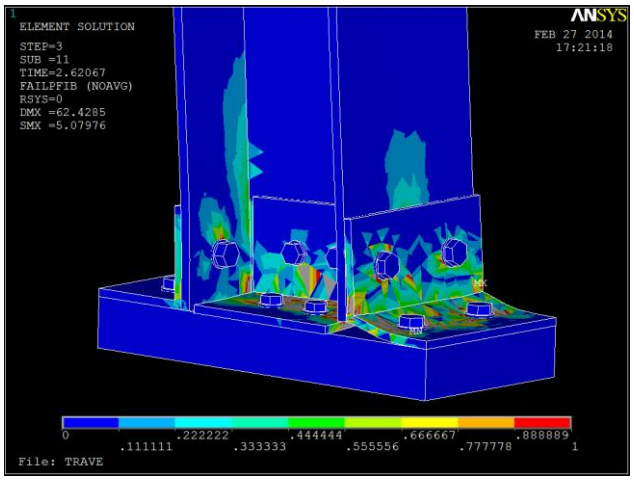

Figure 5.1.3.25. Bending Moment 8906.61Nm

Result for the 3 criteria were similar in terms of bending moment, failure of elements and the displacement, next is the Graph 3 that shows a brief resume of the result for each criteria in terms of bending moment and displacement.

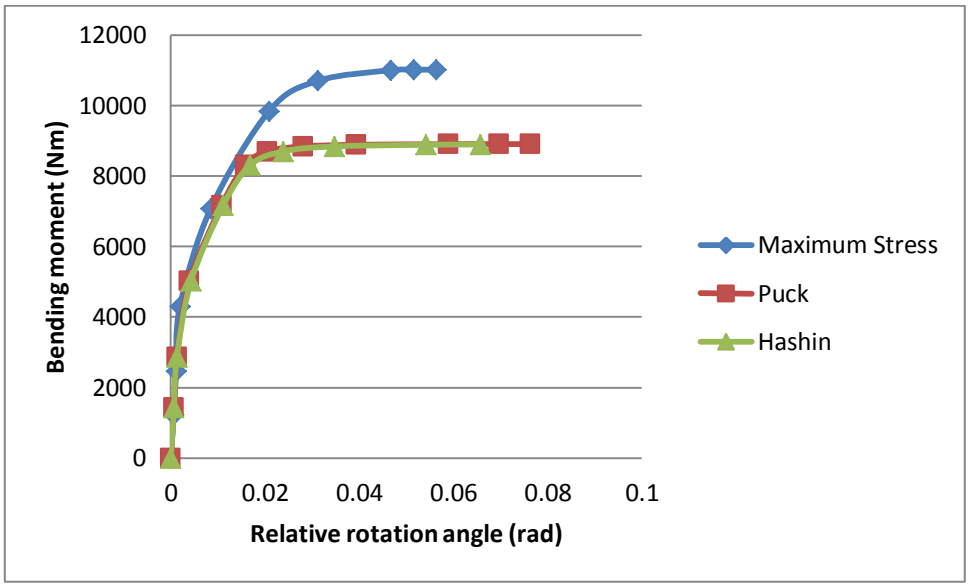

Graph 5.1.3.3. Bending moment-Relative rotation angle

For bending moment under 3000Nm we can see a linear behavior, in fact the 3 curves are practically the same until this point, failure is small predominantly in the right cleat of the flange, after this point is appreciated a nonlinear behavior characterized by the loss of mechanical properties until reach total failure of the connection.

5.1.3.2 Half of failure compression load

Maximum Stress

A half of the failure compression load 37.5 N/mm2, then is applied a bending moment equivalent to 12300Nm in the end of the column. The maximum value of resistance in this case is 11753 Nm substantially more than the previous analysis The maximum relative displacement of the column is 50.67 mm. Damage evolution is illustrated in failures 1, 2, 3, 4, and 5 as before partial failure begins on the right cleat of the flange and then spreads to other elements, column and web cleats.

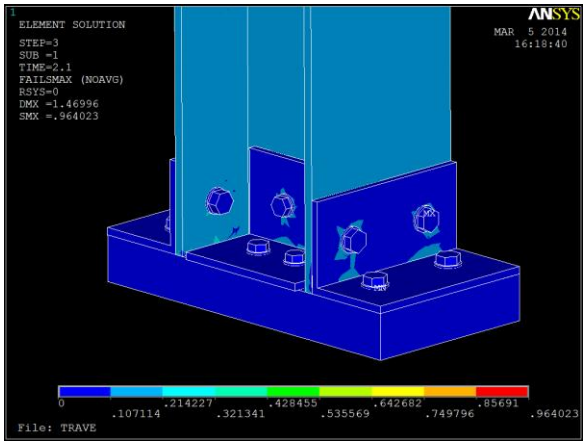

Figure 5.1.3.2.1. Bending Moment 1230Nm

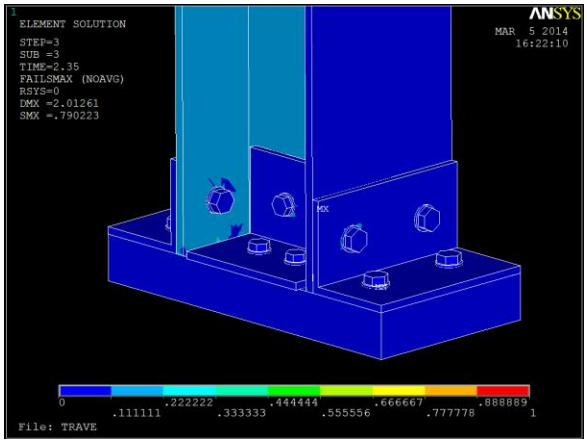

Figure 5.1.3.2.2 Bending Moment 4305Nm

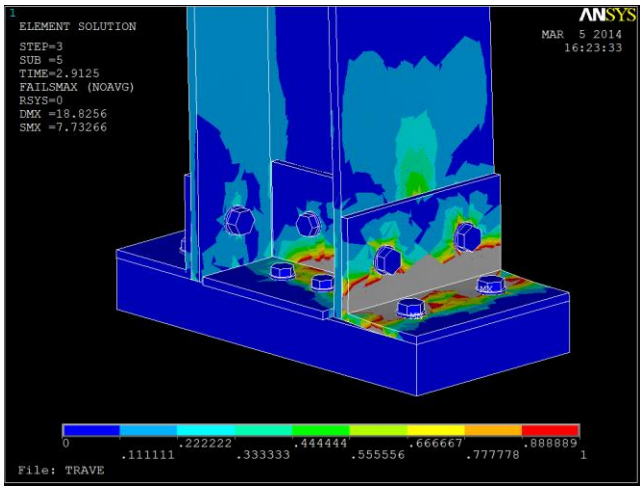

Figure 5.1.3.2.3. Bending Moment 11223.75Nm

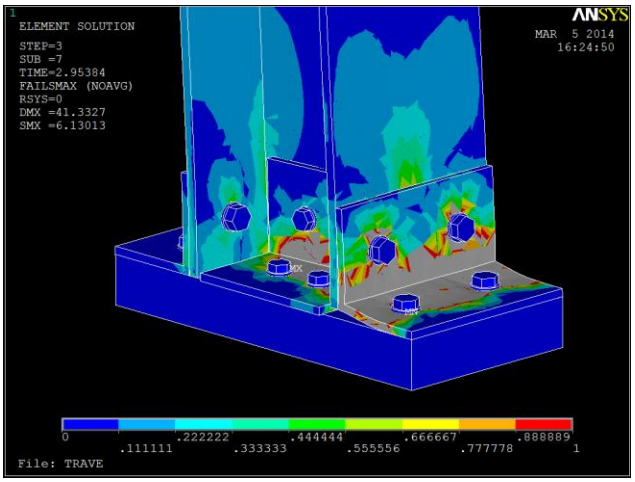

Figure 5.1.3.2.4. Bending Moment 11732.23Nm

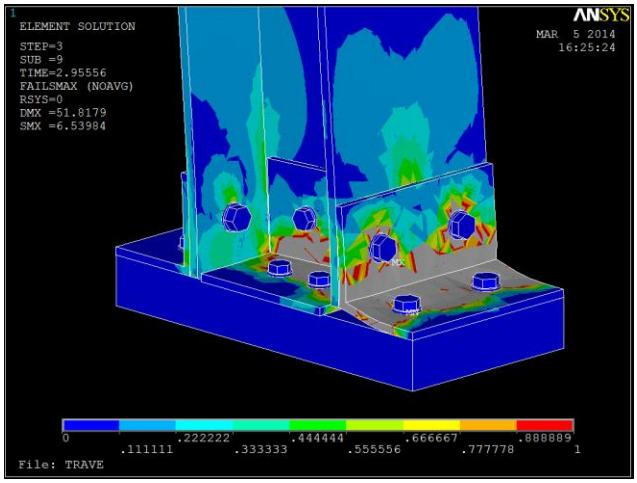

Figure 5.1.3.2.5. Bending Moment 11753.88Nm

Graph 5.1.3.2.1 shows the relation between the relative rotation angle of the column due to bending moment.

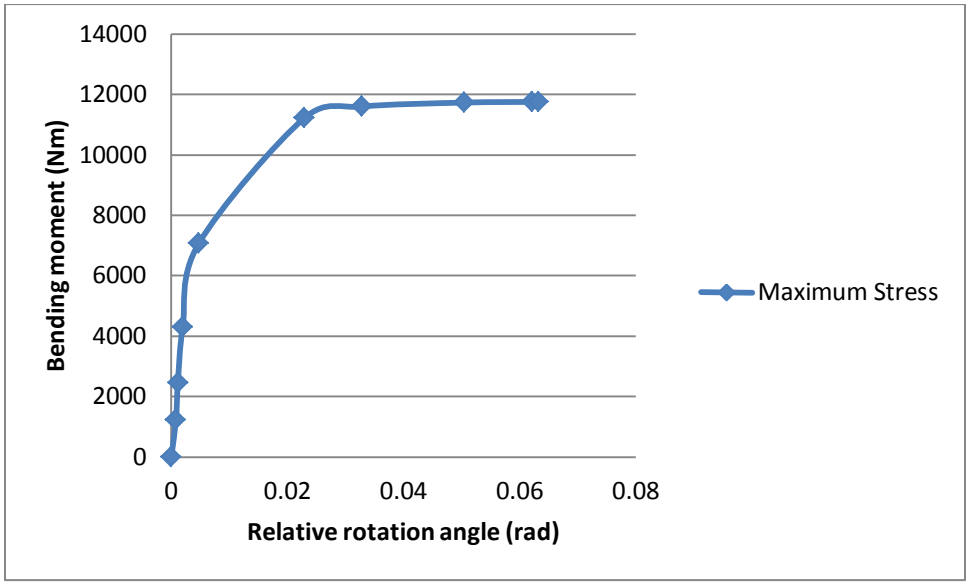

Graph 5.1.3.2.1. Relative rotation angle (rad)-Bending moment (Nm)

Hashin

Images show the spread of the failure in the connection. Analogue to previous analyses failure begins at the right plate of the beam flange, right in the corner then spreads until total failure of the connection. The maximum displacement of the end of the column is 34.133mm and the bending moment 10806.53 Nm. Matrix presents more damage than the fiber, next figures shows the development of the damage.

Matrix

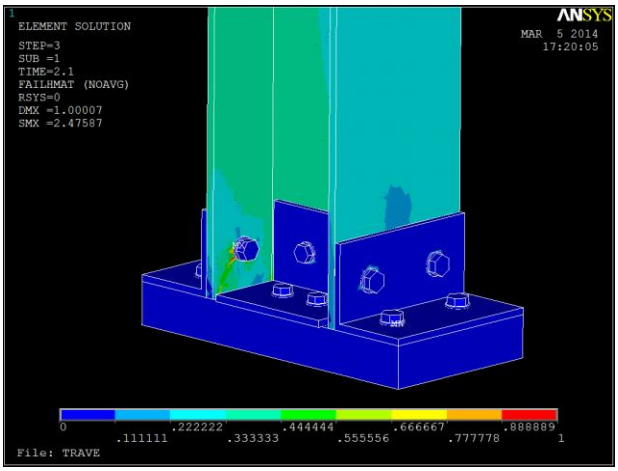

Figure 5.1.3.2.6. Bending Moment 1230Nm

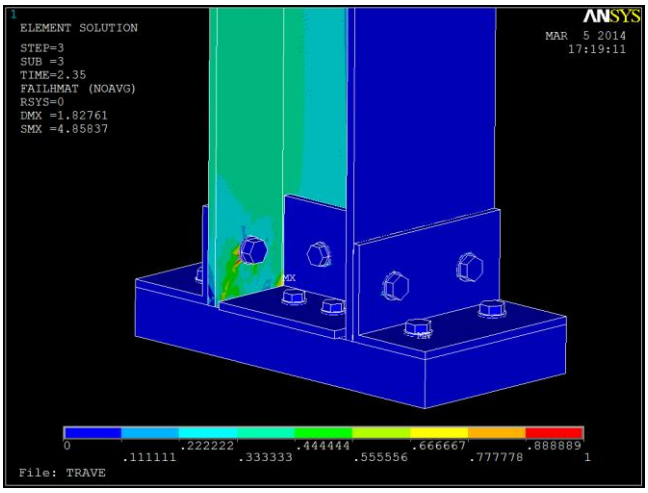

Figure 5.1.3.2.7. Bending Moment 4305Nm

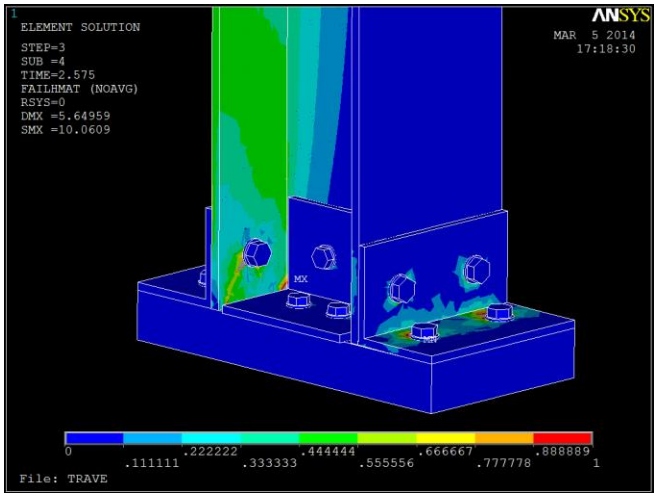

Figure 5.1.3.2.8. Bending Moment 7072.5Nm

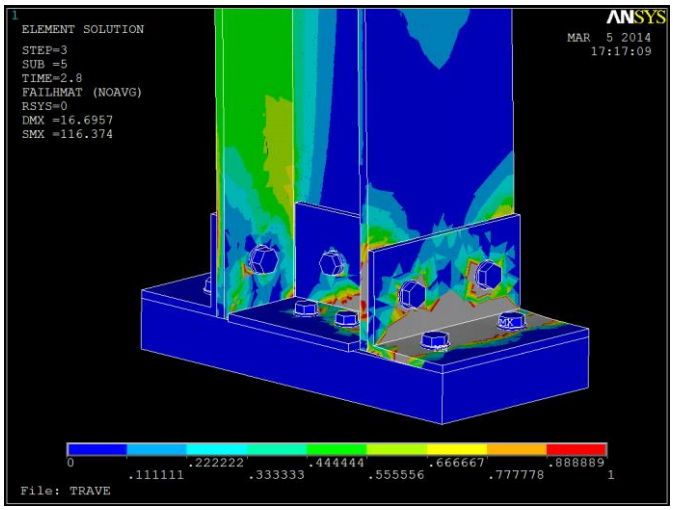

Figure 5.1.3.2.9 Bending Moment 9840Nm

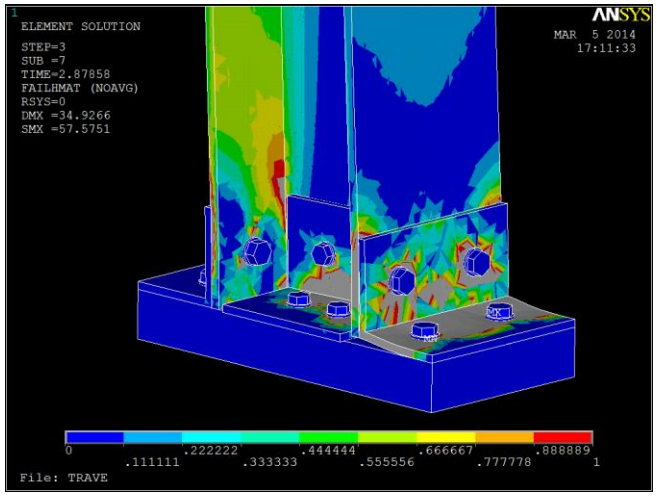

Figure 5.1.3.2.10 Bending Moment 10806.53Nm

Fiber

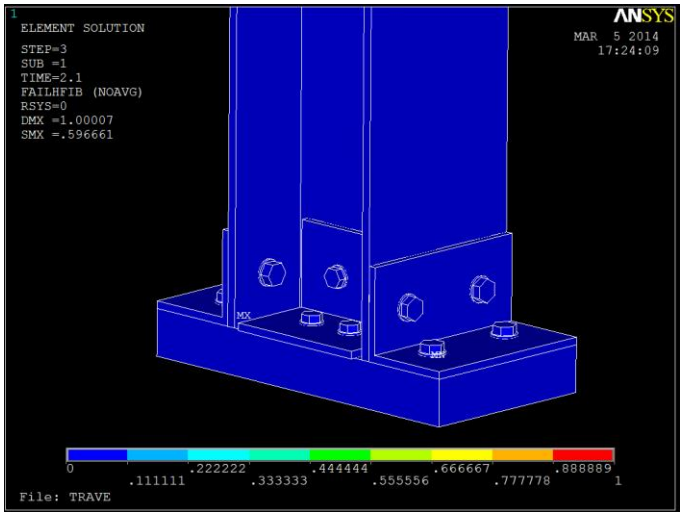

Figure 5.1.3.2.11. Bending Moment 1230Nm

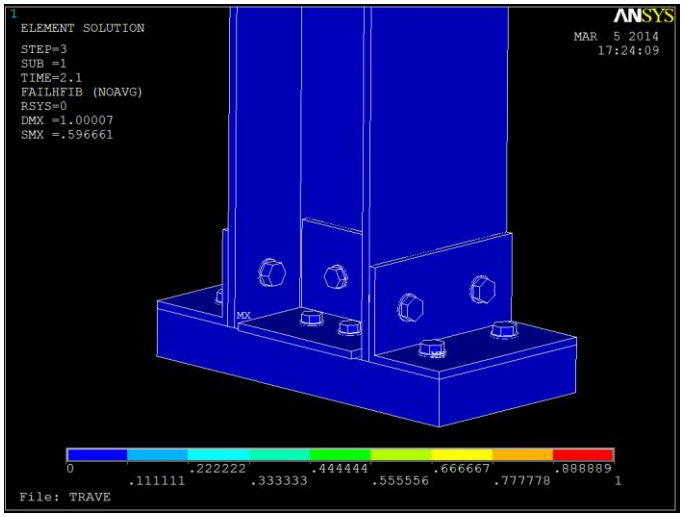

Figure 5.1.3.2.12 Bending Moment 4305Nm

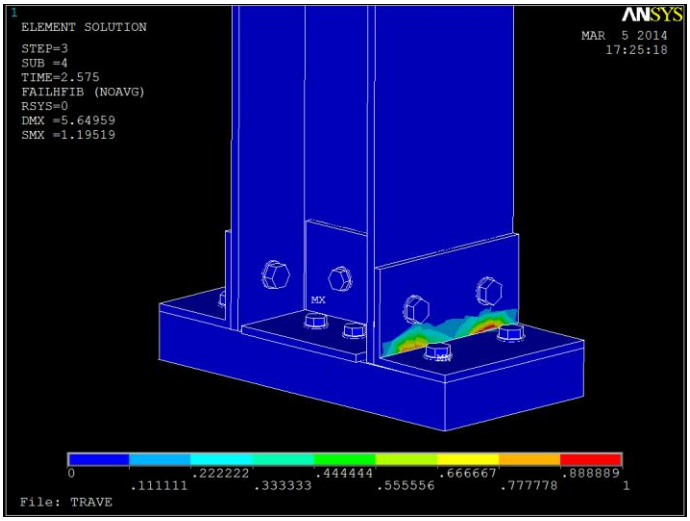

Figure 5.1.3.2.13. Bending Moment 7072.5Nm

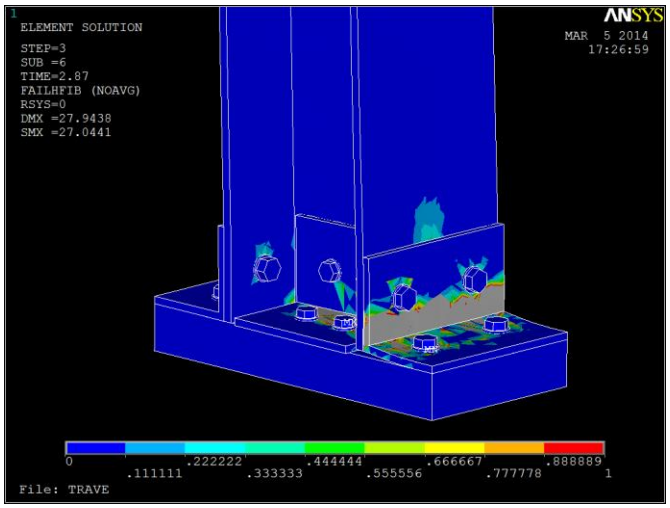

Figure 5.1.3.2.14. Bending Moment 9840Nm

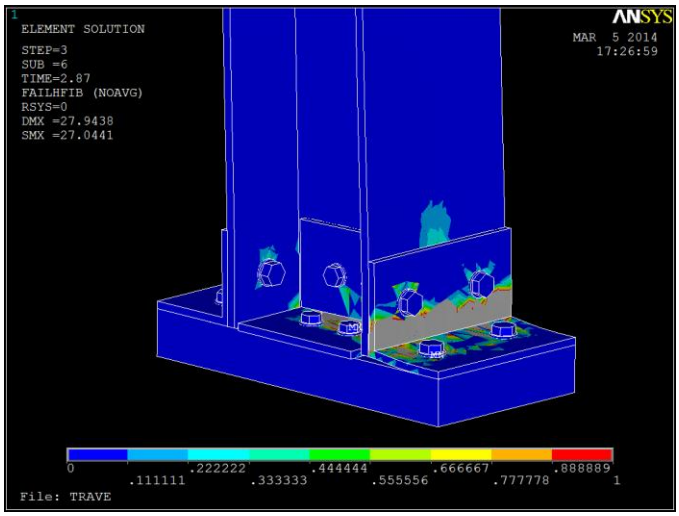

Figure 5.1.3.2.15 Bending Moment 10806.53Nm

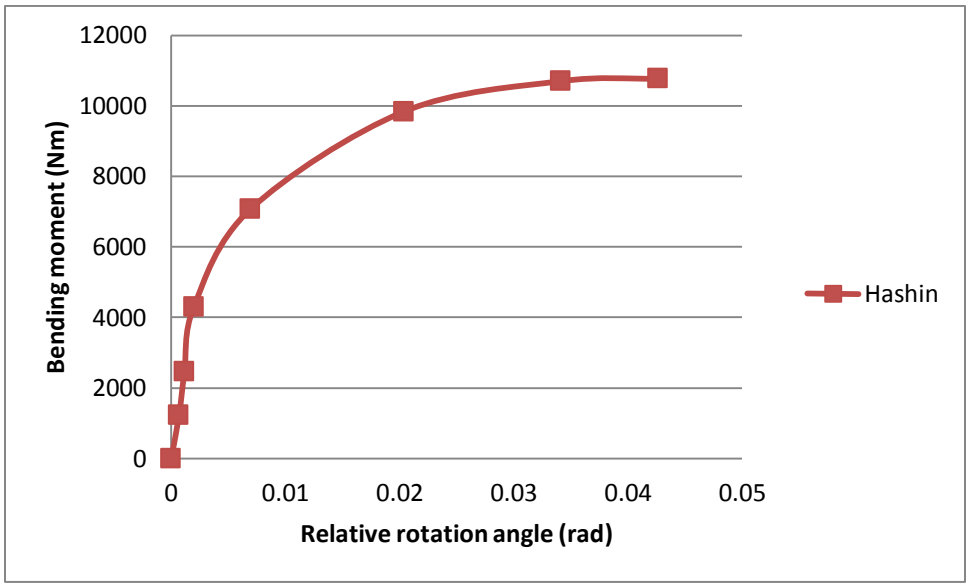

Graph 5.1.3.2.2. Relative rotation angle (rad)-Bending moment (Nm)

Graph 5.1.3.2.2 shows the relation between the relative rotation angle of the column due to bending moment, for bending moment under 3000Nm we can see a linear behavior, until this point failure is small predominantly in the right cleat of the flange, after this point is appreciated a nonlinear behavior characterized by the loss of mechanical properties until reach total failure of the connection.

Puck

Analogue to Hashin, total failure is evident at 10290.6 Nm. The maximum displacement of the end of the column is 47.27. Matrix presents more damage than the fiber, next figures shows the development of the damage.

-Matrix

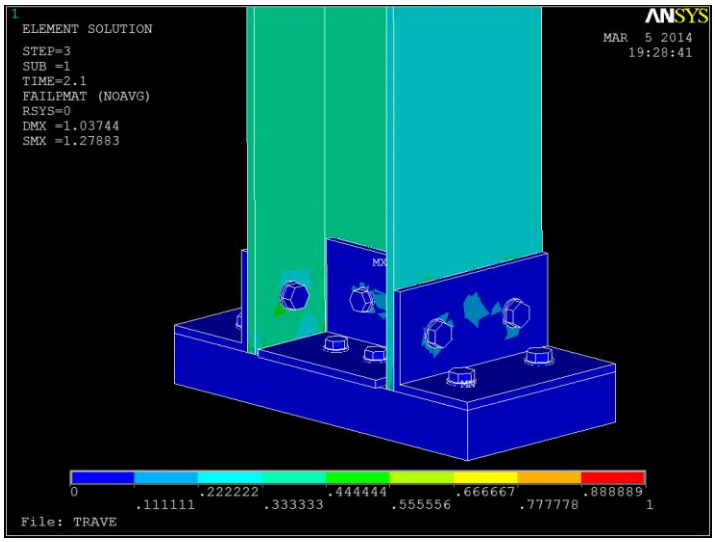

Figure 16. Bending Moment 1230Nm

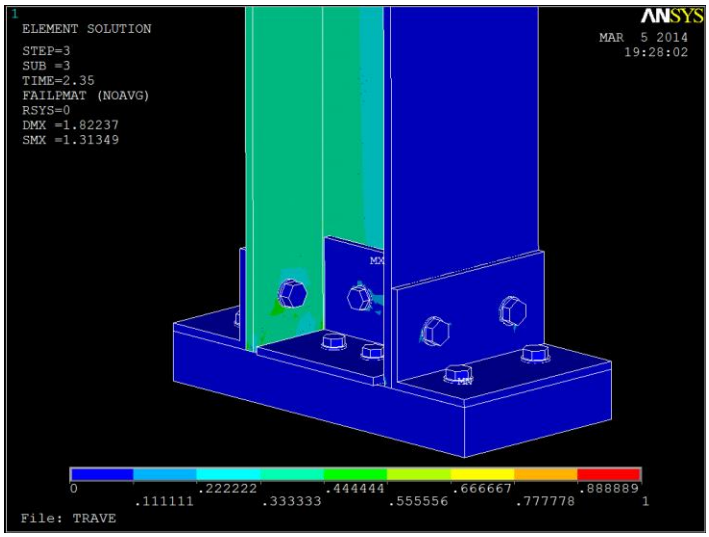

Figure 17. Bending Moment 4305Nm

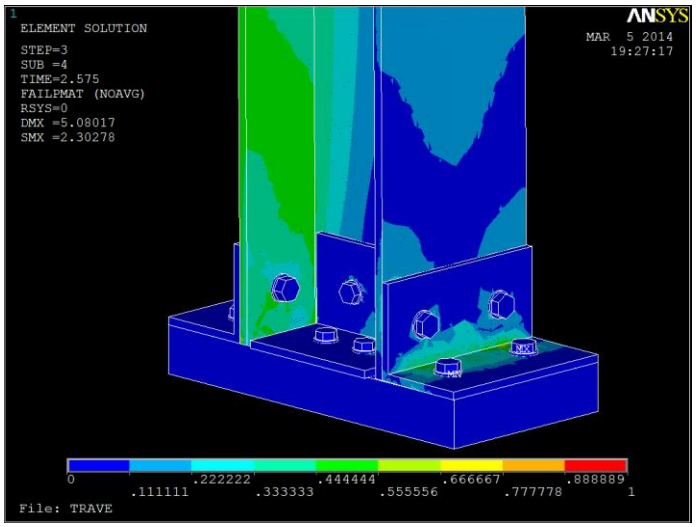

Figure 18. Bending Moment 7072.5Nm

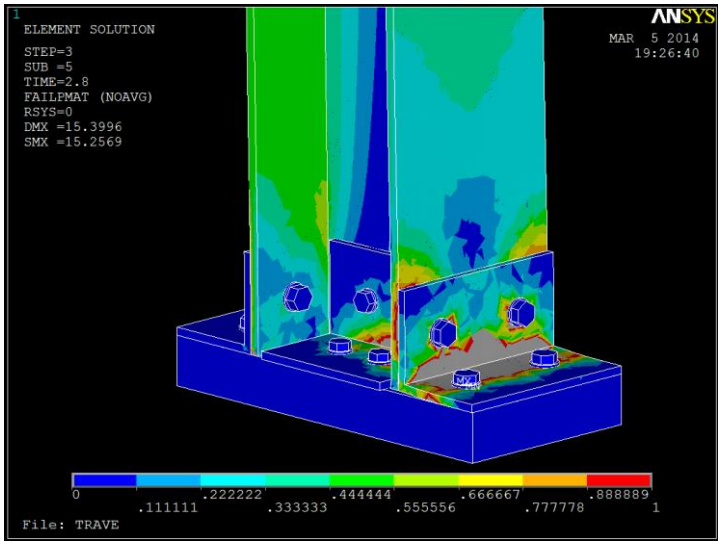

Figure 19. Bending Moment 9840Nm

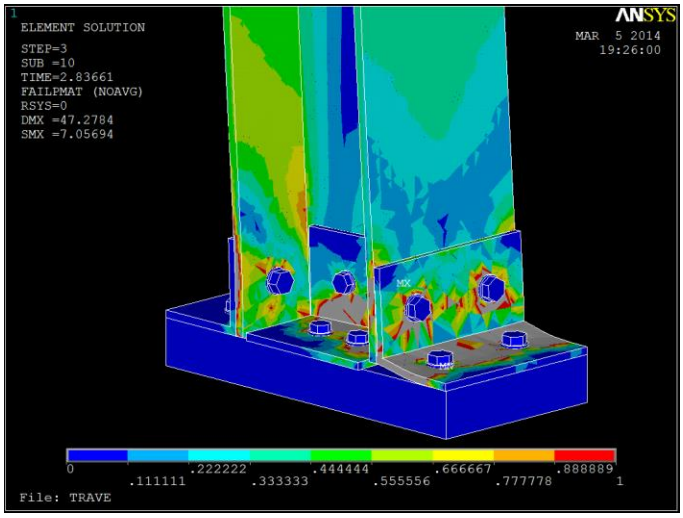

Figure 20. Bending Moment 10290.3Nm

-Fiber

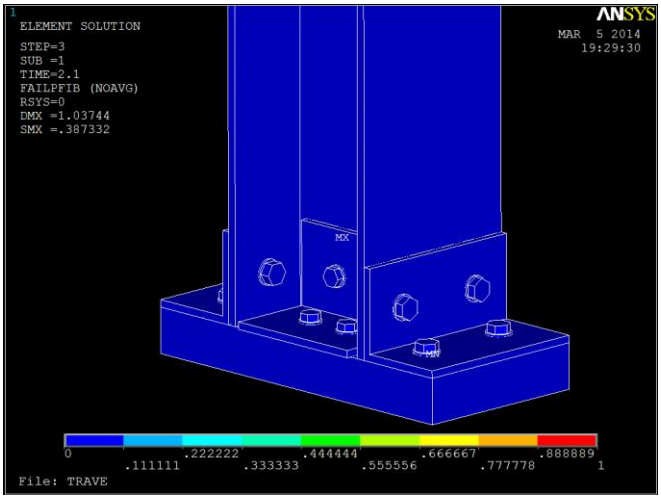

Figure 21. Bending Moment 1230Nm

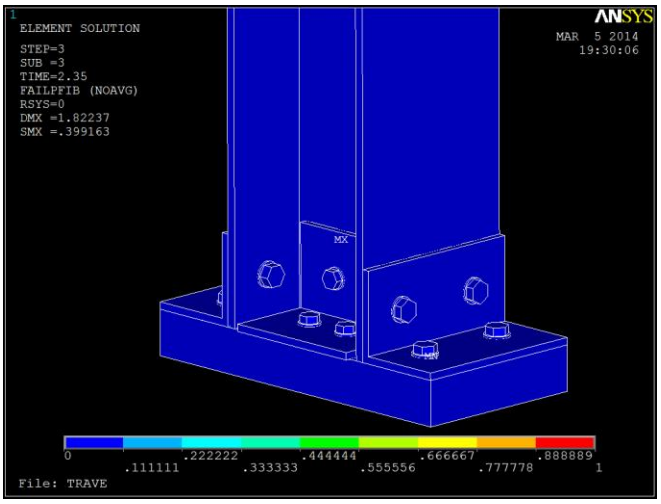

Figure 22. Bending Moment 4305Nm

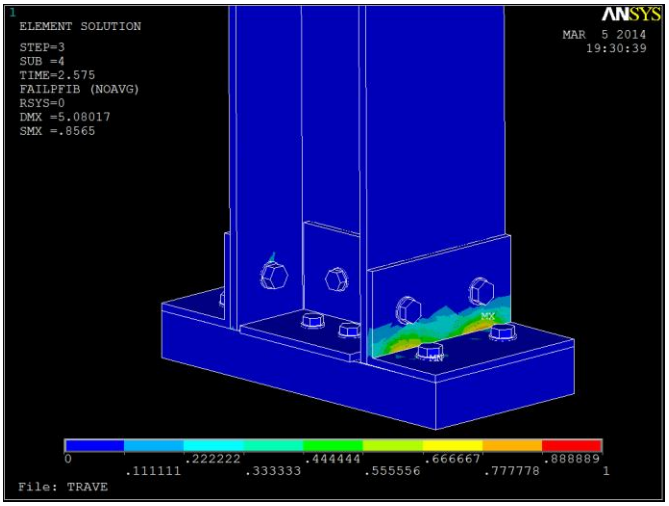

Figure 23. Bending Moment 7072.5Nm

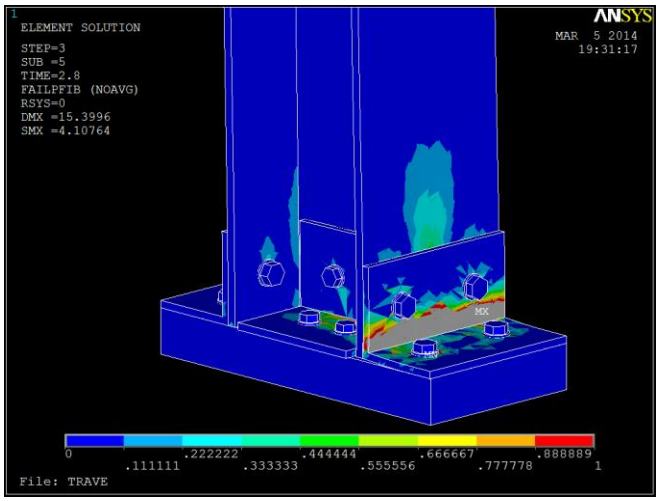

Figure 24. Bending Moment 9840Nm

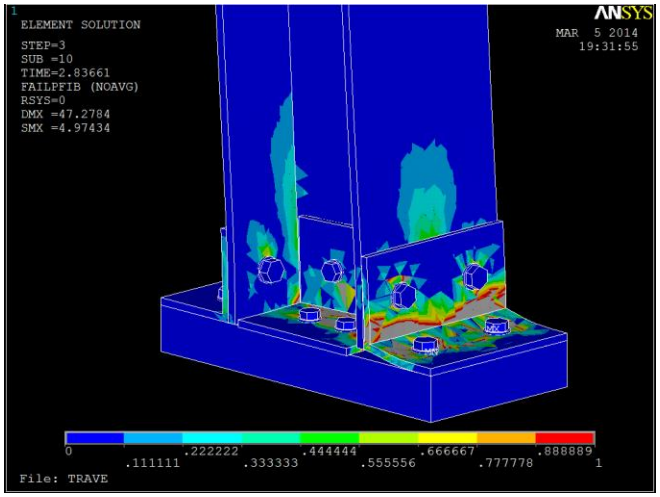

Figure 25. Bending Moment 10290.3 Nm

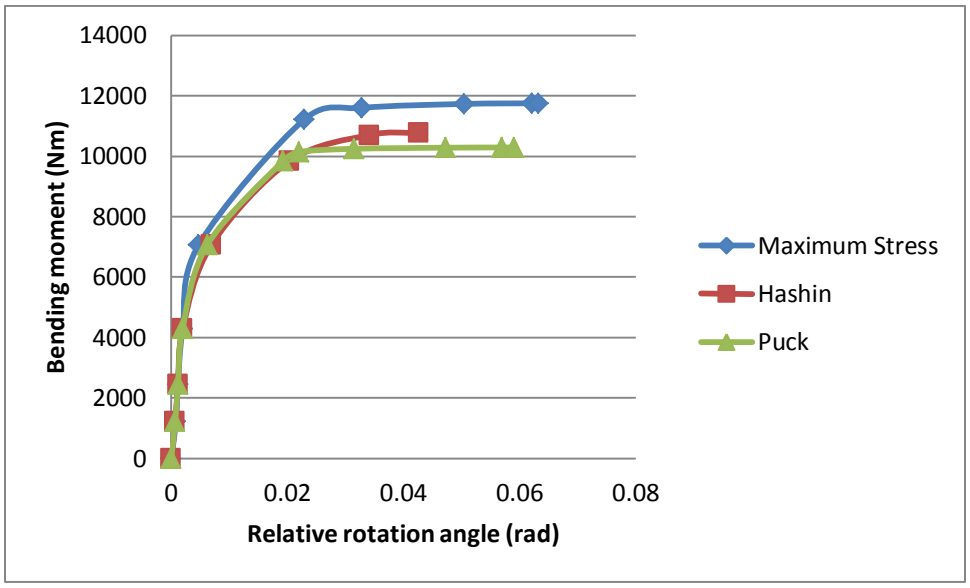

Graph 5.1.3.2.3. Bending moment-Relative rotation angle

For bending moment under 4000Nm we can see a linear behavior, in fact the 3 curves are practically the same until this point, failure is small predominantly in the right plate of the flange, after this point is appreciated a nonlinear behavior characterized by the loss of mechanical properties until reach total failure of the connection.
A brief resume of the results that allows understand better would be, graph 4, 5 and 6, they represent how the connection evolves in all cases of compression and bending moment for each failure criterion. As compression increases the resistance to bending moment increases too, deformations also increases:

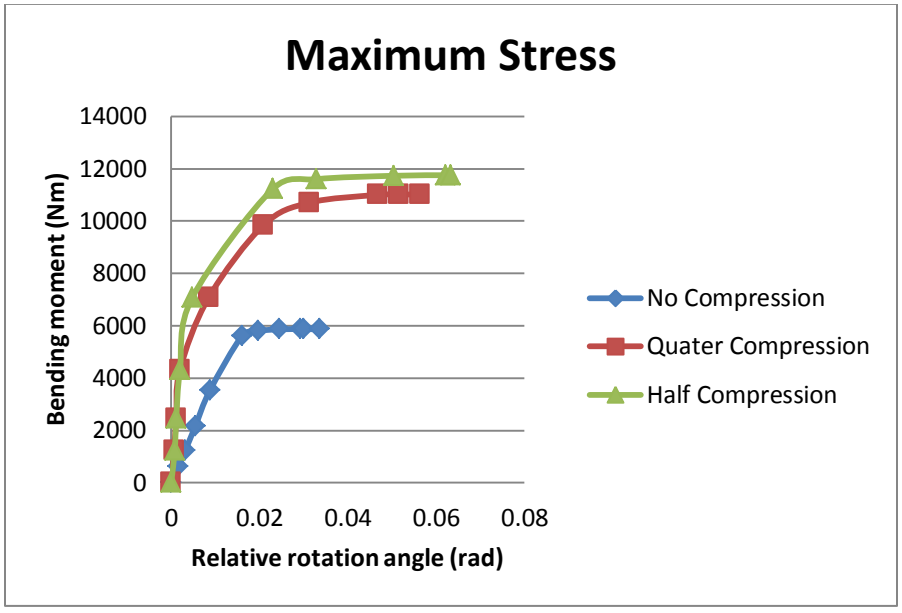

Graph 5.1.3.2.4. Bending moment-Relative rotation angle.

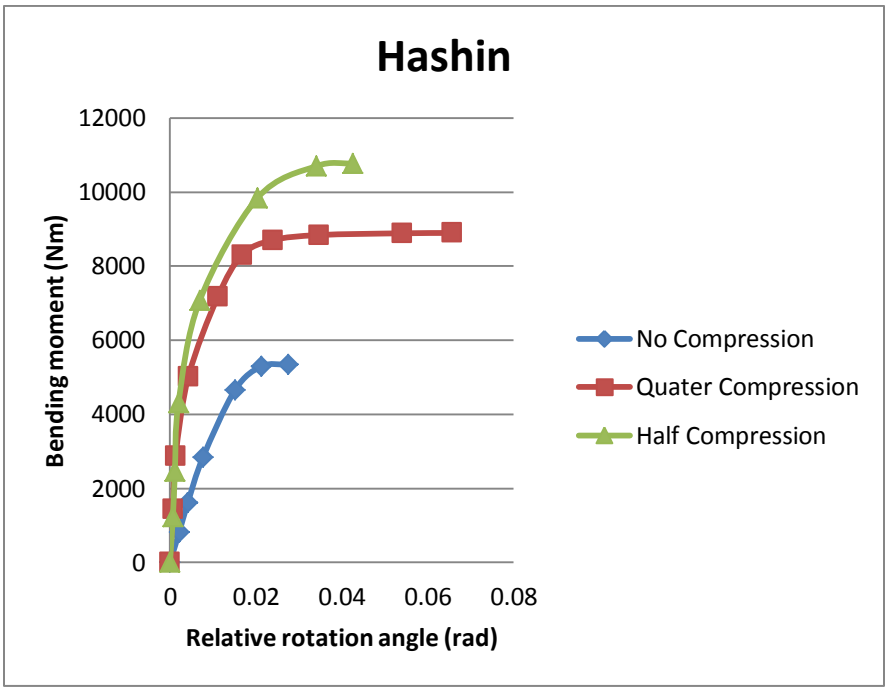

Graph 5.1.3.2.5. Bending moment-Relative rotation angle.

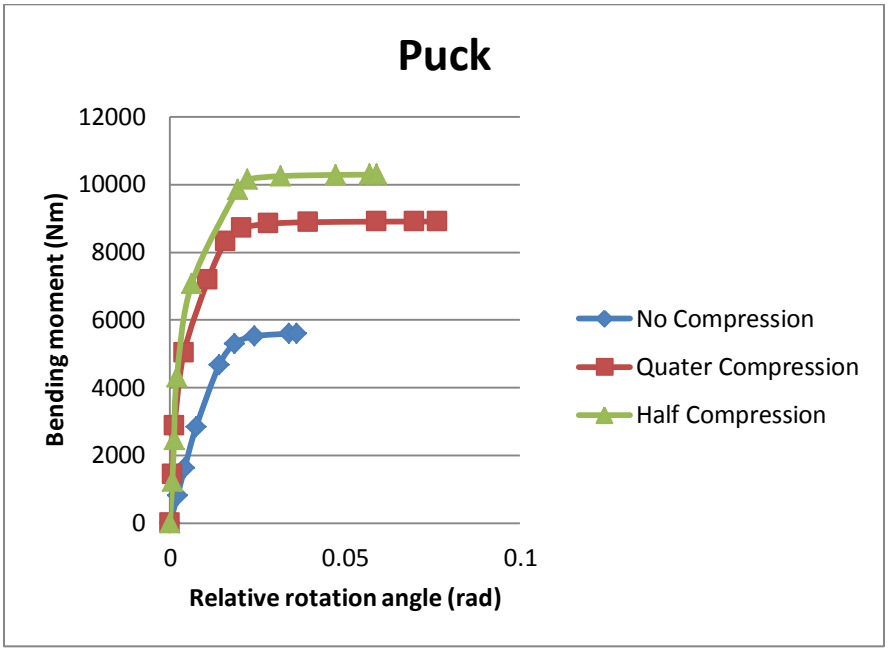

Graph 5.1.3.2.6. Bending moment-Relative rotation angle.

5.1.4 Behavior under hysterical cycles

The objective of this analysis is to calculate the Equivalent Viscous Damping, in other words the dissipated energy of the structure; this dissipation is a cause of non-linearity of the system, interaction of with nonstructural elements, etc.

Equivalent viscous damping is based on a concept first proposed by Jacobsen (1930). He proposed that the maximum displacement of an oscillator with complex damping mechanisms, when subjected to steady state vibratory motion, could be found from an analysis of a viscously damped associated elastic model. The complex damping mechanism in the oscillator could include hysteretic behavior due to yielding. The appropriate level of viscous damping for the associated elastic model could be found by equating the energy dissipated by the oscillator to that dissipated by the associated elastic model. Jacobsen found that his theory, when implemented for mechanical systems under forced steady state vibration, was in close agreement with exact solutions for systems with relatively low levels of non-linearity. For the non-regular vibratory motion Jacobsen suggested that a time average damping would be more representative than the equivalent viscous damping, but that the equivalent viscous damping is more convenient to use.

As a starting point, the equations proposed by other authors differentiate in two parts the viscous damping coefficient:

$$\xi = \xi_0 + \xi_{hyst}$$

Where ξ_0 corresponds due initial elastic viscous damping and ξ_{hyst} equivalent due a nonlinear behavior (hysteretic). For the hysteretic viscous damping the concept used by Jacobsen was based in dissipated and stored energy. Illustrated in the following figure:

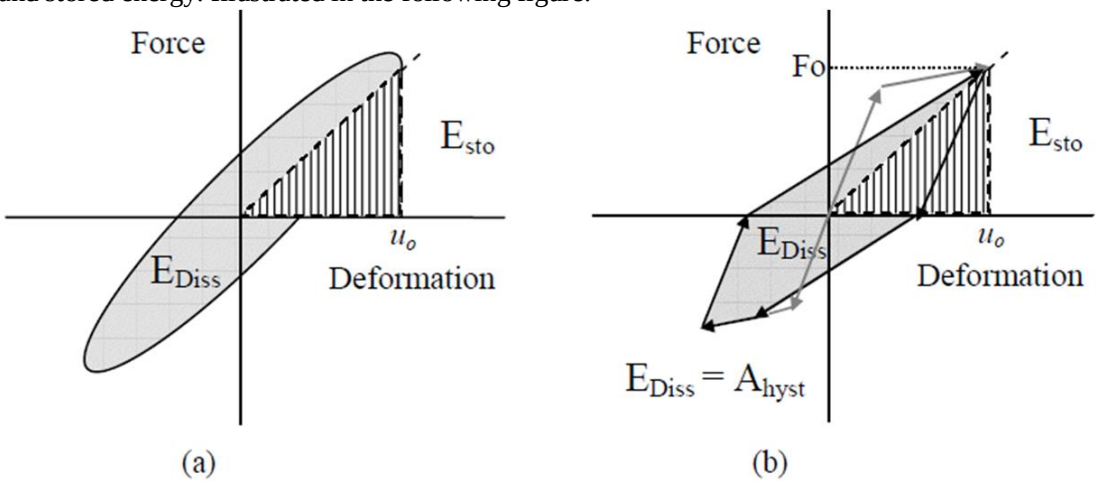

Figure1. Dissipated force for viscous damping and hysteretic cycles.

Is assumed the resonance frequency is the same to the natural frequency of the SDOF, the equation to calculate the hysteretic viscous damping is:

$$\xi_{hyst} = \frac{1}{4\pi}\frac{E_{Diss}}{E_{Sto}} = \frac{1}{2\pi}\frac{A_{hyst}}{F_0 u_0}$$

The connection was requested to hysteretic cycles, under the control of displacement, applying an increasing displacement at the barycenter of the column. The values of displacement are selected small enough to development several cycles and calculated for each one Equivalent viscous damping. Each increment between cycles is 3mm until failure. Results for all failure criteria are:

Viscous Damping (%)

Cycle(mm)	Maximum Stress	Hashin	Puck
wd3	3.144E-05	0.00682	0.00465
6	0.0289	-	-

Table 5.1.4.1.

Graph 1 shows the development of the hysterical cycles for each failure criteria. With Maximum Stress criterion only 2 cycles could be calculated, and for Hashin and Puck criteria only the first cycle, then none may end next cycle due to failure.

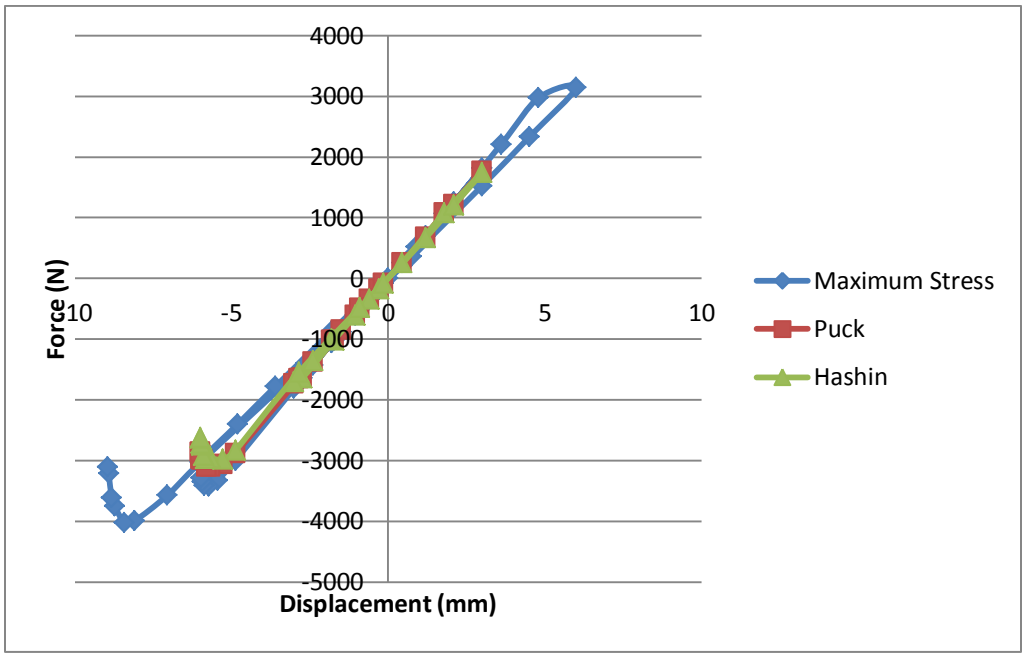

Graph 5.1.4.1. Force – displacement.

Previous analysis were only just with to load steps, first pretension of the bolts and displacements of the end of the column, now in the following analyses are attached another loads steps, namely, compression force. The viscous damping decline as the compression increases. Graph 1 and 2 shows the development of the hysterical cycles varying the compression force in the end of the column, also are calculated values of viscous damping based on Jacobsen theory.

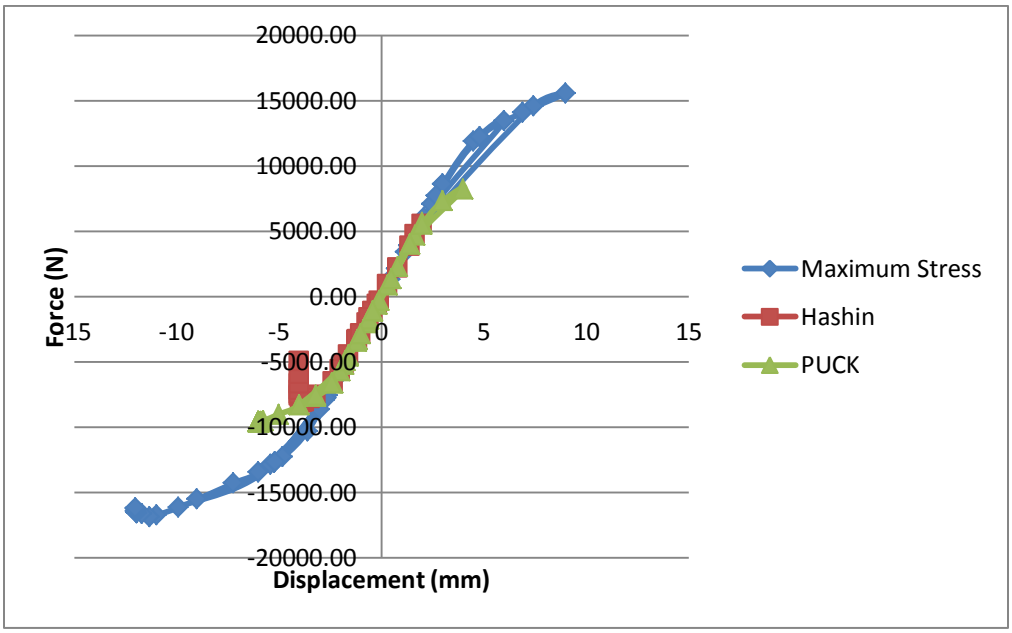

Graph 5.1.4.2. Force – displacement, under quarter failure compression force

Viscous Damping (%)			
Cycle (mm)	Maximum Stress	Hashin	Puck
2	-	0.00218	3.320E-07
3	2.127E-08	-	-
4	-	-	0.00226
6	9.37E-07	-	-
9	1.00E-06	-	-

Table 5.1.4.2 Viscous Damping

Viscous damping varies according to the failure criterion, for maximum stress results damping is almost 0 for all cycles. For Puck and Hashin the results are more similar each other, around 0.0022 % is de common value. Next is graph 2 that shows the development of the hysterical cycles under half failure compression force, the viscous damping for each failure criterion decreases considerably to the point of not be able to develop complete cycles although displacements are reduced.

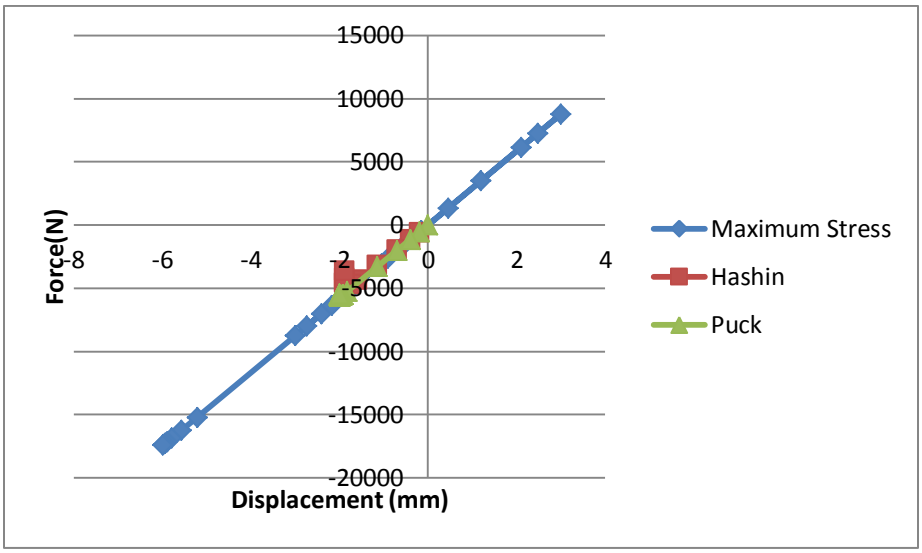

Graph 5.1.4.3. Force – displacement, under half failure compression force

Maximum Stress:

Cycle (mm)	Viscous D. (%)
3	2.52E-7

Table 5.1.4.3. Viscous Damping

Results are only for maximum stress criterion because models with the other criteria couldn't develop a full hysterical cycle. Then analogue to previous analyses were done but changing the compression force until three quarters of the failure compression force, no model couldn't complete a full hysterical cycle, corroborating the loss of energy dissipation increasing the compression force in the column.

5.2 Connection 2

5.2.1 Behavior under bending moment

Bending moment is applied in the end of the column equivalent to 8200Nm, next are presented the result for the 3 failure criteria.

Maximum Stress:

The maximum value of resistance is 3997. Figure 1 shows that failure begins at the right cleat of the beam flange, right in the corner then spreads until total failure of the connection Web cleats are next who are affected; the corner of the plates begins the rupture increasing until failure..

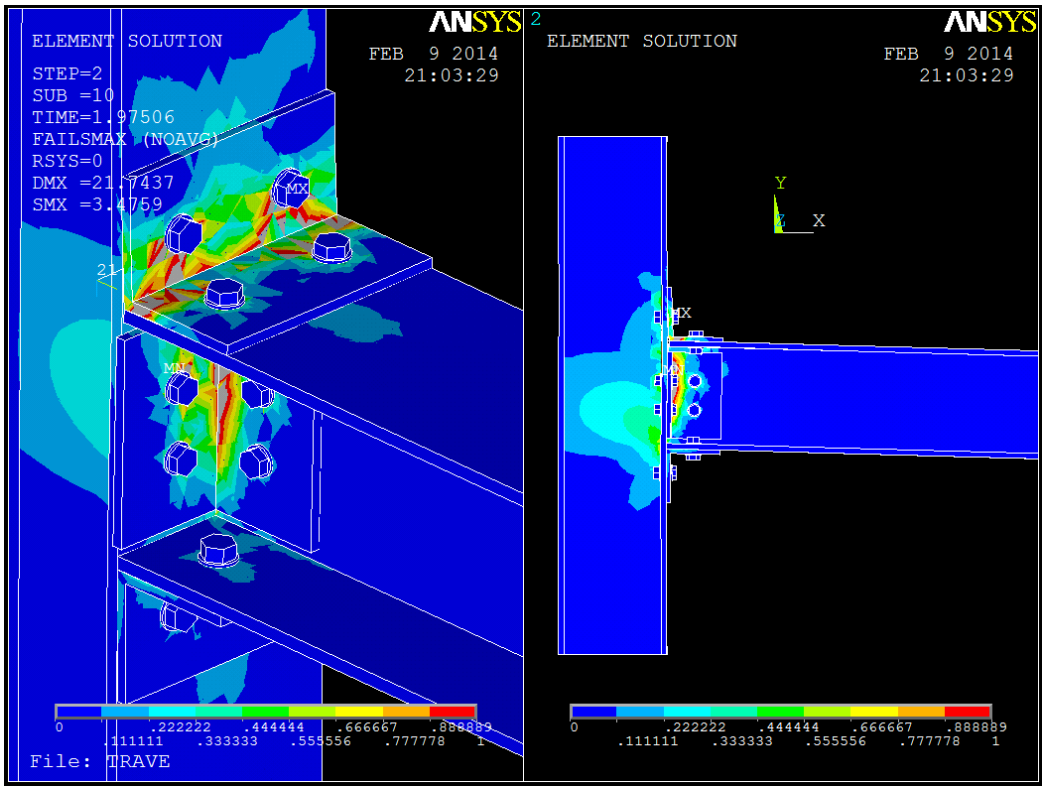

Step 4. Bending Moment 3997.5 Nm.

Puck

Images show the spread of the failure in the connection. Failure begins around 3150Nm, it will continue until reach 5634.5Nm, as before failure begins at the right cleat of the beam flange, right in the corner then spreads until total failure of the connection. Matrix presents more damage than the fiber, next figures shows the development of the damage.

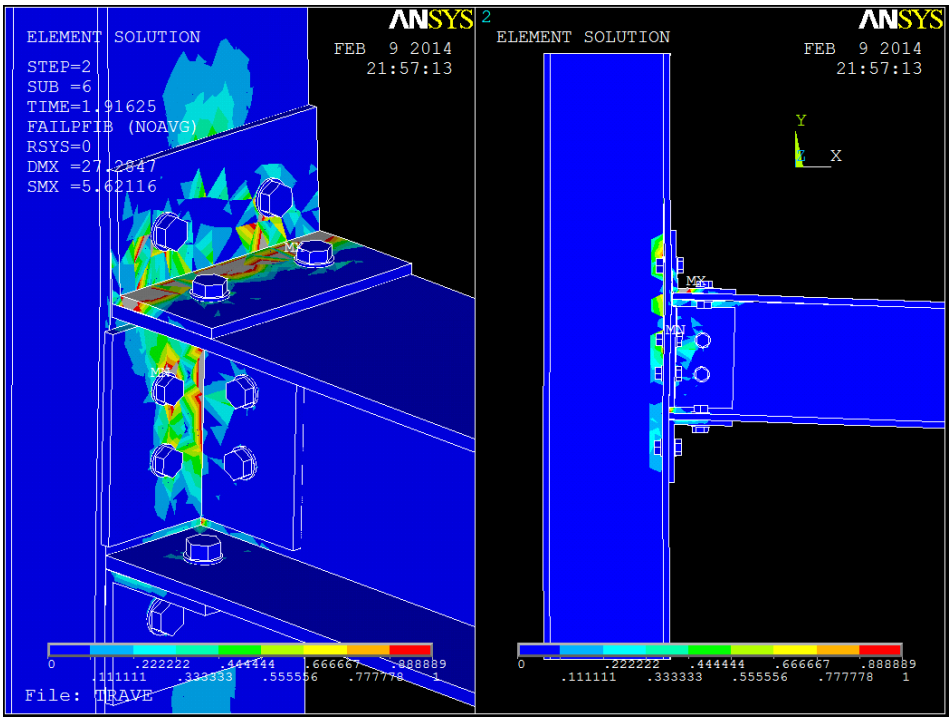

Step 4. Bending Moment 5634.93 Nm.

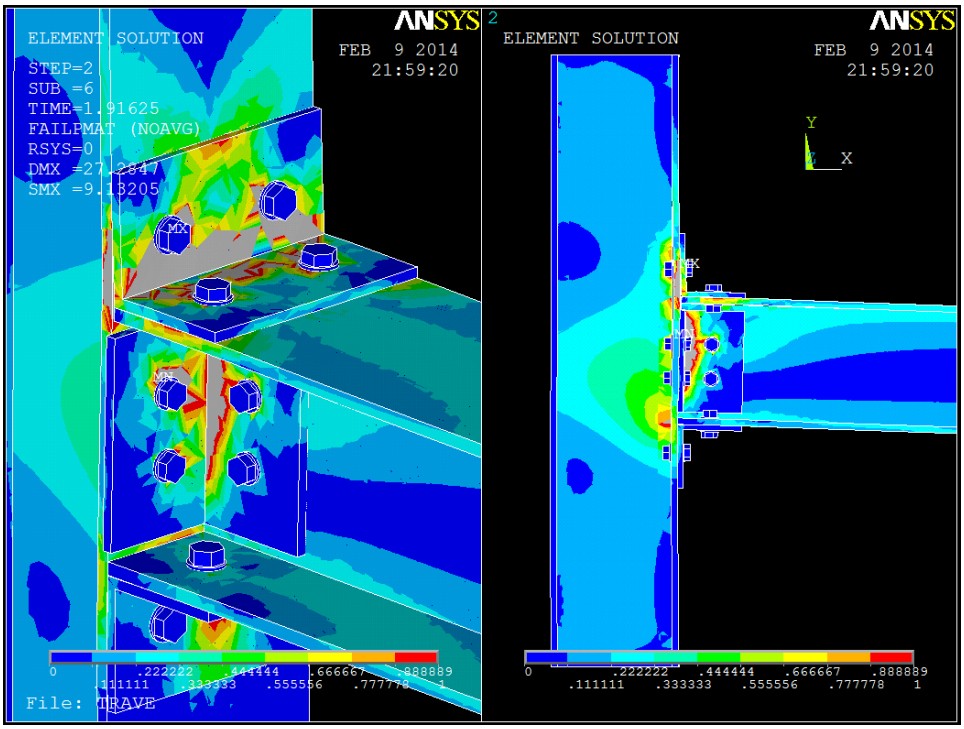

Step 4. Bending Moment 5634.93 Nm.

Hashin

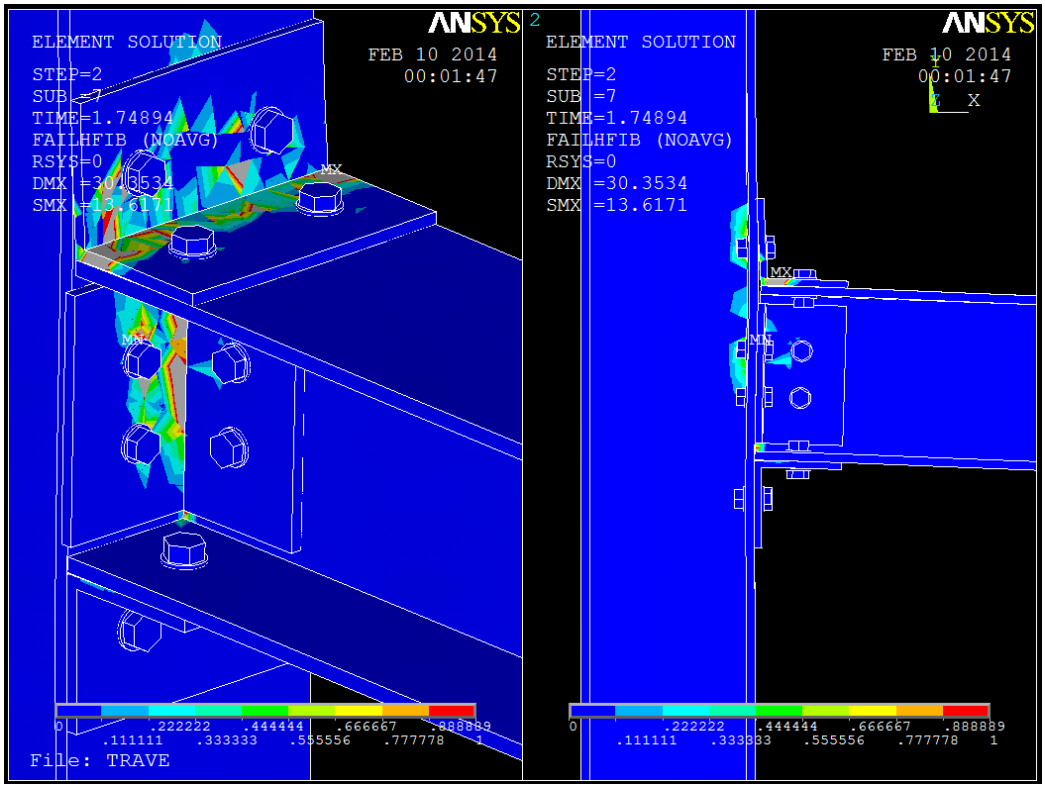

Step 4. Bending Moment 4605 Nm.

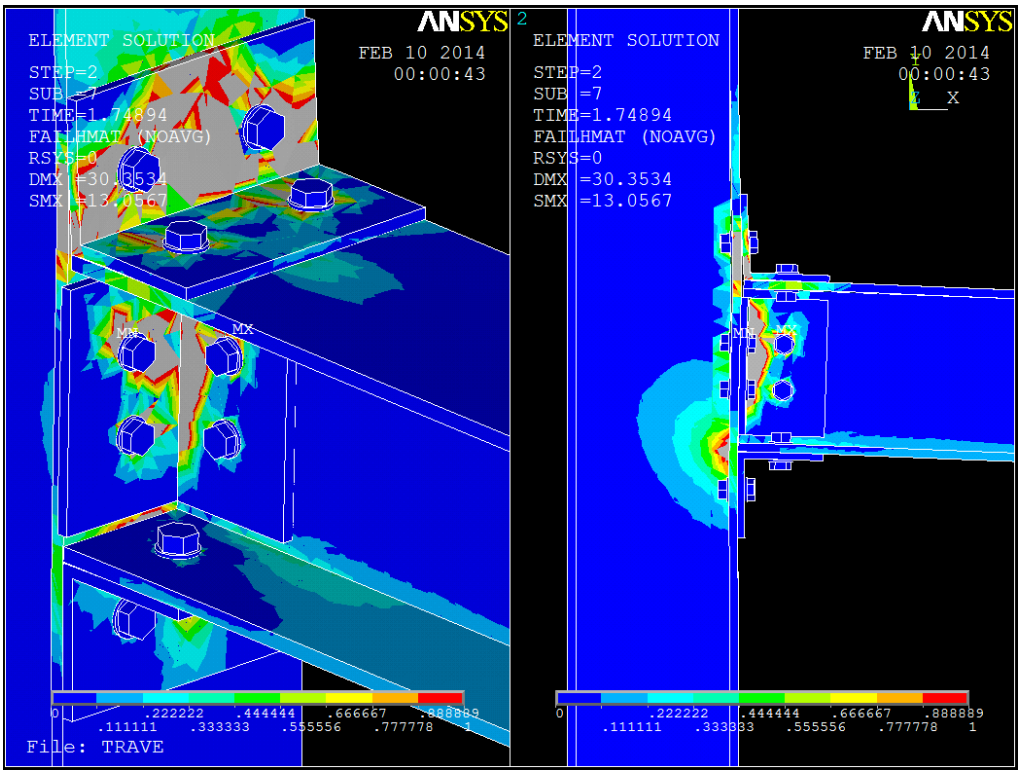

Step 4. Bending Moment 4605 Nm.

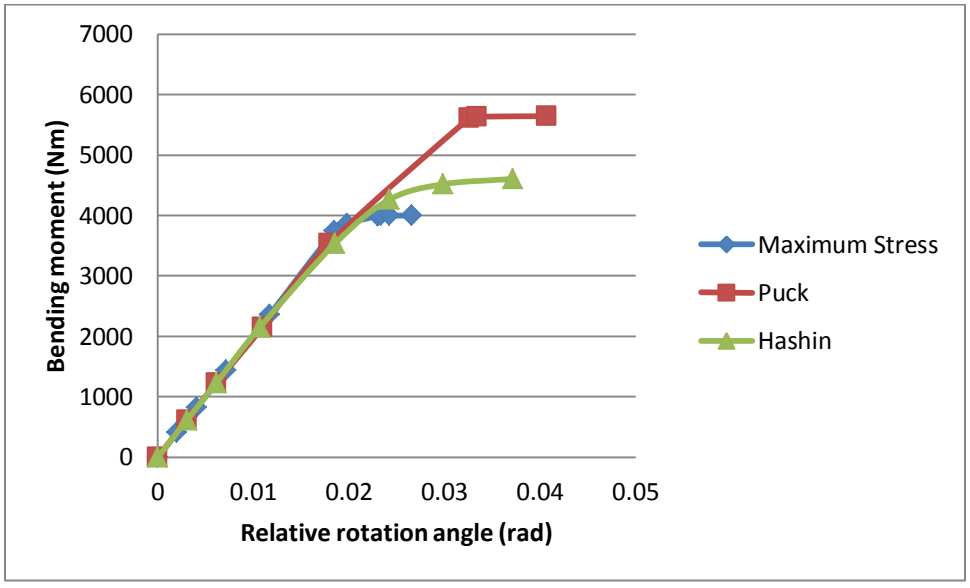

Graph 5.2.1. Bending moment-Relative rotation angle.

5.2.2 Behavior under hysteretic cycles

The connection was requested to hysteretic cycles, under the control of displacement, applying an increasing displacement at the barycenter of the beam. The values of displacement are selected small enough to development several cycles and calculated for each one Equivalent Viscous Damping. Each increment between cycles is 5mm until failure. Results for all failure criteria are:

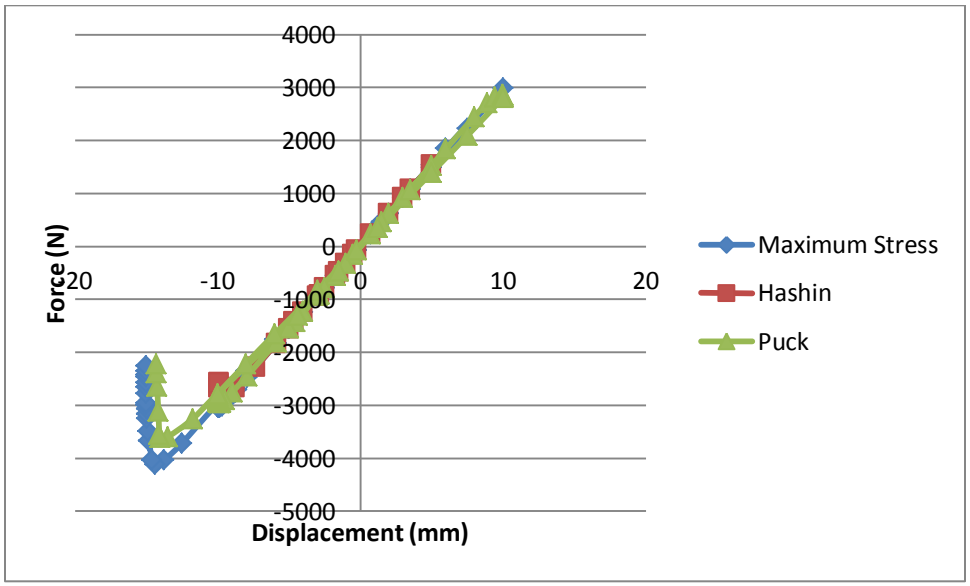

Graph 5.2.2.1. Force – displacement, under half failure compression force

	Viscous Damping (%)		
Cycle (mm)	Maximum Stress	Hashin	Puck
5	0.000399	0.000893	0.00125
10	0.00650	-	0.0160

Table 5.2.2.1. Viscous Damping

6 Comparison of Results with previous analyses.

In this chapter in particular, results obtained for the connection 2 are going to be compared with the final degree project "CAPACITà DISSIPATIVA DI NODI TRAVE-COLONNA IN STRUTTURE PULTRUSE" made by Engineer Antonio Picariello. This project consists in two GFRP pultruded joints, both of them beam-column attached with cleats and bolts made with the same material Figure 6.1 illustrated the geometry of the connectionS:

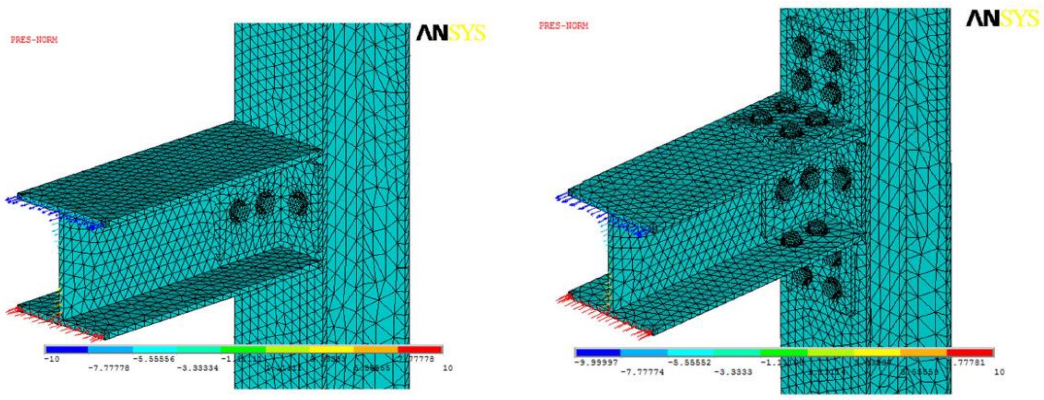

Figure 6.1 Types of connections made in previous analyses.

These to connections were subjected to bending moment and hysteretic cycles at the end of the beam, always analogue to the analyses made to the connection 2. It's very interesting to confront results between connections to verify the behavior of each FEM model. Next graph shows results for all the connections, in particular relation between moment and relative rotation angle:

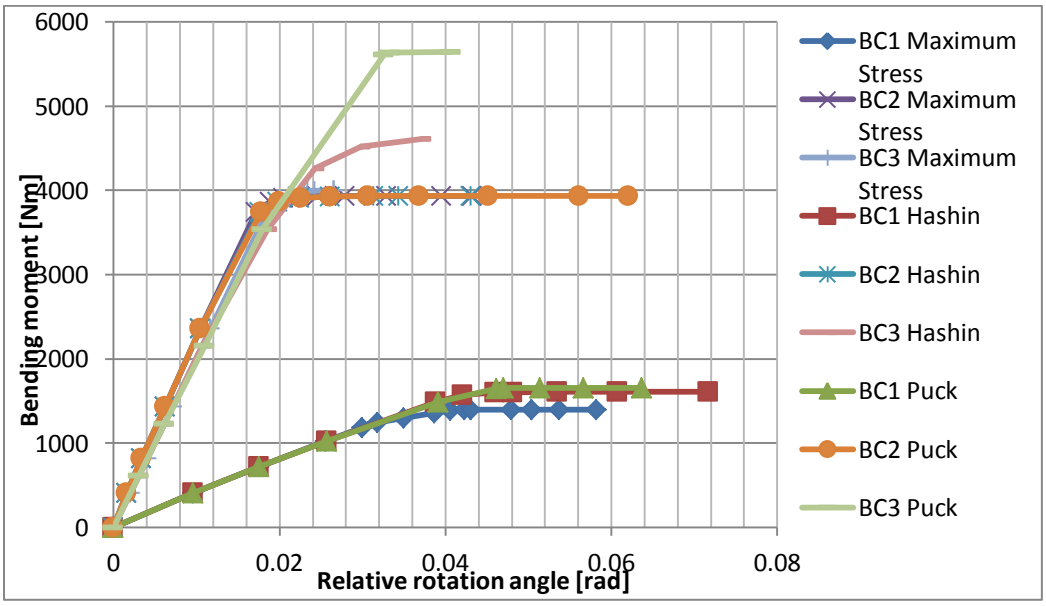

Graph 6.1 Bending moment – Relative rotation angle.

Where BC1 and BC2 are the curves for the connections in Picariello's project, BC3 is the connection 2 model previously, there are important differences between curves, BC1 curves have less stiffness than

the others, it is expected because the connection is attached only with two cleats, instead that BC2 and BC3 curves are more similar between them due to the similar geometry, but nevertheless BC3 resists more bending moment developing less relative rotation angle than BC2.
Next table shows the values of Viscous Damping for each connection and failure criteria, for calculating this values it was necessary to subject to hysteretic cycles each connection, and determine the energy dissipation according to their own geometric and mechanical properties:

	Viscous Damping (%)			
	Cycle (mm)	Maximum Stress	Hashin	Puck
BC1	5	-	0.001343	0.001156
	10	-	0.006511	0.006255
	15	0.018	-	0.07954
	20	-	-	-
BC2	2.5	-	0.001931	0.00193118
	5	0.025	0.140625	0.14
	7.5	0.069	-	-
	10	-	-	-
BC3	5	0.000399	0.000893	0.00125
	10	0.0065	-	0.016

Table 6.1 Bending moment – Relative rotation angle.

It is appreciated that the BC1 and BC2 have more or less same order of magnitude, instead that BC3 (connection 2) is much smaller , namely , energy dissipation is lower in this particularly connection, one of the reasons could be the difference of material in the bolts, producing a different rupture in the cleats.

7 Conclusions

A progressive damage analyses were carried out, of two different connections made of Pultruded GFRP, the first one a column attached to a steel end plate and a second one beam-column connection each one with different material, geometry and stiffness properties. Due to nonlinear behavior load capacity, failure mechanism and energy dissipation vary in each analysis and connection. A common conclusion for each type of connection is that local failure always begins in the cleats due to perpendicular solicitations of the fiber directions and a total collapse is a consequence of massive damage of the matrix, worth noting than local failure exists in the fiber of all pultruded elements but never arrive to a massive collapse. Results vary according to the failure criterion used, however results are consistent among the three, difference are caused thanks to the different procedures that characterizes each one.

In the connection column steel plate, an increase of the axial compressive force is favorable to develop a higher stiffness, resistance to bending moment and relative rotation angle. Results can vary; the increase of resistance to bending moment is roughly about 50%, an important difference to take in account to confront with the energy dissipation. In the other hand, analyses related to hysteretic cycles, energy dissipation decreases as the axial compression force rises, as a first prove of this is less cycles develop by the connection, and minor enclose area in the graphs cycles-displacement, namely, viscous damping with tendency to 0.

In the connection beam-column, results are congruent with previous analyses done in other connections in GFRP, resistance to bending moment vary according to the failure criterion used in the analysis, nevertheless differences between failure criterion are mild. Bolts made in steel changes considerably the mechanical properties of the joint increasing the resistance to bending moment and reducing the relative rotation angle of the joint. Energy dissipation is smaller than connections studied in other analyses, with tendency to 0.

Some improves can be carried out as change the material of the cleats, instead FRP could be made of steel, aluminum or another material that can resist better the tensile and compression stresses.

Numerical and experimental results helps with a better comprehension of the behavior of the material and its properties, can be used to define different coefficients to project structures for different purposes under several effects, as seismic hazard, wind or others.

More numerical an experimental analysis have to be done to improve the normative and regulations of construction with this material.

8 Bibliography

Bank, L. C. (2006). Composites for Construction Structural Design with FRP Materials. New Jersey: Jonh Wiley & Sons.

Creative Pultrusions, I. (2004). The Pultex® Pultrusion Design Manual of Standard and Custom Fiber Reinforced Polymer Structural Profiles

Jacobsen, L. S. (1930). Steady forced vibrations as influenced by damping. *ASME Trans., 52*, 169–181.

Mottram, J. T., & Bass, A. J. (1994). Moment-rotation behavior of pultruded beam-to-column connections.

Russo, S. (2007). Strutture in composito: sperimentazione, teoria e applicazione. Milano: Hoepli.

Smith, S. J., Parsons, I. D., & Hjelmstad, K. D. (1998). An experimental study of the behavior of connections for pultruded GFRP I-beams and rectangular tubes. *Composite Structures, 42*(3), 281

Turvey, G. J. (1997). Analysis of pultruded glass reinforced plastic beams with semi-rigid end connections. *Composite Structures, 38*(1-4), 3-16.

Turvey, G. J. (1998). Single-bolt tension joint tests on pultruded GRP plate - effects of tension direction relative to pultrusion direction. *Composite Structures, 42*(4), 341-351.

Turvey, G. J., & Cooper, C. (2000). Semi-rigid column-base connections in pultruded GRP frame structures. *Computers and Structures, 76*(1), 77-88.

Picariello, Antonio. *CAPACITA' DISSIPATIVA DI NODI TRAVE-COLONNA IN STRUTTURE PULTRUSE*